REACTION KINETICS OF FRESH & SPENT ACID IN DOLOMITE ROCK AT HIGH PRESSURES

BY

Muhammad Ali Khalid

A Thesis Presented to the

DEANSHIP OF GRADUATE STUDIES

KING FAHD UNIVERSITY OF PETROLEUM & MINERALS

DHAHRAN, SAUDI ARABIA

In Partial Fulfillment of the
Requirements for the Degree of

MASTER OF SCIENCE

In

PETROLEUM ENGINEERING

DECEMBER, 2014

KING FAHD UNIVERSITY OF PETROLEUM & MINERALS

DHAHRAN- 31261, SAUDI ARABIA

DEANSHIP OF GRADUATE STUDIES

This thesis, written by **MUHAMMAD ALI KHALID** under the direction his thesis advisor and approved by his thesis committee, has been presented and accepted by the Dean of Graduate Studies, in partial fulfillment of the requirements for the degree of **MASTER OF SCIENCE IN PETROLEUM ENGINEERING.**

Dr. Abdullah S. Sultan
(Advisor)

Dr. Abdullah S. Sultan
Department Chairman

Dr. Sidqi A. Abu-Khamsin
(Member)

Dr. Salam A. Zummo
Dean of Graduate Studies

Dr. Mustapha Abbad
(Member)

22/1/15
Date

Dedication

I dedicate this effort to my parents and my sister.

ACKNOWLEDGMENTS

All praise to the Almighty for his countless blessings bestowed upon me and giving me the strength to complete this work. Without his help nothing is possible. No words of thanks are enough to express my gratitude towards him.

I am proud to have been awarded scholarship by King Fahd University of Petroleum & Minerals throughout my Master's program, for which I am extremely thankful to the University.

I am really grateful to my thesis advisor, Dr. Abdullah Sultan who allowed me the opportunity to work in my area of interest and mentored and guided me throughout the research. His contribution to this work is immense.

I would like to thank my thesis committee members, Dr. Abu-Khamsin and Dr. Mustapha for their valuable input and suggestions throughout my work and I am really honored to have them in my thesis committee.

I would also like to express my thanks to the Center of Petroleum and Minerals at The Research Institute of KFUPM for providing me the funding to conduct my research. In addition, I would like to thank Schlumberger Dhahran Carbonate Research Center (SDCR) for funding this research project under (CPM 2298) and for providing access to conduct experimental work at SDCR. A special acknowledgment to Xiangdong Qiu who helped, facilitated, supported and guided me greatly throughout the research conducted at SDCR. In addition, Nadir Othaibi, also helped me a lot in conducting the Rotating Disk experiments at SDCR.

I would also like to thank Dr. Mohamed Khodja for his continuous help and support in conducting the Micro XCT work for my thesis.

I also thank all my friends at KFUPM especially Zaid Zaffar, who was my support system during this entire time I spent at KFUPM. He is like a brother to me and will always be grateful to him for his unconditional care and immense help during my stay at KFUPM as well as for conducting Micro XCT experiments as a part of my thesis work.

TABLE OF CONTENTS

ACKNOWLEDGMENTS ..... **V**

TABLE OF CONTENTS ..... **VII**

LIST OF TABLES ..... **IX**

LIST OF FIGURES ..... **X**

LIST OF ABBREVIATIONS ..... **XIII**

ABSTRACT (ENGLISH) ..... **XIV**

ABSTRACT (ARABIC) ..... **XVI**

CHAPTER 1 INTRODUCTION **1**

1.1 Rotating Disk Theory **2**

1.2 Mass transfer limited and Surface reaction limited regimes **4**

1.3 Dolomite Dissolution **4**

1.4 Problem Statement and Research Objectives **5**

CHAPTER 2 LITERATURE REVIEW **7**

2.1 Transport and Reaction Kinetics Aspects **7**

2.2 Reaction Kinetics of Limestone Reservoir Rocks **8**

2.3 Reaction Kinetics of Dolomite Reservoir rocks **12**

CHAPTER 3 RESEARCH METHODOLOGY **20**

3.1 Materials **20**

3.2 Equipment **23**

3.3 Methodology **37**

CHAPTER 4 EFFECT OF PRESSURE ON DIFFUSION COEFFICIENT OF FRESH ACID & DOLOMITE 55

4.1 Guelph Dolomite at 1000 psi (15 wt. % HCl) Acid **58**

4.2 Silurian Dolomite at 1000 psi (15 wt. % HCl) Acid **70**

4.3 Silurian Dolomite at 3000 psi (15 wt. % HCl) Acid **82**

4.4 Discussion of Results **91**

CHAPTER 5 EFFECT OF SPENT ACID ON DIFFUSION COEFFICIENT OF DOLOMITE AT HIGH PRESSURE 99

5.1 Silurian Dolomite at 3000 psi (12.5 wt. % Spent HCl) Acid **101**

5.2 Silurian Dolomite at 3000 psi (10 wt. % Spent HCl) Acid **110**

5.3 Silurian Dolomite at 3000 psi (7.5 wt. % Spent HCl) Acid **121**

5.4 Discussion of Results **132**

CHAPTER 6 CONCLUSION & RECOMMENDATIONS 148

APPENDICES 151

APPENDIX A: Summary of Reaction Kinetics Literature Review **151**

APPENDIX B: Detailed Titration Results for Fresh Acid Standardization **151**

APPENDIX C: Detailed Titration Results for Spent Acid Standardization **151**

APPENDIX D: Results for Reaction Kinetics Terms **174**

APPENDIX E: XRD Profile and Molecular Structure of Dolomite **176**

REFERENCES 177

VITAE 172

LIST OF TABLES

Table 2.1 Summary of reaction kinetics literature; HCl and Dolomite rock. 19
Table 3.1 Standard conditions for Calcium and Magnesium..... 36
Table 4.1 Experimental Layout for fresh acid – dolomite…….57
Table 4.2 Experimental conditions for series # 01 – 1000 psi – 15 wt. % acid…….58
Table 4.3 Weight loss values for Guelph dolomite experiments - 1000 psi……..63
Table 4.4 Diffusion Coefficient Analysis calculations, Guelph dolomite – 1000 psi…...66
Table 4.5 Experimental conditions for series # 02 – 1000 psi – 15 wt. % acid…….72
Table 4.6Weight loss values for Silurian dolomite experiments - 1000 psi……..77
Table 4.7 Diffusion Coefficient Analysis calculations, Silurian dolomite – 1000 psi…..80
Table 4.8 Experimental conditions for series # 03 – 3000 psi – 15 wt. % acid…….....86
Table 4.9 Weight loss values for Silurian dolomite experiments - 3000 psi…….....88
Table 4.10 Diffusion Coefficient Analysis calculations, Silurian dolomite – 3000 psi…90
Table 5.1 Experimental Layout for Spent acid – Dolomite……106
Table 5.2 Experimental conditions for series # 01 – 3000 psi – 12.5 wt. % acid……107
Table 5.3 Weight loss values for Silurian dolomite experiments – 12.5 wt. %.....109
Table 5.4 Diffusion Coefficient Analysis calculations, Silurian dolomite – 12.5 wt. %, 3000 psi……...111
Table 5.5 Experimental conditions for series # 02 – 3000 psi – 10 wt. % acid……...116
Table 5.6 Weight loss values for Silurian dolomite experiments – 10 wt. %.....118
Table 5.7 Diffusion Coefficient Analysis calculations, Silurian dolomite – 10 wt. %, 3000 psi……....120
Table 5.8 Experimental conditions for series # 03 – 3000 psi – 7.5 wt. % acid…….….128
Table 5.9 Weight loss values for Silurian dolomite experiments – 7.5 wt. %.....132
Table 5.10 Diffusion Coefficient Analysis calculations, Silurian dolomite – 7.5 wt. %, 3000 psi……..134
Table 5.11 Diffusion Coefficient Calculations, 15 wt. % acid and 17% porosity……...149

LIST OF FIGURES

Figure 3.1 Rotating Disk Apparatus…….....24
Figure 3.2 Titrator…….28
Figure 3.3 Weighing Balance……....28
Figure 3.4 XRD equipment……...29
Figure 3.5 Micro XCT equipment…….....31
Figure 3.6 Atomic Absorption Spectroscopy (AAS)…….33
Figure 3.7 Dolomite disks……..40
Figure 3.8 Experimental Setup of Rotating Disk Apparatus for fresh acid reaction kinetics study……...46
Figure 3.9 Experimental Setup of Rotating Disk Apparatus for spent acid reaction kinetics study……..47
Figure 3.10 Layout of basic flame AAS……....50
Figure 3.11 Schematic plot for determining Diffusion Coefficient……...54
Figure 4.1 Measurement profile of Guelph dolomite XRD……...60
Figure 4.2 Quantitative analysis of Guelph Dolomite XRD……..60
Figure 4.3 Micro XCT image of Guelph dolomite disk before reaction kinetics experiment……62
Figure 4.4 Graph between weight loss vs rpm; Guelph dolomite – 1000 psi……65
Figure 4.5 Diffusion Coefficient Graph (using weight loss results), Guelph dolomite – 1000 psi……68
Figure 4.6 Diffusion Coefficient Graph (using AAS results), Guelph dolomite……...68
Figure 4.7 Micro XCT image of reacted disk at 500 rpm, Guelph dolomite – 1000 psi...70
Figure 4.8 Micro XCT image of reacted disk at 1250 rpm, Guelph dolomite – 1000 psi.71
Figure 4.9 Measurement profile of Silurian dolomite XRD……..…74
Figure 4.10 Quantitative analysis of Silurian Dolomite XRD……...74
Figure 4.11 Micro XCT image of Silurian dolomite disk before reaction kinetics experiment……..76
Figure 4.12 Graph between weight loss vs. rpm; Silurian dolomite, 1000 psi……..79
Figure 4.13 Diffusion Coefficient Graph (using weight loss results), Silurian dolomite, 1000 psi……82

Figure 4.14 Diffusion Coefficient Graph (using AAS results), Silurian dolomite – 1000 psi……...82
Figure 4.15 Micro XCT image of reacted disk at 500 rpm, Silurian – 1000 psi……...84
Figure 4.16 Micro XCT image of reacted disk at 1250 rpm, Silurian – 1000 psi…….85
Figure 4.17 Graph between weight loss vs rpm; Silurian dolomite – 3000 psi…….89
Figure 4.18 Diffusion Coefficient Graph (using weight loss results), Silurian dolomite, 3000 psi……..91
Figure 4.19 Diffusion Coefficient Graph (using AAS results), Silurian dolomite – 3000 psi……...91
Figure 4.20 Micro XCT image of reacted disk at 500 rpm, Silurian – 3000 psi……...93
Figure 4.21 Micro XCT image of reacted disk at 1250 rpm, Silurian – 3000 psi…….94
Figure 4.22 Comparison of computed diffusion coefficients at 1000 psi and 3000 psi....97
Figure 4.23 Comparison of XRD results for Guelph and Silurian dolomite rock …....100
Figure 4.24 Comparison of computed weight loss values at 1000 psi and 3000 psi…...102
Figure 5.1 Graph between weight loss vs rpm; Silurian – 12.5 wt. %, 3000 psi…….110
Figure 5.2 Diffusion Coefficient Graph (using weight loss results), Silurian dolomite, 12.5 wt. %, 3000 psi…….112
Figure 5.3 Diffusion Coefficient Graph (using AAS results), Silurian dolomite, 12.5 wt. %, 3000 psi……..….112
Figure 5.4 Micro XCT image of reacted disk at 500 rpm, Silurian dolomite, 12.5 wt. %, 3000 psi……..114
Figure 5.5 Micro XCT image of reacted disk at 1250 rpm, Silurian dolomite – 12.5 wt. %, 3000 psi…….115
Figure 5.6 Graph between weight loss vs rpm; Silurian – 10 wt. %, 3000 psi……119
Figure 5.7 Diffusion Coefficient Graph (using weight loss results), Silurian dolomite, 10 wt. %, 3000 psi……..122
Figure 5.8 Diffusion Coefficient Graph (using AAS results), Silurian dolomite, 10 wt. %, 3000 psi……...122
Figure 5.9 Micro XCT image of reacted disk at 500 rpm, Silurian dolomite – 10 wt. %, 3000 psi……124

Figure 5.10 Micro XCT image of reacted disk at 1250 rpm, Silurian dolomite, 10 wt. %, 3000 psi……125
Figure 5.11 Micro XCT image of reacted disk at 1250 rpm, Spent 10 wt. % and 10% porosity……127
Figure 5.12 Micro XCT image of Silurian dolomite disk before reaction kinetics experiment – 7.5 wt. %.....130
Figure 5.13 Graph between weight loss vs rpm; Silurian – 7.5 wt. %, 3000 psi…….133
Figure 5.14 Diffusion Coefficient Graph (using weight loss results), Silurian dolomite – 7.5 wt. %, 3000 psi……...136
Figure 5.15 Diffusion Coefficient Graph (using AAS results), Silurian dolomite, 7.5 wt. %, 3000 psi……...136
Figure 5.16 Micro XCT image of reacted disk at 500 rpm, Silurian dolomite, 7.5 wt. %, 3000 psi……...138
Figure 5.17 Micro XCT image of reacted disk at 1250 rpm, Silurian dolomite – 7.5 wt. %, 3000 psi……..139
Figure 5.18 Comparison of weight loss values for 15 wt. % and 12.5 wt. %.....142
Figure 5.19 Comparison of computed diffusion coefficient values for spent acid experiments……..144
Figure 5.20 Comparison of High Resolution Micro XCT Images for spent 12.5, 10 and 7.5 wt. % system……...…145
Figure 5.21 Micro XCT image of top surface of disk – Spent 10 wt. %, 10% porosity..147
Figure 5.22 Micro XCT image of top surface of disk – Spent 10 wt. %, 13% porosity..147
Figure 5.23 Diffusion Coefficient Graph – 15 wt. % acid and 17% porosity……..151
Figure 5.24 Comparison of Reaction regimes for 10% and 17% porosity……..151
Figure 5.25 Comparison of computed diffusion coefficient values for 10% and 17% porosity……152
Figure 5.26 Focused Micro XCT image – 10% porosity and 1000 rpm…….154
Figure 5.27: Focused Micro XCT image – 17% porosity and 1000 rpm……154

LIST OF ABBREVIATIONS

RDA	:	Rotating Disk Apparatus
HCL	:	Hydrochloric
NaCl	:	Sodium Chloride
AAS	:	Atomic Absorption Spectroscopy
VPA	:	Volume Pressure Actuator
XRD	:	X-ray Diffraction
MICRO XCT	:	X-ray Micro computed topography
CO_2	:	Carbon dioxide
KHP	:	Potassium acid phthalate
RPM	:	Rotation per minute
GLDA	:	Glutamic acid diacetic acid
EGLDA	:	Emulsified Glutamic acid diacetic acid

ABSTRACT (ENGLISH)

Full Name : Muhammad Ali Khalid

Thesis Title : Reaction Kinetics of Fresh and Spent acid in Dolomite rock at high pressures

Major Field : Petroleum Engineering

Date of Degree : December, 2014

Carbonate matrix acidizing extends a well's effective drainage radius by dissolving rock and forming wormholes near the wellbore. Wormholing during matrix acidizing of carbonate reservoirs is controlled by the fluid injection rate and acid diffusion coefficient (D_e) which dictates the speed and profile of the wormholes. Injection rate is easily obtained from the job execution whereas the diffusion coefficient is unknown parameter of the fluid and reaction conditions.

Acid diffusion coefficient data used in modelling of wormholing processes are commonly obtained at 1000 psi system pressure, which is too low to represent realistic reservoir conditions. Moreover, the conventional wormhole models use the diffusion coefficient of fresh acid to predict the wormholing process which overestimates the dissolution rate as it is not representative of the wormhole penetration deeper into the formation. In order to properly quantify the acid penetration inside the formation, the diffusion coefficient of acid acquired from high pressure reservoir conditions and representing the level of acid spending at the tip should be employed.

In this research, the effects of diffusion coefficients of HCl acid as it reacts with pure dolomite rock disks were investigated. A rotating disk apparatus was used to obtain the reaction kinetics data at high pressure conditions at various disk rotational speeds (250 –

1250 rpm) at a temperature of 65ºC. Samples of the reacted acid were collected and analyzed using Atomic Absorption Spectroscopy. In addition, the disks were scanned using X-ray micro computed tomography to characterize the 3D image of the disks. The first set of experiments were conducted using 15 wt. % HCl concentration whereas the second set of experiments were conducted at various spent acid concentrations (12.5, 10 & 7.5 wt. %). It was concluded that dissolution rates and diffusion coefficient decreased at high pressure condition since CO_2 was more soluble in aqueous solution and tends to buffer the diffusion of hydrogen ions from the bulk to the rock surface. On the other hand, when the fresh acid was spent to 12.5 wt. %, there was a slight decrease in the diffusion coefficient results because of the slow reaction rate of dolomite. Moreover, HCl/dolomite reaction was mass transfer limited at low disk rotational speeds and reaction limited at high disk rotational speeds. In addition, diffusion coefficient was significantly affected by rock porosity due to variation in surface reaction area which caused increase in dissolution rates as observed by Micro XCT images of the reacted disk.

The new set of kinetics data can be implemented in acidizing job design model which can provide more reliable parameters estimation such as acid injection rate, volume, pumping schedule leading to more accurate production forecast.

ABSTRACT (ARABIC)

ملخص الرسالة

الاسم الكامل: محمد على خالد

عنوان الرسالة: حركية تفاعل الاحماض المركزة والمستهلكة في صخور الدولومايت عند الضغط العالي

التخصص: هندسة البترول

تاريخ الدرجة العلمية: ديسمبر 2014

تقوم عملية تحفيز ابار البترول بتحميض الصخور الكربونية بزيادة مساحة النفاذية وذلك بالتفاعل مع الصخر وتكوين ثقوب ممتدة بالقرب من مدخل البئر. خلال عملية التحميض يتم التحكم في شكل وسرعة تكون الثقوب الحلزونية (wormhole) الممتدة بواسطة معدل الحقن ومعامل انتشار الحمض. من السهل الحصول على معدل الحقن خلال العملية، إلا ان معامل الانتشار يكون عادة مجهول نسبة لنوع السائل وظروف التفاعل.

بناءً على الدراسات السابقة، عادة يتم اخذ معامل الانتشار في عملية تصميم الثقوب الحلزونية عند ضغط 1000 رطل لكل بوصة مربعة والذي يعتبر منخفض مقارنة بالظروف الحقيقية للمكامن. إضافة الى ذلك، فإن نماذج التثقيب الحالية تستخدم معامل انتشار الاحماض المركزة وهو ما يؤدي الى زيادة التوقع في معاملات الانحلال نتيجة لتجاهل امتداد الثقوب داخل الطبقات. و للقيام بقياس امتداد الثقوب بصورة مثلى يجب استخدام معامل انتشار في ظروف مشابهة لظروف استهلاك الحمض وعلى ضغط مماثل لضغط المكمن.

في هذا البحث تمت دراسة معاملات انتشار حمض الهيدروكلوريك عند تفاعله مع صخور الدولومايت. تم استخدام جهاز القرص الدوار للحصول على حركية التفاعل في ظروف ضغط عالية عند سرعات دوران متفاوتة (250 – 1250 دورة في الدقيقة) وذلك عند درجة حرارة تعادل 65 درجة مئوية. تم تحليل عينات من الحمض المستهلك باستخدام جهاز الامتصاص الذري الطيفي. إضافة الى ذلك تم مسح الأقراص باستخدام التصوير المقطعي الدقيق باستخدام الاشعة السينية للحصول على صور ثلاثية الابعاد. تم القيام بالمجموعة الأولى من التجارب باستخدام تركيز ثابت لحمض

الهيدروكلوريك يعادل 15 % من الحجم، اما المجموعة الثانية فقد استخدمت فيها قيم متفاوتة لتراكيز الحمض المستهلك (12.5، 10 و7.5 % من الحجم). من خلال التجارب تبين ان معدلات التحلل ومعامل الانتشار تقل قيمتهما عند درجات الضغط العالية وذلك بسبب تكون غاز ثاني أكسيد الكربون والذي تزيد ذوبانيته ويميل الى حجز انتشار ايون الهيدروجين من المحلول الى الصخر. في المقابل، وجد ان هنالك نقصان طفيف في النتائج عندما تم استهلاك حمض الهيدروكلوريك بنسبة 12.5% من الحجم وذلك بسبب ضغط تفاعل صخر الدولومايت. علاوة على ذلك، يعتبر تفاعل حمض الهيدروكلوريك مع الصخر عملية انتقال مادة محدودة عند السرعات المنخفضة لدوران القرص في حين ان التفاعل يكون محدود عند السرعات العالية للقرص الدوار. إضافة الى ذلك فقد تأثر معامل الانتشار بشكل كبير بمسامية الصخر نسبة لاختلاف مساحة سطح التفاعل وهو ما ادي الى زيادة معدلات التحلل والتي تم ملاحظتها بواسطة التصوير المقطعي الدقيق باستخدام الاشعة السينية.

يمكن استخدام معلومات التفاعل الحركي المتحصل عليها في تصميم عمليات التحميض وهو ما سيساعد على التنبؤ الموثوق بمعاملات التفاعل لمعدل حقن الحمض والحجم وجدولة الضخ، الذي سينعكس على دقة التنبؤ بالإنتاج.

CHAPTER 1

INTRODUCTION

Acidization is concerned with the application of acids and acid mixtures to dissolve porous and non-porous minerals. The main purpose of the process is to remove wellbore formation damage and/or dissolve a portion of the rock and hence enhance permeability in the near wellbore region by the techniques of matrix and fracture acidization (Lund, 1973). The use of different methods for stimulation of oil, gas and water wells has become a common practice in the petroleum industry. It is considered of great importance to optimize the treatment design as well as predict the post treatment performance (Anderson, 1991).

Matrix acidizing is concerned with injection of acid or acid mixtures through wellbore into formation matrix at pressures less than fracture pressure in order to enhance the productivity or injectivity of hydrocarbon. The reservoir rock characteristics are altered as the acid reacts with clays and minerals present. This process is employed where natural boundaries are to be maintained so as to prevent gas or water production or in chalk formations (Adenuga, 2013). On the other hand, fracture acidizing is a hydraulic fracturing treatment for carbonate formations in which acid-etched channels serve as very high conductivity flow paths along the face of the fracture (George, 1986).

1.1 Rotating Disk Theory

Rotating disk apparatus (RDA) is widely used to study diffusion coefficients, dissolution rates, reaction order and activation energy of the reservoir rocks (Taylor *et al.*, 2003). In heterogeneous reaction rate measurements, rates due to chemical reaction processes are differentiated from rates attributed to mass transfer processes. A rotating disk apparatus provides an opportunity to compare rates due to transport processes from rates as a result of chemical processes. Using the theory of mass transfer to rotating disk, it is possible to appraise the amount of diffusional resistance in the rotating disk system (Adenuga, 2013).

For the rotating disk theory to be valid, certain experimental considerations needs to be satisfied. The theory is invalidated as a result of change in the evolution of the gaseous reaction product CO_2 at the solid liquid interface. In addition, the theory of rotating disk will remain valid for a system with finite geometry though it was derived assuming an infinite disk and fluid medium (Lund *et al*., 1973).

In order to investigate the reaction of a fluid with a solid surface using RDA, the following condition must be conformed to (Adenuga, 2013):

i. Flow in the vicinity of the disk must be laminar i.e. the Reynolds number must be in between 10^4 and 10^5.
ii. The disk is assumed to be an infinite plane; hence the disk diameter must be larger than the thickness of the diffusion layer boundary.
iii. The disk is assumed to be spinning in a fluid of infinite volume.

Newman (1965) showed that for Newtonian fluids, the rate of mass transfer, J_{mt}, to the rotating disk instrument in laminar flow regime is given by:

$$J_{mt} = \frac{0.62048\,(S_c)^{-2/3}\,(v\omega)^{1/2}}{1 + 0.2980\,(S_c)^{-1/3} + 0.1451\,(S_c)^{-2/3}} \times (C_b - C_s)$$

Where J_{mt} = rate of mass transfer of HCl to a rotating disk, mole/s. cm^2

v = kinematic viscosity, cm^2/sec

ω = disk rotational speed, rad/sec

C_b = bulk concentration of acid, moles/ cm^3

C_s = surface concentration of acid, moles/ cm^3

S_c = Schmidt number = v / D

D = diffusivity of HCl, cm^2/sec

Lund *et al.* (1973) described the rate of the surface reaction dependence on concentration by the power law model expression that can be represented by:

$$-r_{HCl} = k\,C_s^n$$

Where $-r_{HCl}$ = rate of reaction in moles/s.cm^2

k = reaction rate constant in (moles/cm^2.s) (mole/cm^3)$^{-n}$

n = reaction order, dimensionless

C_s = surface acid concentration in moles/cm^3

1.2 Mass transfer limited and Surface reaction limited regimes

The reaction between acid and the carbonate rock is described in three steps (Lund et al., 1973):

i. The transport of H^+ ions from the solution to the surface of carbonate
ii. The reaction of H^+/carbonate taking place on the surface of carbonate
iii. The transport of the reaction products from the carbonate surface to the bulk solution

The slowest step is considered as the rate determining step during acid-rock reactions. If the slowest step is the diffusion of the reactants or the products to and from the rock surface, then the reaction is mass transfer limited. If the slowest step is the surface reaction itself, then the reaction is considered as surface reaction limited (Taylor, 2009).

In the rotating disk experiment, both of these regimes can occur. At low rotational speeds, the acid dissolution rate increases as the disk rotational speed increases which is considered as the mass transfer limited regime. On the other hand, when the acid dissolution rate is constant at high rotational speeds, then the reaction is considered as surface reaction limited regime. Between the two extremes of diffusion limitation and reaction limitation, there will be a region where the dissolution rate will be a complex function of disk rotational speed.

1.3 Dolomite Dissolution

The reaction of HCl with dolomite is given as follows:

$$4HCl + CaMg(CO_3)_2 \rightarrow CaCl_2 + MgCl_2 + 2H_2O + 2CO_2$$

In this reaction, 4 moles of HCl react with 1 mole of dolomite to form calcium and magnesium chloride, CO_2 and water. The HCl-dolomite reaction is considered as heterogeneous reaction because it occurs between a liquid and a solid.

1.4 Problem Statement and Research Objectives

Current understanding of wormholing process during carbonate matrix acidizing needs to be revisited for better description because of two major reasons:

i. The impact of pressure on diffusion coefficients and reaction rate
ii. The lack of reaction kinetics data of spent acids.

1.4.1 Impact of pressure on diffusion coefficient and reaction rate

Pressure has significant impacts on the diffusion coefficient and the reaction rate. Conventional wormhole models use diffusion coefficient obtained from the system pressure of 1000 psi to predict the wormholing process. It is claimed that 1000 psi is sufficient to keep the evolved CO_2 in solution. However, using the reaction kinetics data obtained from 1000 psi may overestimate the dissolution rate. Recent studies indicate that the pressure value of 1000 psi is not sufficient to keep the CO_2 in solution and does not represent true reservoir conditions. The reaction rate estimated at higher pressures is less as compared to the reaction rate estimated at 1000 psi condition. Moreover, using data from core flow experiments conducted at 1000 psi in a wormhole design model may lead to an underestimation of wormhole penetration at pressures above 1000 psi (Qiu, 2014).

1.4.2 Lack of kinetics data of spent acids

The second drawback in modelling wormholing phenomena is the lack of reaction kinetics of spent acids with dolomite rock. As wormhole penetrates into the reservoir, the acid concentration at the fine tips could be significantly lower than that of the fresh acid, especially in low permeability rocks. The tip of the wormhole could be saturated with reaction products (Calcium & Magnesium ions) which hinder further reaction by limiting mass transfer of hydrogen ions to the rock surface. The capacity of acid to extend wormhole is significantly reduced. The dissolution kinetics at the tip of the wormhole is dictated by the reaction kinetics parameters of spent acid.

The conventional wormhole models use the diffusion coefficient of fresh acid to predict the worm holing process which is not representative as the wormhole penetrates deeper into the formation. Using fresh acid reaction kinetics data can thereby overestimate the dissolution rate. In order to properly quantify the acid penetration deep into the formation, a diffusion coefficient representing the level of acid spending at the tip should be employed (Qiu, 2013).

Owing to the above two shortcomings in current understandings, the main objective of the thesis were as follows:

i. Study the reaction kinetics of HCl with Dolomite at high pressure using fresh acid (15 wt. % HCl).
ii. Study the reaction kinetics of HCl with Dolomite at high pressure using various spent acid concentrations (12.5, 10 and 7.5 wt. %).

CHAPTER 2

LITERATURE REVIEW

2.1 Transport and Reaction Kinetics Aspects

Fredd & Fogler (1999) studied the effects of transport and reaction on the phenomenon of wormhole formation for a wide range of fluid systems including strong acids, weak acids and chelating agents. These fluid systems are influenced by a variety of transport and reaction processes such as the transport of reactants to the surface, the reversible surface reactions and the transport of products away from the surface. When these transport and reaction processes are taken into account, a common dependence of the dissolution phenomenon on the Damkohler number is observed. There exists an optimum Damkohler number at which a minimum number of pore volumes are required for channel breakthrough and form wormholes. Moreover, an optimum kinetic parameter exists at which wormhole formation is most efficient. Together, the Damkohler number and the kinetic parameter provide a complete description of the dissolution phenomenon.

Experiments were conducted at pressure ranges of 1000-2200 psi and temperatures of about 50°C and 70°C. The degree of transport/reaction limitations was quantified by a kinetic parameter Γ. The dimensionless kinetic parameter is defined as the ratio of the surface reaction rate constant to the overall dissolution rate constant.

It was found that the number of pore volumes to breakthrough and the wormhole structures were found to be influenced by the degree of transport/reaction limitations. These limitations were quantified by the dimensionless kinetic parameter.

2.2 Reaction Kinetics of Limestone Reservoir Rocks

2.2.1 Reaction Kinetics of HCl with Calcite

It is generally assumed that the reaction of HCl acid with limestone reservoir rock is much more rapid than acid reaction with dolomite reservoir rock. According to (Lund, 1975), calcite marble reacts with 1M HCl approximately 650 times faster than dolomite marble at 25°C. The dissolution of pure calcite marble in hydrochloric acid using a rotating disk system was studied. Experiments were carried out under 800 psig varying acid concentrations between 0.1 to 9 N HCl at temperatures of -15.6, 1 and 25°C. The disk rotation speed lie in the range of 100-500 rpm. It was concluded that at 25°C, the reaction is mass transport limited even at high rotational speeds (500 rpm). On the other hand, both mass transfer and reaction limited regimes were found to limit the dissolution rate of calcite at -15.6°C.

Taylor *et al.* (2004) were the first to show this assumption to be false in some cases depending on the mineral impurities found in limestone rocks. Trace amounts of clay impurities in limestone rocks reduce the acid dissolution rate making it similar to a fully dolomitized rock. They studied the effect of acid additives on the calcite dissolution rate and the results showed that polymer had a significant effect on calcite dissolution rate. It changed the reaction from mass transfer limited to surface reaction limited due to polymer adsorption at the rock surface. Iron (III) reduced the reaction rate of calcite at low rotational

speeds due to the formation of iron hydroxide precipitate which was not evident at high rotational speeds. Citric acid also reduced the dissolution rate of calcite especially at high rotational speeds due to the formation of calcium citrate on calcite surface. The quaternary amine corrosion inhibitor also decreased the dissolution rate of calcite. Nonionic surfactant had no significant effect on acid dissolution rate of calcite. On the other hand, mutual solvent increased the acid dissolution rate for calcite by 9%.

2.2.1.1 Effect of Reaction Products and Spent HCl Acid on Diffusion Coefficient

Conventional wormhole propagation models neglect the effect of reaction products on reaction kinetics which resulted in significant errors in stimulation field treatment. (Qiu, 2013) studied the impact of reaction products on reaction kinetics and described the laboratory procedures to obtain it. Rotating disk apparatus was used to compare the dissolution rate of a partially spent system- 15% HCl spent to 10% HCl- to a 10% fresh HCl solution using limestone core samples by varying disk rotational speeds. It was found that the reaction rate for the partially spent system is lower as compared to fresh acid system. Moreover, diffusion coefficient of a spent acid system is significantly lower than the fresh acid system (30% less). The experiment also concluded that the reaction products (CO_2 and counter ions) buffered the diffusion of H^+ ions in the spent acid mixture, decreasing the mass transfer coefficient which resulted in slower dissolution rates.

Qiu *et al.* (2014) studied the effects of diffusion coefficients of HCl acid as it reacts with calcite using a rotating disk apparatus. Moreover, they also investigated the impact of pressure (1000 and 3000 psi) on the diffusion coefficient and the reaction rate. It was found that the diffusion coefficient of HCl acid is low at high pressure as compared to low pressure. At low pressure, CO_2 is present in gaseous phase increasing the movement of

hydrogen ions from the acid solution to the surface of rock. Thus, the mass transfer coefficient is significantly increased. However, at high pressure, CO_2 tends to stay in aqueous phase which slows down the reaction of HCl and the calcite rock samples.

2.2.2 Reaction Kinetics of Organic Acid with Calcite

Al-Douri *et al.* (2013) formulated a new organic acid (phosphorus based and iron based) to stimulate deep wells in carbonate reservoirs. Reaction kinetics of the new organic acid was studied using rotating disk apparatus with calcite samples at 150, 200 and 250°F by varying disk rotational speeds (100-1500 rpm).

Firstly, reaction-rate experiments were conducted using the phosphorus based acid. It was found that the calcium concentration increased with the disk rotational speed at low temperatures. However, at high temperatures, the calcium concentration increased linearly for a certain period of time and then plateaued for the remainder of the reaction. The calcium concentration reached a maximum value of 2500 mg/l at 150°F and at 250°F whereas 4500 mg/l at 200°F. It was noted that the calcium concentration decreased when the temperature escalated from 200°F to 250°F due to the formation of phosphorus precipitate (calcium phosphate) on the core face.

Moreover, it was found that at low temperatures (150°F), the reaction was controlled by surface reaction kinetics at disk rotational speeds higher than 500 rpm. However, at high temperatures, the reaction was controlled by mass transfer reaction kinetics.

In order to cure the problems associated with precipitation, the organic acid was modified and an iron based catalyst was added to perform the reaction rate experiments at fixed rotational speed (1000 rpm) and temperatures of 200°F and 250°F. It was concluded that

the reaction rate of the iron based acid at 200°F and 250°F was less as compared to phosphorus based acid.

2.2.3 Reaction Kinetics of Chelating Agent with Calcite

Rabie *et al.* (2011) studied the rate of reaction of chelating agent (GLDA). The effect of pH (1.7, 3.8 & 28) and disk rotational speed (100-1800 rpm) was investigated at 150, 220 and 300°F. The reaction of calcite and GLDA was mass transfer limited up to 1800 rpm. It was found that the calcite dissolution is a strong function of temperature and increased significantly by increasing the temperature. The rate of dissolution at pH 3.8, 1000 rpm and 80°F increased six times when the temperature was increased to 200°F. On the other hand, calcite dissolution rate was decreased due to the increase in the pH conditions. The reaction at pH 3.8 and 13 were less dependent on disk rotational speed which showed that the reaction was surface limited at these pH values.

2.2.4 Reaction Kinetics of Emulsified Chelating Agent with Calcite

Sayed *et al.* (2013) studied the reaction kinetics of an emulsified chelating agent (EGLDA) and limestone rock at a temperature of 230°F covering a disk rotational speed range from 100 to 1500 rpm. Moreover, the reaction rate of calcite in EGLDA was measured at temperatures of 250 & 300°F at 1000 rpm and these data were compared to the work done by (Ahmed Rabie, 2011). It was concluded that emulsified GLDA achieved dissolution rates and diffusion coefficient that are less by two orders of magnitude as compared with emulsified acid at the same conditions.

2.3 Reaction Kinetics of Dolomite Reservoir rocks

2.3.1 Reaction Kinetics of HCl with Dolomite

Lund *et al.* (1973) studied the dissolution of pure dolomite marble in hydrochloric acid with the aid of rotating disk system. Measurements were conducted at a pressure of 600 psig with varying acid concentrations between 0.01 N HCl and 9 N HCl at temperatures of 25, 50 and 100°C rotating the disk speed from 50 to 500 rpm. It was found that the dissolution of dolomite was reaction limited at low temperatures (25 and 50°C) even at low rotational speeds which was in contrast with the dissolution rate of calcite and HCl. However, the dissolution rate was diffusion limited at high temperatures at relatively high rotational speeds. Moreover, reaction order of HCl concentration at the dolomite surface was found to be temperature dependent.

Anderson (1991) measured the reactivity of five San Andres dolomite samples and a 'reference' quarried rock; Kasota dolomite; using rotating disk system. Measurements were conducted at 1000 psi at a disk rotational speed of 120 rev/min using five different HCl acid strengths (1-5 N) with varying temperature conditions (80-180°F). The reaction constant (K) and reaction order (n) were calculated and compared with Lund et al. work (Kaiser Dolomite). It was found that for acid concentrations above 1 N, Kasota dolomite dissolution rate was independent of disk rotational speed. Reaction order (average value = 0.366) did not increase with temperature which was in contrast with Lund's work showing less temperature dependence. Moreover, reaction constant show less temperature dependence for Kasota dolomite as compared to Kaiser Dolomite. The values of activation energy for Kasota and Kaiser Dolomites were 7.37 and 22.5 kcal/gmol respectively. The

variation in reactivity data was also observed when dolomite samples of San Andres formation were tested. The values for activation energy ranged from 3.38 to 5.27 kcal/gmol, significantly less than the industry-accepted value for dolomite which is 22.5 kcal/gmol. In addition, the value for n varied from 0.131 to 0.392 showing no temperature dependence. It was concluded form the above study that different dolomite samples demonstrate different surface kinetics and reactivity data. Moreover, data generated from actual formation cores (San Andres dolomite) was considered more representative than data generated from quarried rock samples (Kasota & Kaiser).

2.3.1.1 Effect of rock mineralogy on reactivity

Acid reaction rates and reaction rate coefficient of a rock from deep dolomitic gas reservoir was studied (Taylor *et al.*, 2004). Measurements were conducted from room temperature to 85°C at rotational speeds from 100 to 1000 rpm and acid concentrations of 0.2 to 17 wt. % using rock samples that range from pure calcite to pure dolomite. Reactivity of the rock varied from values expected for pure calcite marble to those expected for pure dolomite marble as the reaction rates depended on rock mineralogy and presence of clays. Samples of calcite (containing less than 5 wt. % dolomite) with clay and without clay reacted in a different manner. Coating of clay material on the surface of rock after reaction had an inhibiting effect on acid reaction. Similar results were obtained with dolomite marbles with clay i.e. reduction of the acid reaction rate with rock. In addition, additional experiments were performed with rocks that were high in dolomite content at 23, 50 and 85°C. It was found that at higher temperatures, reaction rate was rapid and resulted in nonlinear effects. The slope of the curve was increased which cause an increase in the dissolution rate

because rapid reaction of the rock produces a rough texture that increased the surface area of the rock.

The dissolution rates of reservoir rock from a deep dolomitic gas reservoir in Saudi Arabia (275°F, 7500 psi) at temperatures of 23 and 85°C with 1 M HCl concentration at a disk rotational speed of 800 rpm was studied (Taylor et al., 2006). The main objective of the work was to study the impact of mineralogy on reservoir rock reactivity. Eight distinct rock types that varied in composition from 0 to 100% dolomite were used in the study. It was found that trace amounts of clay impurities in limestone reservoir rocks reduce the acid dissolution rate by a factor of 25 which makes the acid reactivity of these rocks similar to that of a fully dolomitized rock. Formation of a stable clay layer at the reacting surface of the rock act as a physical barrier to acid reaction. Clays such as illite and mixed layer illite/smectite reduce the dissolution rates significantly. Rock samples containing 99% dolomite were more reactive due to the less amount of clay deposition on the surface of dolomite crystals. Moreover, it was also found that rock samples containing anhydrite interact with HCl solution created fine anhydrite needles that cause formation damage in tight carbonate reservoirs. In addition, the dissolution of anhydrite affected the calculation of dissolution rates leading to reduction in acid reaction by 16%. On the other hand, preferential dissolution of calcite cause mechanical loss of dolomite crystals resulted in high dissolution rates as compared to homogeneous rock of similar calcite and dolomite content.

2.3.1.2 Effect of Additives on dissolution rate

Taylor *et al.* (2004) evaluated the effect of a large number of additives on acid dissolution rates of calcite and dolomite rock samples over a wide range of rotational speeds at 23 &

50°C. The additives include polymer, corrosion inhibitor, surfactant, mutual solvent, citric acid and dissolved iron (III). It was found that the dissolution rate of calcite in 1 M HCl at room temperature was mass transfer limited. However, the dissolution rate of dolomite was surface reaction limited.

It was found that polymer decreased the dissolution rate of dolomite marble significantly at high rotational speeds because of polymer adsorption at the rock surface. At low rotational speeds, the reduction was less pronounced as compared to calcite dissolution rate. However, mutual solvent increased the dissolution rate of dolomite by 29%. The reaction of iron (III) and dolomite resulted in surface deposition of iron hydroxide at rotational speeds less than 200 rpm which had an inhibiting effect on the dissolution rate at low rotational speeds.

2.3.1.3 Effect of sequential vs. single measurements on reaction rate

Taylor *et al.* (2009) examined different ways that acid reaction rates are measured with rotating disk apparatus and the factors that affect the results. It was found that sequential measurements would give high error in calculation of reaction rate after nearly 500 seconds from the initial acid-rock contact as compared to single measurements because the data in the first 500 seconds is linear and can be used to estimate the dissolution rate. But as the reaction proceeds, the dissolution rate increases because the surface area of the rock surface increases resulting to error in measurements.

2.3.1.4 Effect of rock porosity on dissolution rate

Rock porosity also have a significant effect on measurements. The acid dissolution rate increases as the porosity of the rock increases because it depends on the surface area of the

rock disk. A low porosity rock minimizes this effect. Rock composition should be adequately verified as it affects the determination of dissolution rate of the rock by the acid (Taylor *et al*., 2009).

2.3.2 Reaction Kinetics of Organic Acid with Dolomite

Adenuga *et al.* (2013) studied reaction kinetics of dolomite with 0.866N organic acids (acetic and formic acid) as well as Chelating Agents (GLDA) by varying the disk rotational speeds from 100 – 1500 rpm at 250°F. It was noted that as the disk rotational speed increased, magnesium concentration increased for all the acids. The dissolution rate was also determined using the plot of concentrations vs. reaction time and it was found that the reaction rate of GLDA solution was comparatively lower when compared to organic acids. It was also established that rate of dissolution of dolomite in GLDA was surface reaction limited at lower rotational speed values. However, at higher rotational speed, the reaction was mass transfer limited.

Acetic acid showed variations as the rotational speed increased throughout the range. However, for formic acid, the reaction was mass transfer controlled until 1000 rpm. Diffusion coefficients were determined for organic acids and GLDA by plotting dissolution rate vs. square root of disk rotational speeds. The diffusion coefficient of GLDA was less as compared to organic acids.

It was concluded that GLDA was more retarder than formic and acetic acid. Moreover, it is better suited for stimulation into a dolomitic reservoir than organic acids because their reaction rate was fast at high temperatures leading to inadequate acid penetration and wormhole creation into the formation.

2.3.3 Reaction Kinetics of Emulsified Acid with Dolomite

The reaction kinetics of a new emulsified acid (0.5, 1.0 and 2.0 vol% emulsifier concentrations) was studied with dolomite core plugs using a rotating disk apparatus at a temperature of 230 °F by varying disk rotational speeds from 100 – 1500 rev/min (Sayed *et al*., 2012). The main objective of the study was to optimize the design of carbonate acidizing treatments using emulsified acid.

Weight loss measurements were conducted and it was noted that that the weight loss percentage increased as the disk rotational speed increased and decreased with increasing the emulsifier concentration which affirms that the overall reaction rate of emulsified acid decreased by increasing the emulsifier concentration. It was also noted that the amount of calcium and magnesium concentrations decreased as the emulsifier concentration increased. However, the concentrations increased as the rotational disk speed increased.

For low emulsifier concentration (0.5 vol %), the rate of dissolution increased proportionally with the rotational speed indicating a mass transfer limited reaction. Whereas the emulsified acid-dolomite reaction was determined as surface controlled at higher emulsifier concentrations.

It was also established that as the emulsifier concentration increased, the diffusion coefficients decreased leading to reduction in reaction rates confirmed by the weight loss measurement results.

2.3.4 Reaction Kinetics of Dolomite in aqueous solutions

The effect of pH on the dissolution kinetics of HCl with dolomite was studied by (Busenberg and Plummer, 1982). They measured the dissolution rate of dolomite over a

range of pH (0 to 10), carbon dioxide pressure (0-1 atm) and temperature (1.5 – 65 ˚C). It was found that the dissolution rate was dependent on pH (pH < 6 and constant at pH > 8). Moreover, the dissolution rate was dependent on the carbon dioxide pressure over the entire range of pH.

Herman and White (1985) studied the dissolution kinetics of three stoichiometric dolomite specimens (hydrothermal single crystal, microcrystalline sedimentary rock and coarse grained marble) in aqueous carbonate solutions. The dissolution experiments were conducted initially at under saturated condition set by CO_2 at 1 atm. The reaction was followed by measuring concentrations of calcium, magnesium and bicarbonate and pH over time at 0, 15 and 25 °C. It was found that dissolution rates of pure forms of dolomite were not significantly affected by mineralogy. The dissolution rate values increased by decreasing the grain size of the sample. Moreover, the observed initial rates were dependent upon disk spinning speed. However, the spinning speed became a less important factor as the saturation state of the solutions increased and as temperature decreased.

Dissolution rates of calcite, dolomite and magnesite were measured at 25 °C and pH from 3 to 4 as a function of salinity (0.001 M ≤ NaCl ≤ 1 M) and partial pressure of CO_2 (10-3.5 ≤ pCO_2 ≤ 55 atm) by (Pokrovsky *et al*.,2005). It was found that the effect of pCO_2 was insignificant as compared to that of pH. Dolomite dissolution rate increases with increasing pCO_2 at 1≤ pCO_2 ≤ 10 atm and stays constant when pCO_2 is further increased to 50 atm. These rates depend on the stirring velocity and increases by a factor of 2-3 from 200-2500 rpm reflecting moderate transport contribution to dissolution. Moreover, dolomite dissolution rates were independent of ionic strength between 0.1 and 1 M NaCl and 5 to 50 atm pCO_2.

Table 2.1: Summary of reaction kinetics literature; HCl and Dolomite rock.

Paper Ref No	Year	Main Author	Rock Sample	Temperature	Pressure	Concentration of HCl	Rotational Speed (rpm)	Brief Summary of the paper
SPE 4348	1973	Lund, Fogler, McCune & Ault	Dolomite	25, 50 & 100 ˚C	1000	0.01 N - 9 N (0.0365 - 33 wt%)	50 - 500	No study was done related to diffusion coefficient measurements. Dissolution of HCl with dolomite was studied.
Chemical Engineering Science, Vol 28, pp. 691-700	1973	Lund, Fogler and McCune	Dolomite	25, 50 & 100 ˚C	1000	0.01 N - 9 N (0.0365 - 33 wt%)	50-500	No study was done related to diffusion coefficient measurements. Dissolution of HCl with dolomite was studied.
SPE-20115-PA	1991	Anderson	Dolomite	93 ˚C	1000	1 - 5 N (3.6 - 18.3 wt %)	120	No study was done related to diffusion coefficient measurements. Reactivity data of San Andreas dolomite was presented to be used in fracture-acidizing simulators to allow more accurate simulation.
PETSOC-2003-068	2003	Taylor, Ghamdi & Nasr El Din	Dolomite	85 ˚C	-	0.2 - 17 wt%	100 - 1000	Diffusion Coefficient, dissolution rates, raection rates, reaction order and activation energy were calculated for a deep dolomitic gas reservoir in Saudi Arabia.
SPE-80256-PA	2004	Taylor, Ghamdi & Nasr El Din	Dolomite	23 & 50 ˚C	1000	1 M (3.6 wt%)	100, 200, 400, 800 & 1000	Diffusion Coefficient measurements were not done. Effect of additives on the dissolution rate of dolomite in HCl was studied.
SPE-89417-PA	2006	Taylor, Nasr El Din, Mehta	Dolomite	23 & 85 ˚C	1000	1 M (3.6 wt%)	800	No study was done related to diffusion coefficient measurements. Dissolution rate from a deep dolomitic gas reservoir (8 samples) in Saudi Arabia were calculated to investigate the effect of mineralogy on reservoir rock reactivity.
PETSOC-09-06-66-P	2009	Taylor & Nasr El Din	The paper discuss the acid reaction rate of calcite and dolomite with Rotating Disk Apparatus published by authors in recent years. The effects of single vs. sequential measurements, rock porosity, rock composition (sulpahte), rock mineralogy and additives were discussed.					

CHAPTER 3

RESEARCH METHODOLOGY

For our research, an experimental Rotating Disk Apparatus (RDA) was used to study the kinetics of fresh and spent acid with dolomite rock. The apparatus consists of an ISCO pump, a thermally controlled accumulator, a reaction vessel with a magnetic drive assembly, associated pressure regulators, valves, temperature and pressure displays and controllers. A data acquisition system was used to monitor the temperature and pressure inside of the reaction vessel. The RDA was modified to handle high pressure reaction kinetics. In order to achieve high back pressures, a gas booster was used. A brief description of all the materials and the equipment as well as the detailed procedure followed in the experiments is described below.

3.1 Materials

3.1.1 Core Sample

Silurian Dolomite and Guelph Dolomite cores of 12” length and 1.5” diameter were used in the experiments. The core samples were procured from Kocurek Industries (USA). The porosity of the cores lies in the range of 10% – 19%. The supplier specified brine permeability was in the range of 45-100 md and gas permeability was in the range of 100-170 md. In addition, the core samples contain 98% dolomite with minute traces of silica.

3.1.2 Acid (HCl)

Concentrated hydrochloric acid (ACS reagent grade, 37 wt. %) was used to prepare 15 wt. % HCl acid which was eventually used to conduct the reaction kinetics experiments.

3.1.3 Chemicals

Chemicals such as sodium hydroxide (NaOH) and potassium acid phthalate (KHP; $HKC_8H_4O_4$) were required to conduct standardization of acid and base solutions. Sodium hydroxide powder was required to prepare 0.1 M NaOH and to standardize HCl. However, potassium acid phthalate was required to standardize NaOH. An organic compound, Phenolphthalein, was required to indicate the end point of titration process. Moreover, Nitric acid (HNO_3) was also used to prepare calibration standards needed for AAS calibration.

3.1.4 Distilled Water

Second grade distilled water was used to prepare 15 wt. % acid, standardization purposes as well as preparing standards for AAS. In addition, it was also used to clean the entire RDA system before and after experiment in order to avoid corrosion and rusting of the lines and other equipment parts due to interaction with HCl acid. First grade distilled water was required to prepare dilution samples which were used to measure calcium and magnesium concentration using AAS.

3.1.5 Dolomite Powder

Dolomite cores were crushed to powder form using the crushing machine. The dolomite powder was used to conduct spent acid experiments in RDA system.

3.1.6 Gas Cylinders

Industrial grade nitrogen (N_2) gas was obtained in sufficient quantity in the form of gas cylinders. Nitrogen gas was used to pressurize the reaction vessel in order to keep CO_2 in solution during the RDA experiment. In addition, acetylene and nitrous oxide gas cylinders were also required to measure calcium and magnesium concentrations using AAS.

3.1.7 Teflon tubing

The circumference of the dolomite disks used in conducting the RDA experiments were covered using shrink wrap teflon tubing that allows only the lower face of the disk to be exposed to HCl acid.

3.2 Equipment

3.2.1 Rotating disk experimental setup

The principal instrument used in the reaction kinetic experiments was the rotating disk apparatus. The rotating disk apparatus used in this work was manufactured by Autoclave Engineers as shown in Figure 3.1. The predominant components of the apparatus includes reaction vessel, accumulators, ISCO pump, gas booster system, associated pressure regulators, flow lines and valves, temperature and pressure displays and data acquisition system. All acid wetted surfaces such as the reaction vessel, acid reservoir i.e. accumulators and liquid flow lines were fabricated from Hastelloy which is an acid resistant alloy. All other parts of the apparatus were fabricated from stainless steel.

A brief description of the main components of the system is given below.

- *Reaction Vessel* was the main component of the RDA system equipped with magnetic drive assembly where the reaction between dolomite disk and HCl acid takes place. It was designed for high temperature and high pressure use. The maximum capacity (volume) of the vessel was 1000 ml. The ID of the vessel was 3". The dolomite disks were attached to the rotating shaft; the disk is submerged in the acid solution (reactant solution) which is transferred to the disk surface by convection and molecular diffusion. A one inch gap is maintained between the surface of the fluid and the top of the reaction vessel and a pressure of 1000/3000 psi is maintained above the fluid to keep the gaseous by-products (carbon dioxide) in solution. Ethylene-propylene O-ring provide a seal between the end plates and reactor wall. Magnetic coupling through the reactor wall was chosen to connect the

Figure 3.1: Rotating Disk Apparatus

rotating sample holder and rotor to the shaft from the electric drive motor. Vessel cooling coil permit introduction of cooling to the vessel contents for rapid heat transfer in the case of thermal overshoot or removal of exothermic reaction energies. Liquid sampling line, acid injection line and thermowell were also welded on the wall of the vessel. A thermocouple was located in the thermowell of the reactor vessel used to read the temperature signal inside of the reaction vessel. In addition, to provide safety to the RDA system, back pressure regulator was employed to apply and control the back pressure. Moreover, rupture discs that have a +6/-3% manufacturing tolerance and a $\pm$ 5% burst tolerance were also installed in the safety head assembly. The rupture disc burst pressure should never exceed the design pressure of the vessel system. To avoid premature failure of the rupture disc from fatigue, the system operating pressure should ideally be only 70% of the disc burst pressure.

- *Thermally controlled accumulators* were used as a liquid reservoir mounted vertically having a maximum volume of 700 ml. A thermocouple attached to the side of the liquid reservoir supplies the temperature signal to the controller. For spent acid reaction kinetic experiments, two accumulators were used. One accumulator was used as a liquid (acid) reservoir whereas the second accumulator was used to place the dolomite rock powder.
- *ISCO pump* or the dual cylinder Volume-Pressure Actuator (VPA Series 32) provided by DCI Corporation was required to pump the acid from the accumulator to the reaction vessel. In addition, it was also used to pump acid from first accumulator to second accumulator for spent acid reaction kinetic studies. It

consists of five separate elements; two single cylinder VPA pumps, a valve manifold to switch flow between the two pumps, an operator interface terminal and pump control electronics. The operator interface terminal is a panel-mount controller with a touch screen color display. The pump can be controlled in either a flow-control mode or in a pressure-control mode.

- *Flow lines* were required to connect the liquid reservoir and the reaction vessel and the pump to the liquid reservoirs. Moreover, flow line was also needed to connect the two accumulators for spent acid reaction kinetic studies.
- *Data acquisition system* or Universal Reactor Controller (URC series of Autoclave Engineers) incorporates all the features necessary to safely and accurately monitor or control the reactor's temperature, pressure and mixer speed.
- *Gas booster* was used to handle high back pressure (3000 psi) during reaction kinetic experiments.

3.2.2 Titrator

In order to perform standardization of acid and base solutions, 15 wt. % HCl acid and the reacted acids after the experiment, titration was performed using the Titrator that includes burette and NaOH reservoir (container). In addition, two volumetric flasks (50ml and 250 ml), pipette syringe, three glass beakers and three magnetic stirrers were required to perform the titration process. Stirring machine was also required to stir the solution inside the beakers by setting the rotational speed around 200 rpm. The Titrator is shown in Figure 3.2.

3.2.3 Analytical Weight Balance

A high accuracy analytical weight balance (Scientech, SA210D) was used to measure the weight of the disks before and after the experiment, measurement of dolomite powder as well as different chemicals used for titration purpose. The weight balance is shown in Figure 3.3.

3.2.4 XRD (X-ray Diffraction)

The atomic planes of a crystal cause an incident beam of X-rays to interfere with one another as they leave the crystal. The phenomena is called X-ray Diffraction (XRD).

X-ray powder diffraction (XRD) is a rapid analytical technique primarily used for phase identification of a crystalline material, minerals and can provide information on unit cell dimensions. Identification is achieved by comparing the X-ray diffraction pattern. In our work, XRD equipment (Miniflex II) produced by "Rigaku Japan" was used to determine the purity of dolomite rock samples which were eventually used to prepare dolomite disks used for reaction kinetic studies (Figure 3.4). The basic elements of the XRD machine includes the following:

- *Monochromatic X-ray tube* which is the source of x-rays
- *Sample holder*
- *Goniometer* is the platform that holds and moves the sample, tube or detector
- *Data collector/detector* counts the number of x-rays scattered by the sample

Figure 3.2: Titrator

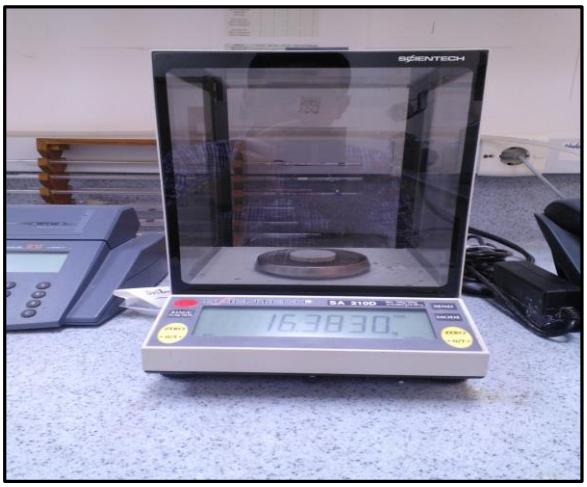

Figure 3.3: Weighing Balance

Figure 3.4: XRD equipment

3.2.5 X-ray micro computed tomography (micro XCT)

Micro XCT (Versa XRM-500, XRadia product) was used for the 3D visualization, characterization and analysis of multiphase systems at the micron level of voxel resolution. Figure 3.5 shows the Micro XCT machine. In our work, the equipment was employed to scan the dolomite disk before and after the reaction kinetic experiments.

The external features of the equipment includes the following:

- *X-ray chamber* which is made of solid lead to protect from any radiation leakage
- *Terminal panel* where the operator can monitor and manipulate samples through a surveillance camera and screen
- *Main frame* for data acquisition
- *Power Adapter*

The internal features of the Micro XCT system includes the following:

- *X-ray source* to generate x-rays
- *Sample stage* to penetrate the sample/disk on the stage with x-rays passing through the filter
- *Detector* to measure the intensity of the transmitted radiation
- *Granite rock foundation* to avoid any tilt, motion or vibration during the scan

Figure 3.5: Micro XCT equipment

The sample stage was able to rotate through a full 360º and raise or lower the sample in a certain range. The source and the detector can also be moved forward or backward to adjust the distance or the axial position to obtain a better field of view and x-ray intensity. Source, sample stage and detector movement can be done using the operating software for this Micro XCT system. The spatial relationship of each unit can be adjusted at the micron level. Sample status and movement can be observed through the surveillance camera displayed on the terminal monitor.

A consecutive scan with a short exposure time can also help catch the sample position with the software. This automated system keeps the user safe and allows for higher resolution of images. In addition, working distances between source, sample and detector are typically around 100 mm, so that full tomography even for larger samples can be achieved. Moreover, multiphase particles having a size on the order of 10 microns can be imaged in 3D due to sub-micron resolution of the x-ray detector.

3.2.6 Atomic Absorption Spectrometer (AAS)

The calcium and magnesium concentrations from the reacted samples were measured using the Atomic Absorption Spectrometer provided by Thermo Scientific (Model: ICE 3000 Series). It is used for the quantitative determination of chemical elements using the absorption of optical radiation by free atoms in the gaseous state. AAS used is shown in Figure 3.6.

Figure 3.6: Atomic Absorption Spectroscopy (AAS)

The basic components of an atomic absorption instrument includes the following:

- *Light Source* that emits the spectrum of the element of interest. The hollow cathode lamp is the only type of light source widely used in AAS. Its main feature is the narrow absorbing spectral line. The lamp may be expected to run in excess of 5000mA hours without failure. It is also known as a fine line source capable of producing spectra where fine structure can be studied. The cathode is a hollowed-out cylinder constructed entirely or in part of the metal whose spectrum is to be produced. The anode and cathode are sealed in a glass cylinder filled with neon or argon. The glass cylinder has a quartz or UV glass window for optimum transmittance of the emitted radiation. The optimum fill gas is selected that gives the best lamp intensity while taking into consideration spectral interferences from either neon or argon. A red glow is observed in lamps filled with neon, while argon filled lamps have a blue glow. Hollow cathode lamps are available for more than 60 elements.
- *Atomizer/Flame* is an absorption cell in which the atoms of the sample are produced. A combustion flame provides the most convenient, stable and economic source of atomic vapors. For the production of free atoms, flame temperature is very important. A range of temperatures from 2000 to 3000K can be produced from fuel and oxidant mixtures. Propane, hydrogen and acetylene can be used as fuel gases and sir or nitrous oxide as the oxidant. The two oxidant/fuel combinations used almost exclusively in atomic absorption today are air-acetylene and nitrous oxide-acetylene. Air/acetylene flames are used for elements which do not form highly refractory oxides such as calcium, chromium, cobalt, iron, magnesium,

molybdenum, nickel, strontium and the noble metals. It is extensively used as it enables the determination of 30 common elements. The temperature of the air-acetylene flame is about 2300 °C. On the other hand, the nitrous oxide-acetylene flame has a maximum temperature of about 2900 °C and is used for the determination of elements which form refractory oxides. It is also used to overcome chemical interferences that may be present in flames of lower temperature.

- *Monochromator* is used for light dispersion. The function of the monochromator is to isolate light emitted from the primary radiation source and to isolate the most intense resonance line from non-absorbing lines close to it. These lines may come from the cathode metal or the filler gas in the hollow cathode lamp. A monochromator should be capable of separating two lines 0.1nm apart or less when operating at minimum slit width.
- *Detector* which measures the light intensity and amplifies the signal. The most common type of detector is the Photomultiplier. The detector must be able to cover the spectral range from 190-860nm. An important characteristic of a photomultiplier are its dark current and noise which increases as the voltage is applied. An amplification factor of greater than 100 is achieved by increasing the voltage over the dynode system.
- *Display/read out device* that shows the reading after it has been processed by the instrument electronics.

The standard conditions required for determination of calcium and magnesium using AAS are presented in Table 3.1:

Table 3.1 Standard conditions for Calcium and Magnesium

Standard Conditions	Calcium (Ca)	Magnesium (Mg)
Atomic Number	20	12
Atomic Mass	40.08	24.305
Primary Wavelength	422.7nm	285.2nm
Band pass	0.5nm	0.5nm
Emission wavelength	239.9nm	285.2nm
Flame type	Nitrous oxide/acetylene	Air/acetylene
Fuel flow rate	4 – 4.4L/min	0.9 – 1.2 L/min
Signal	1 mg/L gives about 0.4A	0.3 mg/L gives about 0.4A
Atomizer temperature	2600 °C	2800 °C

3.3 Methodology

3.3.1 Experimental Plan

In order to accommodate the effect of various factors on the diffusion coefficient measurements, it was decided to conduct a number of experiments. The experimental layout was divided in two main parts:

i. The first part deals with the reaction kinetics measurements of fresh acid (15 wt. % HCl) and dolomite rock.
ii. The second part deals with the reaction kinetics measurements of various spent acid concentrations and dolomite rock.

The experiments were designed to depict reservoir conditions, thus some of the parameters were kept constant. These include:

i. Temperature: 65˚C or 150°F
ii. Rock type: Dolomite
iii. Core: Guelph Dolomite & Silurian Dolomite
iv. Acid type: Hydrochloric Acid (HCl)
v. Disk diameter: 1.5 inch
vi. Disk thickness: 0.27 inch

The parameters that were varied to study the reaction kinetics are mentioned below:

i. Concentration of HCl acid
    - Fresh acid: 15 wt. % HCl
    - Spent acid: 12.5, 10 & 7.5 wt. % HCl

ii. Pressure: 1000 & 3000 psi

iii. Disk rotational speeds: 250, 500, 750, 1000 & 1250 rpm

A methodology was devised to conduct these experiments which is detailed as under:

3.3.2 Experimental Methodology

3.3.2.1 XRD Analysis of Dolomite rock sample

The first step in conducting the reaction kinetic experiments was to determine the purity of the dolomite rock samples using XRD. Guelph and Silurian Dolomite were used to prepare disks and conduct reaction kinetic measurements. The rock samples should contain greater than 95% dolomite content and very less traces of clay or silica.

X-ray diffraction is based on constructive interference of monochromatic X-rays and a crystalline sample. Sample was prepared by finely grinding 10 gram of the dolomite rock so that the powder becomes completely homogeneous to minimize inducing extra strain (surface energy) that can offset peak positions, and to randomize orientation. Powder less than ~10μm (or 200-mesh) in size was preferred. The powder was then placed on to a sample surface. A glass slide was smeared uniformly on the sample surface to assure a flat upper surface. Finally, the sample was loaded in the sample holder present inside the XRD machine.

X-rays were generated by a cathode ray tube, filtered to produce monochromatic radiation, collimated to concentrate, and directed toward the sample. The interaction of the incident rays with the sample produces constructive interference (and a diffracted ray) when conditions satisfy Bragg's Law ($n\lambda = 2d \sin \theta$). This law relates the wavelength of electromagnetic radiation to the diffraction angle and the lattice spacing in a crystalline

sample. These diffracted X-rays are then detected, processed and counted. By scanning the sample through a range of 2θ angles, all possible diffraction directions of the lattice should be attained due to the random orientation of the powdered material. Conversion of the diffraction peaks to d-spacing allows identification of the mineral because each mineral has a set of unique d-spacing.

3.3.2.2 Porosity measurements

After conducting XRD and estimating the purity of the rock sample, the next step was to estimate the porosity of Silurian and Guelph core samples. The porosity of the rock should be low to minimize the effects of surface area. High porosity rock acts to increase the surface area of the rock. Because the acid dissolution rate depends on the surface area of the rock disk, the dissolution rate will appear to increase as the porosity of the rock increases.

3.3.2.3 Dolomite Disk preparation

After conducting XRD and estimating the porosity of the rock sample, the next part was to prepare the dolomite disks using the core samples. Dolomite core plugs were cut into disks that were approximately 1.5 inch in diameter and 0.27 inch in thickness as shown in Figure 3.7. The disk faces were successively polished with 120, 320 and 400 mesh carborundum. The disks were then soaked in 0.1 M HCl for 30 to 35 minutes and thoroughly rinsed with deionized water. Disk preparation was identical for all experiments since disk surface preparation has an effect on results.

Figure 3.7: Dolomite disks

3.3.2.4 Weight loss measurement of dolomite disks (before experiment)

The next step after preparation of the disk was to measure the weight of all the dolomite disks using Weighing Balance before conducting reaction kinetic experiments.

3.3.2.5 Micro XCT of dolomite disks (before experiment)

Dolomite disks prepared from Guelph and Silurian dolomite core samples were then scanned using Micro XCT technique to characterize and visualize the 3D image of the disks at the micron level of voxel resolution before conducting reaction kinetic experiments. It also helps in examining whether the dolomite disks contain natural pores and fractures which will help in understanding the dissolution mechanism of the dolomite disks.

The foundation of x-ray computed tomography is to measure the x-ray attenuation of the sample with an appropriate detector. The dolomite disk (sample) is placed on the sample holder/container to hold the sample on the stage in a fixed, steady position during scanning of the sample. The first consideration for the container is to stabilize the sample during the scan while rotating through different angles; the second consideration is the mass attenuation coefficient of the container which has to be as low as possible, yet still providing sufficient support and stability for the sample.

3.3.2.5.1 Process of Micro XCT

X-ray photons are generated from a point source, penetrate the sample, are absorbed and then the attenuated beams were collected on the detector. The sample absorbs a certain amount of x-ray photons as determined by sample density, atomic number, thickness and linear attenuation coefficient. The x-ray photons which escape from the sample were

captured by the detector and the intensity measure creating a radiograph or “projection”. The projection of x-ray photons is defined for a specific angular position. A collection of projections at different angles in a full rotation can be processed for a three dimensional reconstruction known as “back projection”. The back projected image is a 3D matrix composed of linear attenuation coefficients for the sample. The variation in voxel intensity distinguishes the structure and material characteristics.

3.3.2.5.2 Scan Conditions

Image creation for CT analysis is based on material properties such as density, mineral composition and atomic number. The image quality for the CT scan depends on the difference in attenuation coefficients and scan conditions are determined by this difference. The significant scan conditions are presented below:

- Mass attenuation coefficient increases with an increase in x-ray photon travel distance. In other words, the further the distance between x-ray source and detector, the lower the x-ray intensity that will be measured. Under this consideration, a combination of distance, energy level and exposure time can be adjusted to obtain a better image quality.
- Exposure time is also a decisive factor for the CT scan. Material density and elemental composition decides the energy level (voltage) and exposure time decides attenuation coefficient reading for the sample. For a heavier, thicker or higher atomic number material, a long exposure time is required to collect enough x-ray photons.

3.3.2.6 HCl preparation and standardization

After conducting Micro XCT, the following steps were conducted to prepare 15 wt. % HCl acid and standardize it.

- 15 wt. % HCl was prepared using concentrated hydrochloric acid (ACS reagent grade, 37 wt. %) and distilled water. The volume of 37 wt. % HCl required to prepare 15 wt. % HCl was 366.19 ml.
- The next step was to prepare 0.1 M NaOH which was used for standardization purposes of the HCl acid. Standardization is the process of determining the exact concentration of a solution. Titration is one type of analytical procedure often used in standardization. In titration, an exact volume of one substance was reacted with a known amount of another substance.
- After preparing 0.1 M NaOH, it was standardized with potassium acid phthalate (KHP, $HKC_8H_4O_4$) to determine the molarity of NaOH. The following reaction takes place when NaOH and KHP reacts:

$$\boldsymbol{HKC_8H_4O_4 + NaOH \rightarrow NaKC_8H_4O_4 + H_2O}$$

- The last step was to standardize 15 wt. % HCl with the prepared NaOH and determine its molarity. The following reaction takes place when NaOH and HCl reacts:

$$\boldsymbol{NaOH + HCl \rightarrow NaCl + H_2O}$$

3.3.2.7 Reaction Kinetics Measurement

Rotating Disk Apparatus (RDA) was used to conduct reaction kinetic measurements. Figure 3.8 and 3.9 shows the schematic of RDA for fresh as well as spent acid reaction kinetics studies. The testing procedure of a typical experiment is described as follows:

- The dolomite disk was mounted on the rotating shaft. The circumference of the disk was covered using shrink wrap teflon tubing that allows only the lower face of the disk to be exposed to HCl acid.
- For spent acid experiments, a precise and measured amount of dolomite powder was introduced into the accumulator. The amount of powder used was computed to stoichiometric ally equate to the level of acid "spending" required - e.g. 15% HCl spent to 12.5%, 10% or 7.5%.
- In order to keep CO_2 in solution, the reaction vessel was then pressurized to the desired level with nitrogen (back pressure) and the temperature for both reaction vessel and the acid accumulator were heated to the same temperature i.e. 65ºC.
- Once stabilized, the acid was transferred from the accumulator to the reaction vessel and disk rotation was started at a particular rpm already set in the control panel of data acquisition system.
- For spent acid, the injected acid was left to completely react with the carbonate powder under desired pressure and temperature conditions. Once reacted the concentration of the spent acid solution, the corresponding counter ions and CO_2 represent a true "partially spent acid" system at the same conditions. Once stabilized and all the powder was reacted, the second stage of the reaction was initiated. A metered volume of water was used to displace the piston to submerge

the rotating disk in the partially spent acid solution and start the disk reaction process.

- A 5 - 10 ml sample of reaction products was taken every two minutes in an accurately timed 10 minute reaction process. The sampling tube was purged prior to each sample collection. All volumes of collected and discarded fluids were recorded.
- The reaction was stopped after 10 minutes by draining the fluid through the sampling tube drops which drop the level of acid below the marble disk.
- The mass of the remaining disk sample was then weighed to determine the weight loss as a second comparison for diffusion coefficient.

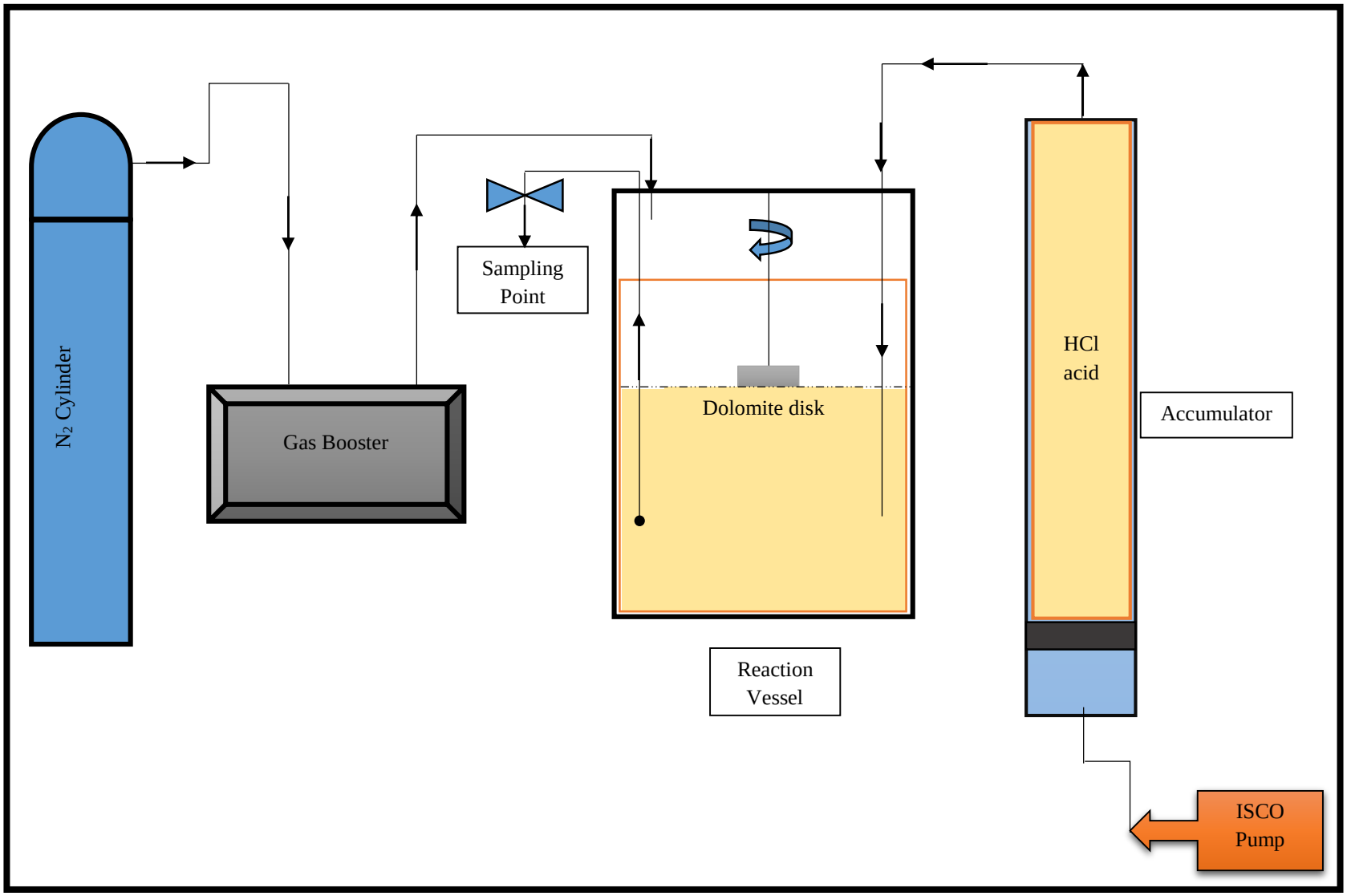

Figure 3.8: Experimental Setup of Rotating Disk Apparatus for fresh acid reaction kinetics study

Figure 3.9: Experimental Setup of Rotating Disk Apparatus for spent acid reaction kinetics study

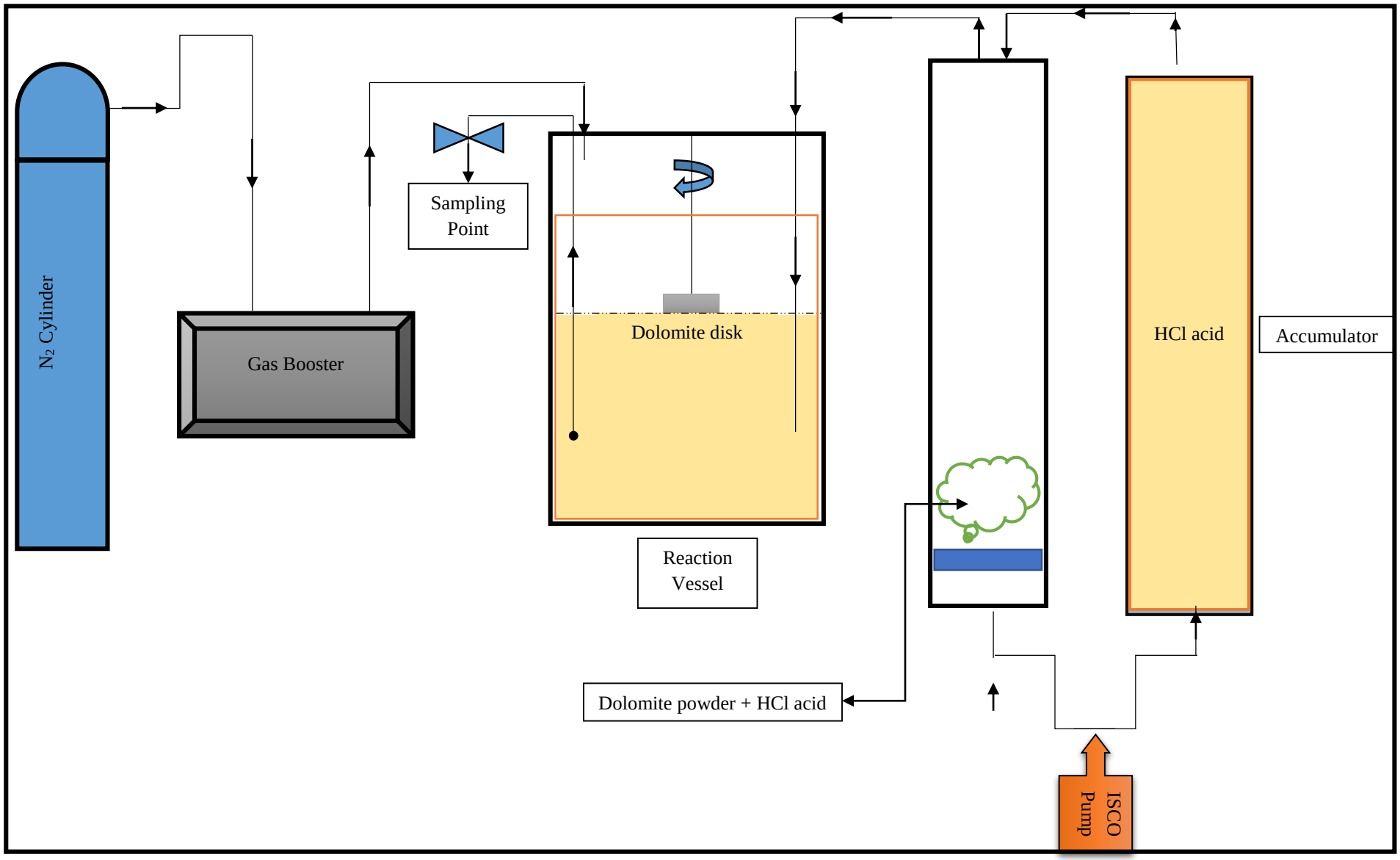

3.3.2.8 Weight loss measurement of dolomite disks (after experiment)

After conducting the experiment on the dolomite disk, the disk is dried in the oven and the weight of the disk is measured using the Weighing Balance to calculate the weight loss (ΔW).

3.3.2.9 Micro XCT of dolomite disks (after experiment)

The reacted dolomite disks for 500 rpm and 1250 rpm (for each series of experiment) were scanned using Micro XCT to characterize the nature of reaction at different experimental conditions. The procedure of conducting the scan had been discussed in earlier section.

3.3.2.10 Titration Analysis of the reacted acid

Once each experiment was conducted, titration analysis was performed on the acid drained from the reaction vessel to evaluate the molarity of the acid. This step had great significance in spent acid reaction kinetic experiments as the molarity of the acid was used as a quality check as well as to determine that the dolomite powder was completely dissolved in the acid during the experiment.

3.3.2.11 Analytical Analysis

The last step in the experimental methodology was to conduct Atomic Absorption Spectroscopy (AAS). It is an analytical technique used for quantitative determination of elements present in the samples. Each collected sample in the reaction kinetics experiment was analyzed using AAS to determine the Ca^{2+} or Mg^{2+} ions concentration in order to determine the dissolution rate as well as the diffusion coefficient. The samples collected from the experiments were diluted with first grade distilled water up to the calculated dilution factor.

3.3.2.11.1 Principle of AAS

The basic principle of Atomic Absorption is that the "ground state" atom absorbs light energy of a specific wavelength as it enters the "excited state." As the number of atoms in the light path increases, the amount of light absorbed also increases. By measuring the amount of light absorbed, a quantitative determination of the amount of analyte can be made. The use of special light sources and careful selection of wavelengths allow the specific determination of individual elements.

3.3.2.11.2 Preparation of Calibration Standards

The correct preparation of standards and calibration graph was an important step before using the diluted samples to determine the elements concentration. When preparing calibration standards, it is important to select the correct acid. The correct acid will keep the metal ions in solution and improve solution lifetime. Nitric Acid (HNO_3) was used to prepare the calibration standards. In order to prepare 2.2 wt. % HNO_3, 4000 ml of first grade distilled water was mixed with 88 gm of Nitric acid powder and stirred thoroughly at 300 rpm for 15 – 30 minutes. After preparation of 2.2 wt. % HNO_3, calcium and magnesium standards were prepared according to the required concentrations (100 ppm, 10 ppm, 5 ppm etc.). In order to prepare 100 ppm calcium standard, it is diluted from 1000 ppm to 100 ppm in a 200 ml volumetric flask. The calculation is shown below:

$$\boldsymbol{C_1V_1 = C_2V_2}$$

$$\boldsymbol{1000 * V_1 = 100 * 200}$$

$$\boldsymbol{V_1 = 20\ cc}$$

Now 20 cc of calcium standard was added in 200 ml volumetric flask and HNO_3 solution was added until the maximum limit of the flask had reached. Similarly, all the subsequent Ca and Mg standards for further concentrations were prepared and stored in clean labelled bottles to avoid contamination. The prepared calibration standards were used to plot the calibration graph which is a graph between sample absorbance and concentration. The R^2 should be greater than or equal to 0.997 showing the accuracy of the prepared calibration standards.

3.3.2.11.3 AAS process

The layout of a basic flame atomic absorption spectrometer is shown in figure 3.10.

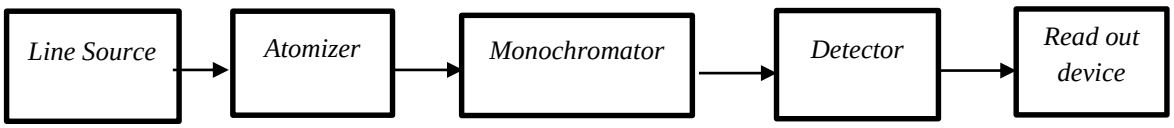

Figure 3.10: Layout of basic flame AAS

The basic steps of conducting AAS are mentioned below:

- The diluted sample was drawn up at high velocity through a capillary tube to a fine jet, which forms a liquid aerosol or mist, using the Nebulizer, before injection into the flame.
- Light from a line source of characteristic wavelength for the element being determined passes through the flame into which has been sprayed a fine mist of the sample solution.
- The region of the spectrum to be measured was selected by a monochromator.
- The isolated spectral line falls on the detector and the output was amplified and sent to a read out device.

- The intensity of the resonance line was measured twice, once with the sample in the flame and once without. The ratio of the two readings was a measure of the amount of absorption, hence the amount of element in the sample.

A number of effects contribute to the uncertainty in the final signal displayed on the read out device. The sources of error are mentioned as follows:

- Fluctuations in hollow cathode lamp emission signal
- Detector shot noise
- Electronic noise
- Flame fluctuations
- Inaccuracies in the read out device
- Random and systematic errors in sample preparation
- Inter-element interferences

3.3.2.12 Determination of Diffusion Coefficient

After conducting the experiments and AAS, the final step was to determine the diffusion coefficient. Diffusion coefficient measurement is a significant step to properly investigate the impact of reaction products on acid/rock reaction. Mass transfer rate is a function of local fluid velocity, fluid viscosity and structure and diffusion coefficient. Flow rate and fluid viscosity are accessible but acid diffusivity is not an easy property to measure. The knowledge of the diffusivity of hydrogen ions from the bulk solution to the rock surface is the key in characterizing the rate of dissolution of carbonate reactions.

The stoichiometric dissolution reaction of dolomite with hydrochloric acid is given as:

$$CaMg(CO_3)_2 + 4H^+ \rightarrow Ca^{2+} + Mg^{2+} + 2CO_2 + 2H_2O \quad (1)$$

(Lund, 1973) described the rate of the surface reaction dependence on concentration by the power law model expression that can be represented by:

$$-R_{H+} = k\, C_s^n$$

Where, R_{H+} = rate of dissolution of dolomite (or calcite) in HCl in moles/s.cm^2

k = reaction rate constant in (g moles/cm^2.s) (g mole/cm^3)$^{-n}$

n = reaction order, dimensionless

C_s = surface acid concentration in mole /cm^3

The reaction rate constant can be related to temperature using Arrhenius equation:

$$k = k_o e^{\frac{-E_a}{RT}}$$

Where, k_o = pre-exponential factor or frequency factor

E_a = activation energy in kcal/gmol

($-E_a/R$) = slope of the straight line plot of k_r as a function of absolute temperature

The mass transfer limited regime is represented by the diffusion rate given as follows:

$$J_{mt} = k_{mt} * (C_b - C_s) \quad (2)$$

Where, J_{mt} = mass transfer rate of HCl from the bulk solution to the disk in gmoles/cm^2.s

K_{mt} = mass transfer coefficient in cm/sec

C_b = bulk acid concentration in mole/cm^3

C_s = surface acid concentration in mole/cm^3

The mass transfer coefficient in a rotating disk reactor has been introduced by (Levich, 1962) given as:

$$K_{mt} = 0.62\, D^{2/3}\, \nu^{-1/6}\, \omega^{1/2} \quad (3)$$

Where ν = kinematic viscosity (cm^2/sec)

D = diffusion coefficient (cm^2/sec)

ω = disk rotation speed (rad/sec)

At steady state condition, the flux of H^+ ions to the surface of the rock disk is equal to twice the flux of Ca^{2+} or Mg^{2+} ions leaving the surface.

$$J_{mt} = 2 * J_{Ca^{2+}} \; or \; J_{mt} = 2 * J_{Mg^{2+}} \qquad (4)$$

Combining equation (2) and (3), the reaction flux can be expressed as:

$$J_{H+} = 0.62 \, D^{2/3} \, \nu^{-1/6} \, \omega^{1/2} \, (C_b - C_s) \qquad (5)$$

When the reaction is mass transfer limited, then $C_s << C_b$, then equation (5) will yield:

$$\frac{J_{H+}}{0.62 * \nu^{-1/6} * C_b} = D^{2/3} \; \omega^{1/2}$$

Substituting equation (4) in the above equation, the following equation can be derived:

$$\frac{J_{Ca^{2+}}}{0.31 * \nu^{-1/6} * C_b} = D^{2/3} \; \omega^{1/2} \; or \; \frac{J_{Mg^{2+}}}{0.31 * \nu^{-1/6} * C_b} = D^{2/3} \; \omega^{1/2}$$

The above derived equation was used to evaluate the diffusion coefficient. A graph of $F = \frac{J_{H+}}{0.31 * \nu^{-1/6} * C_b}$ vs. $\omega^{1/2}$ was plotted which yields a straight line representing the mass transfer limited regime. The slope ($D^{2/3}$) of the straight line provided the value of diffusion coefficient. Figure 3.11 shows the schematic plot of "F" function vs. disk rotational speed.

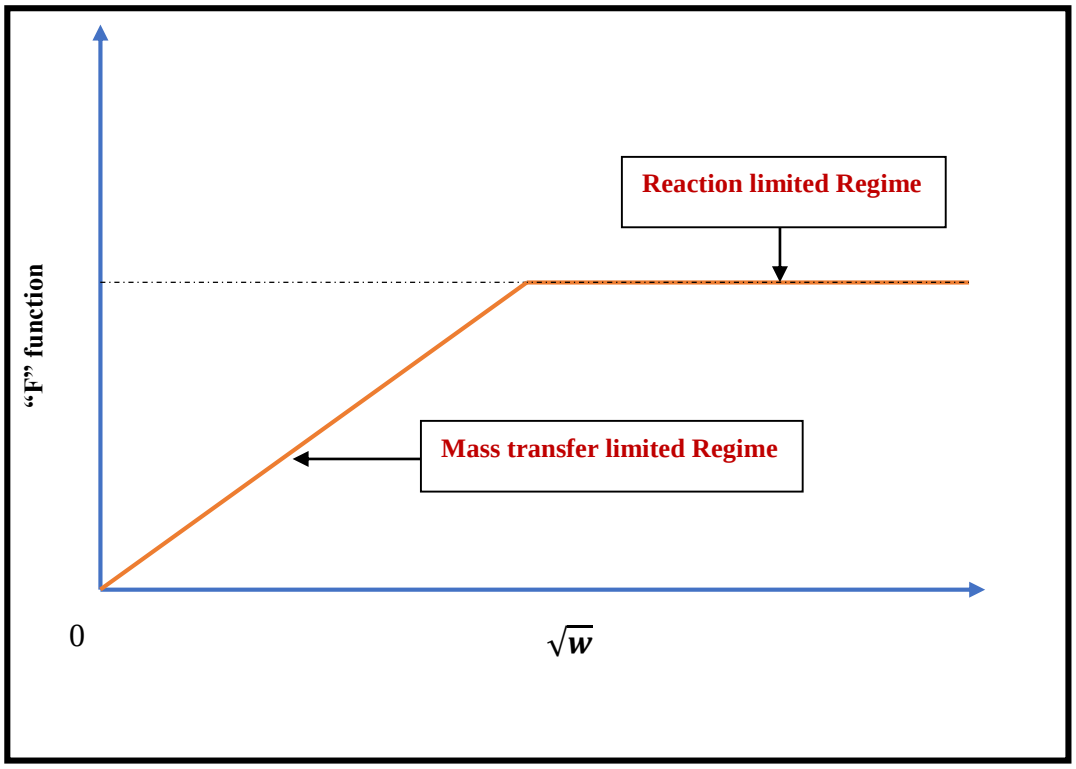

Figure 3.11: Schematic plot for determining Diffusion Coefficient

CHAPTER 4

EFFECT OF PRESSURE ON DIFFUSION COEFFICIENT OF FRESH ACID WITH DOLOMITIC ROCK

Carbonate matrix acidizing extends a well's effective drainage radius by dissolving rock and forming wormholes from the wellbore. Wormholing during matrix acidizing of carbonate reservoirs is controlled by the fluid injection rate and acid diffusion coefficient (De) which dictates the speed and profile of the wormholes. Injection rate is easily obtained from the job execution whereas the diffusion coefficient is a hidden parameter of the fluid and reaction conditions. The rotating disk instrument is widely used in petroleum industry to study the kinetics of acidic fluids and chelating agents with dolomite/calcite rocks which allows the determination of rock dissolution rates and diffusion coefficients.

Pressure has significant impacts on the diffusion coefficient. Conventional wormhole models use diffusion coefficient obtained from the system pressure of 1000 psi (or below) to predict the worm holing process which is too low to represent realistic reservoir conditions resulting in significant overestimation of the results.

Lund *et al.* (1973) studied the dissolution of pure dolomite marble in HCl acid at a pressure of 600 psig with varying acid concentrations between 0.01 N – 9 N HCl at temperatures of 25, 50 and 100°C rotating the disk speed from 50 to 500 rpm. It was concluded that the dissolution of dolomite was reaction limited at low temperature and diffusion limited at

high temperature ranges. However, the dissolution of calcite marble with HCl acid was found to be mass transport limited even at high disk rotational speeds. Moreover, calcite marble reacted approximately 650 times faster as compared to dolomite marble at 25°C (Lund *et al.*, 1975).

Busenberg and Plummer (1982) studied the effect of pH using dolomite and aqueous solution. It was concluded that reaction rate was dependent on pH at pH values less than 6 and constant at pH > 8.

Anderson (1991) measured the reactivity of San Andres dolomite with HCl acid using different dolomite samples at 120 rpm and temperatures of 80 and 120°F. It was concluded that different dolomite samples show different surface kinetics.

Taylor *et al.* (2004) examined the effects of acidizing additives on acid reaction rates of calcite and dolomite rock. The additives include polymer, corrosion inhibitor, surfactant, mutual solvent, citric acid and dissolved iron (III). It was found that dissolution rate of calcite was mass transfer limited in 1 M HCl at room temperature but the dissolution rate of dolomite was surface reaction limited.

Taylor *et al.* (2004 & 2006) studied the relationship between acid reaction rate and rock mineralogy for a deep dolomitic gas reservoir. Their results showed that mineralogy significantly affects the reaction rate. Moreover, clay content (< 1 wt. %) decreased the reaction rate of limestone rock by up-to a factor of 25.

The main objective of this research is to study the reaction kinetics of dolomite rock with fresh acid (15 wt. %) at temperature of 65°C at two different pressure ranges:

- Low pressure i.e. 1000 psi
- High pressure i.e. 3000 psi

In order to fulfill the above mentioned objective, fifteen experiments were conducted to study the impact of pressure on the diffusion coefficient of fresh acid and dolomite rock. The experiments were divided into three sets as shown in Table 4.1. The results for each of the three series of the experiments are described in the following sections.

Table 4.1: Experimental Layout for fresh acid – dolomite

HCl concentration (wt. %)	Dolomite Core Used	Pressure (psi)	Disk Rotational Speeds (rpm)				
			250	500	750	1000	1250
15	Guelph Dolomite	1000	Exp 1	Exp 2	Exp 3	Exp 4	Exp 5
	Silurian Dolomite	1000	Exp 6	Exp 7	Exp 8	Exp 9	Exp 10
	Silurian Dolomite	3000	Exp 11	Exp 12	Exp 13	Exp 14	Exp 15

4.1 Guelph Dolomite at 1000 psi (15 wt. % HCl) Acid

The experimental parameters to conduct experiments for Guelph Dolomite at 1000 psi (15 wt. % HCl) Acid which will be referred to as Series # 01 are listed in Table 4.2.

The first series experiments were conducted using Guelph Dolomite rock. Guelph dolomite contain small holes and natural fractures present inside the core. The core was 12" in length and 1.5" in diameter. The pressure range for this series was 1000 psi. Total five experiments were conducted starting from low disk rotational speeds (250 rpm) to high disk rotational speed (1250 rpm). The Guelph dolomite porosity was measured and found to be 10%. The following sections present the detailed results for series 01 experiments.

Table 4.2: Experimental conditions for series # 01 – 1000 psi – 15 wt. % acid

Experiment Parameters	
Rock Type	Dolomite
Core Type	Guelph Dolomite
Temperature, ˚C	65
Pressure, psi	1000
Acid Type	HCl
Concentration of HCl, wt. %	15
Disk Rotational Speeds, rpm	250, 500, 750, 1000, 1250

4.1.1 XRD Analysis of Guelph Dolomite

XRD was conducted to determine the purity of Guelph dolomite rock sample. The XRD results showed that the purity of the dolomite sample was approximately 99% dolomite. Figure 4.1 shows the measurement profile of the XRD conducted. Figure 4.2 shows the quantitative analysis report for dolomite phase identification. It was found that Guelph dolomite contained 99% dolomite content with minute traces of silicon oxide.

4.1.2 Micro XCT of Guelph Dolomite (before experiment)

Guelph dolomite disks were prepared and scanned using Micro XCT to characterize the 3D image of the disks. Micro XCT equipment was operated at a voltage of 120kv and 10W power source. In addition, the scan time per dolomite disk was 90 minutes (approximately).

Figure 4.3 shows the Micro XCT image of the Guelph dolomite disk before conducting the reaction kinetics experiment. It is evident from the image Guelph dolomite contains natural holes and fractures inside the rock. The rock porosity is low (10%) but the pore structure of the rock imaged through micro XCT predicts the reaction rate to be high. Moreover, the rock has a rough surface.

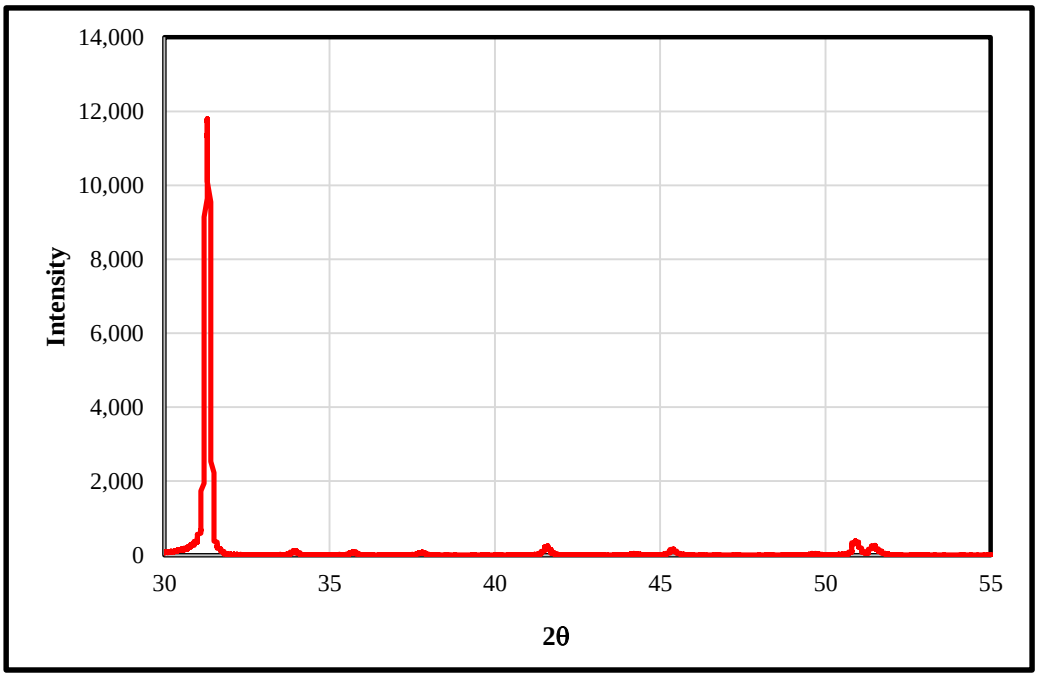

Figure 4.1: Measurement profile of Guelph dolomite XRD

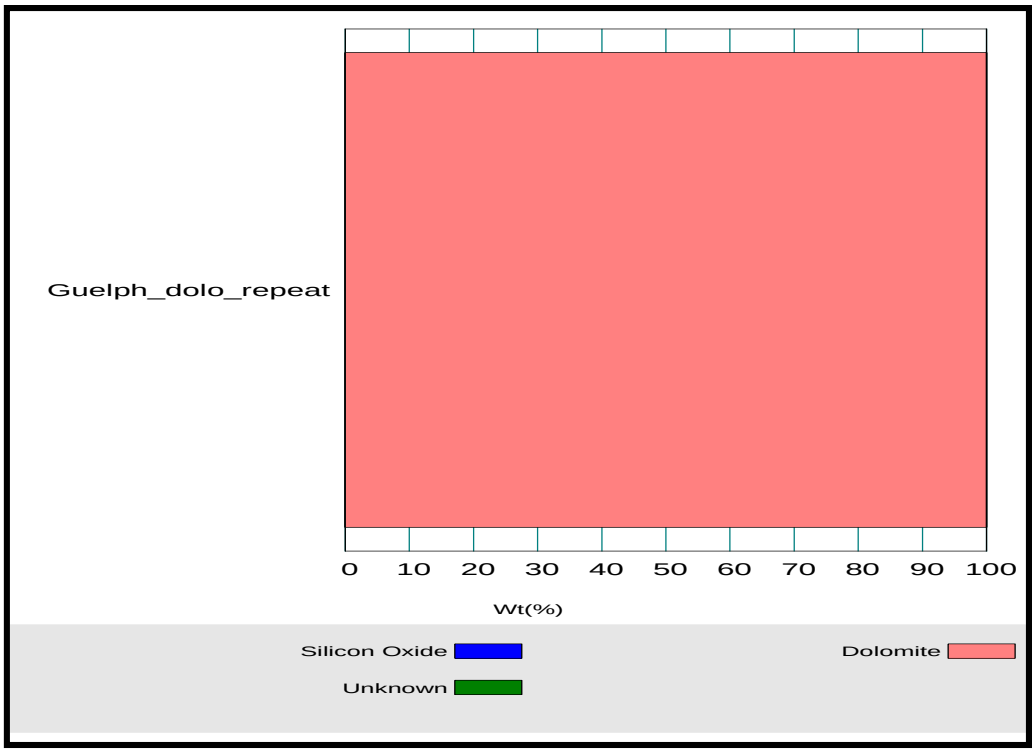

Figure 4.2: Quantitative analysis of Guelph Dolomite XRD

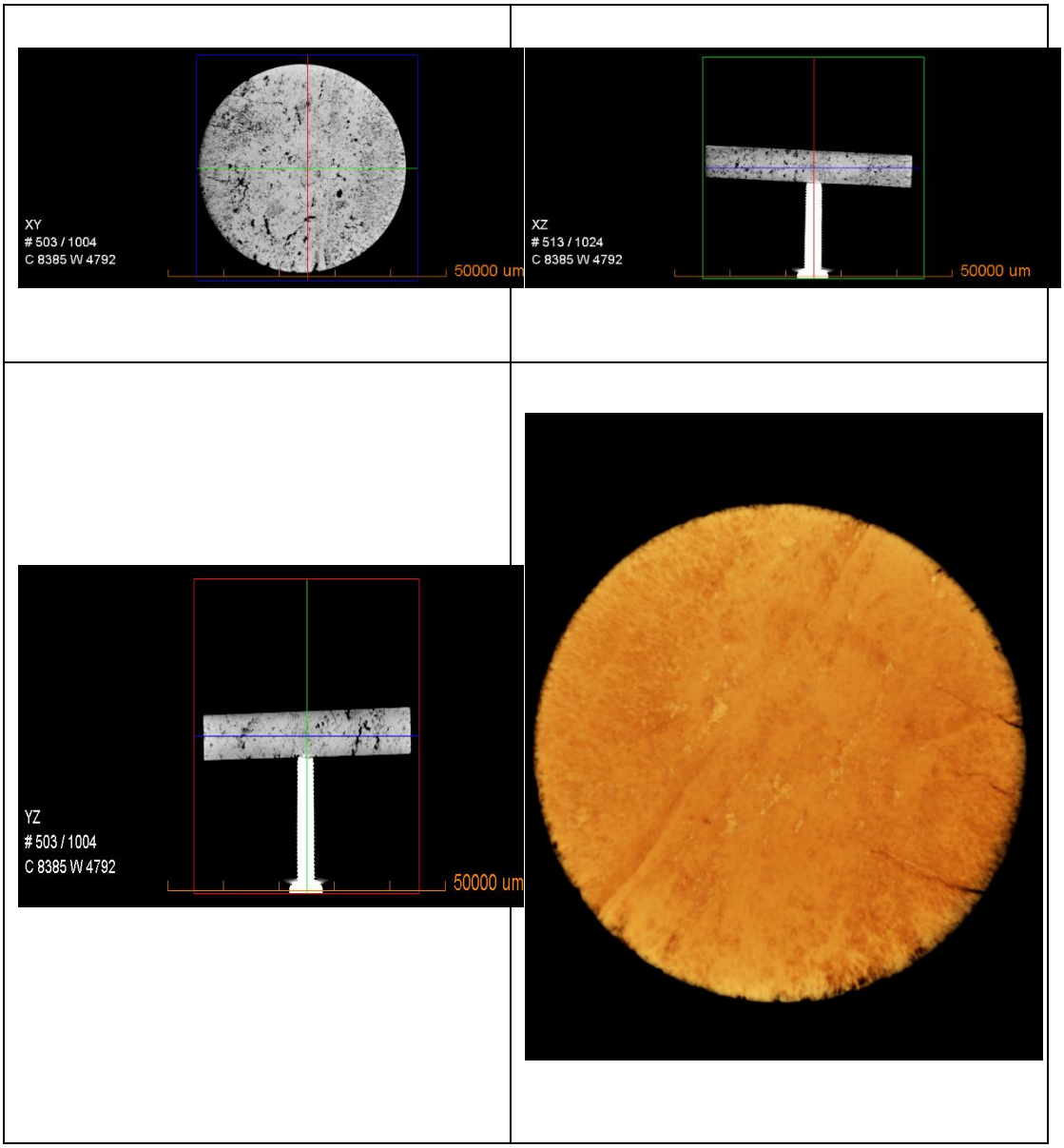

Figure 4.3: Micro XCT image of Guelph dolomite disk before reaction kinetics experiment

4.1.3 Preparation and standardization of 15 wt. % HCl acid

HCl acid was prepared to obtain 15 wt. % acid concentration which was used for reaction kinetics experiment. The molarity of fresh acid was determined using titration process and average value was found to be 4.38 M.

4.1.4 Reaction Kinetics experiment

Rotating Disk Apparatus was used to conduct reaction kinetics measurement. A total of five experiments were conducted using Guelph dolomite disks starting from 250 rpm to 1250 rpm. The detailed procedure to conduct the experiment was described in Chapter 03. The weight of the disks were measured before and after conducting each experiment which was used as a comparison for diffusion coefficient calculations. Table 4.3 shows the weight loss values for each experiment.

Table 4.3: Weight loss values for Guelph dolomite experiments - 1000 psi

Disk Rotational speed rpm	Weight of disk before experiment, gm	Weight of disk after experiment, gm	Weight loss (ΔW), gm
1250	16.82	10.148	6.67
1000	16.129	10.34	5.82
750	15.92	10.12	5.8
500	15.85	11.93	3.92
250	15.538	12.44	3.098

Figure 4.4 shows the graph between weight loss and disk rotational speeds. It can be observed that the weight loss increases as the disk rotational speed increases. However, the difference in weight loss between 1000 rpm and 750 rpm is minimal. Moreover, the increasing trend of the weight loss values depicts that the reaction between Guelph dolomite and HCl acid at 1000 psi will be mass transfer limited.

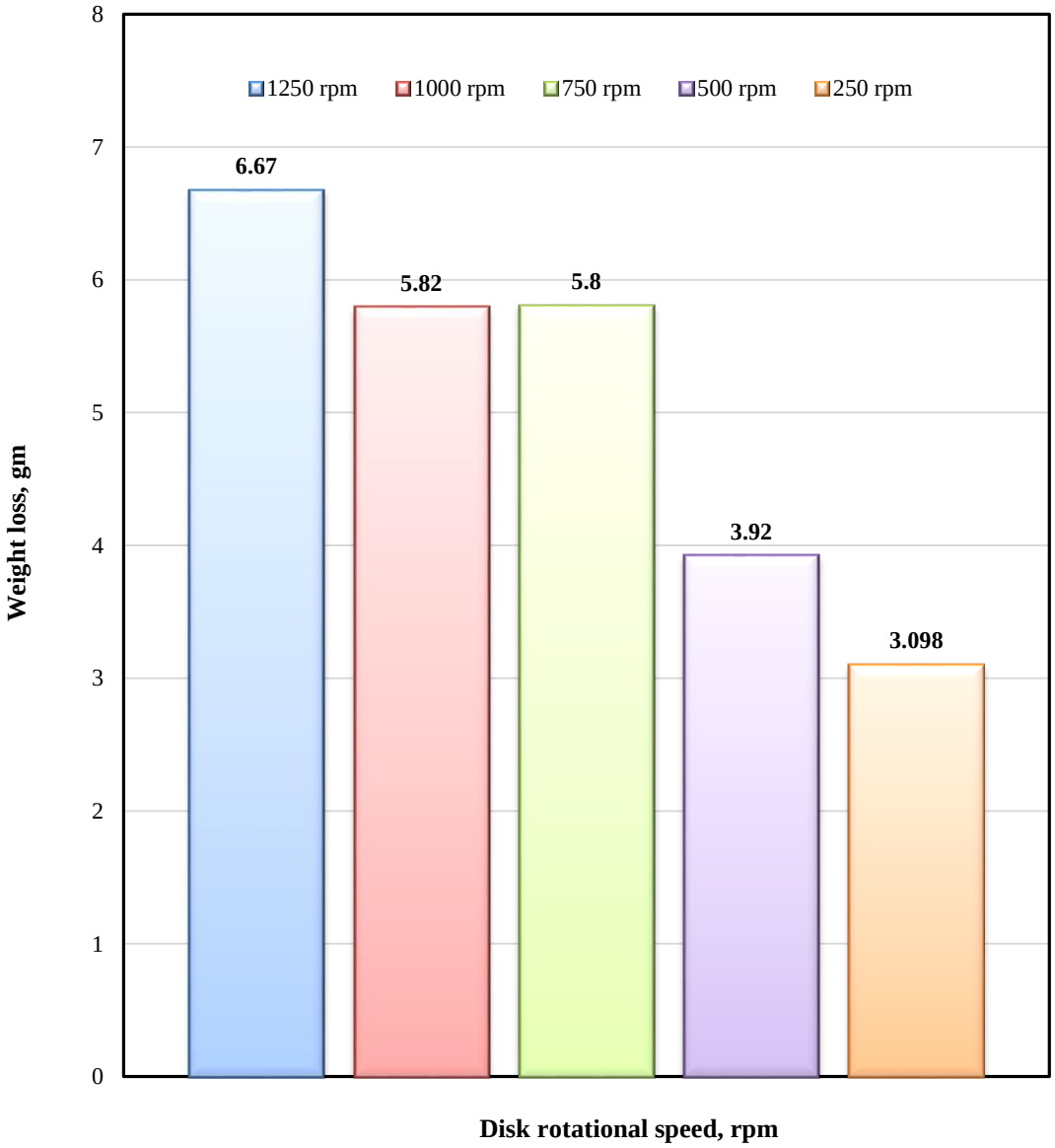

Figure 4.4: Weight loss of Guelph sample as function of RPM at 1000 psi

4.1.5 Diffusion Coefficient Analysis

As discussed in chapter 3, the samples collected from the reaction kinetics experiment were then diluted and their calcium and magnesium concentrations were determined using AAS. The concentrations were then used to calculate dissolution rates as well as the diffusion coefficient. Table 4.4 shows the calculated values for dissolution rates and "F" function using weight loss results as well as using AAS results.

Table 4.4: Diffusion Coefficient Analysis calculations, Guelph dolomite – 1000 psi

Disk rotational speed rpm	$\sqrt{w}$ **rad/sec**	**Dissolution rates mole/s.cm^2**	**F (using weight loss results)**	**F (using AAS results)**
1250	11.4419	0.0000065238	0.002025219	0.002117362
1000	10.2339	0.0000056717	0.00176069	0.001723924
750	8.8628	0.0000057110	0.001772905	0.001772524
500	7.2365	0.0000038271	0.001188059	0.001216897
250	5.1170	0.0000030617	0.000950471	0.000982292

Figure 4.5 and Figure 4.6 shows the graph between "F" function vs. the square root of disk rotational speed using weight loss results and AAS results respectively. It can be observed that the reaction between Guelph dolomite and fresh acid was mass transfer limited as the reaction rate increases with disk rotational speed in both the figures. Moreover, the reaction rate increased significantly at high disk rotational speeds due to the presence of natural pores and fractures inside the Guelph dolomite disks.

Using the slopes in Figure 4.5 and 4.6, diffusion coefficient was obtained. The diffusion coefficient obtained using weight loss and AAS results was **2.83×10^{-06} cm^2/sec.**

4.1.6 Micro XCT of dolomite disks (after experiment)

The reacted dolomite disks for 500 rpm and 1250 rpm were scanned using Micro XCT to characterize the nature of reaction and describe the pore structure. It was observed that at 500 rpm, the dissolution was less as compared to 1250 rpm. At high rotational speed, the acid penetrated deep inside the disk and created holes. Moreover, the due to the presence of natural pores, the acid penetrated at the sides of the disk which were covered by teflon tubing. It can also be observed that a small portion of the disk was completely dissolved by the acid. At 1250 rpm, the center portion of the disk was severely affected by acid-rock reaction resulting in small holes reaching the top surface of the disk. However, at 500 rpm, no holes were created and the dissolution of the disk by acid was uniform. Figure 4.7 and 4.8 shows the Micro XCT images of the disk used in 500 rpm and 1250 rpm experiments, respectively.

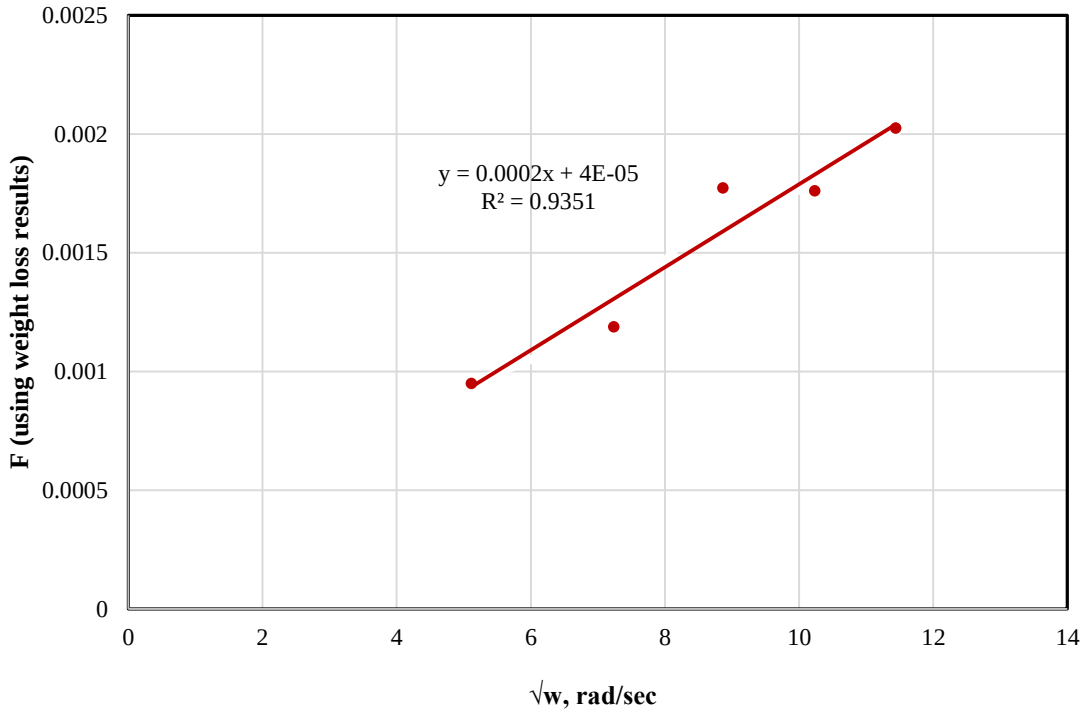

Figure 4.5: Diffusion Coefficient Graph (using weight loss results), Guelph dolomite – 1000 psi

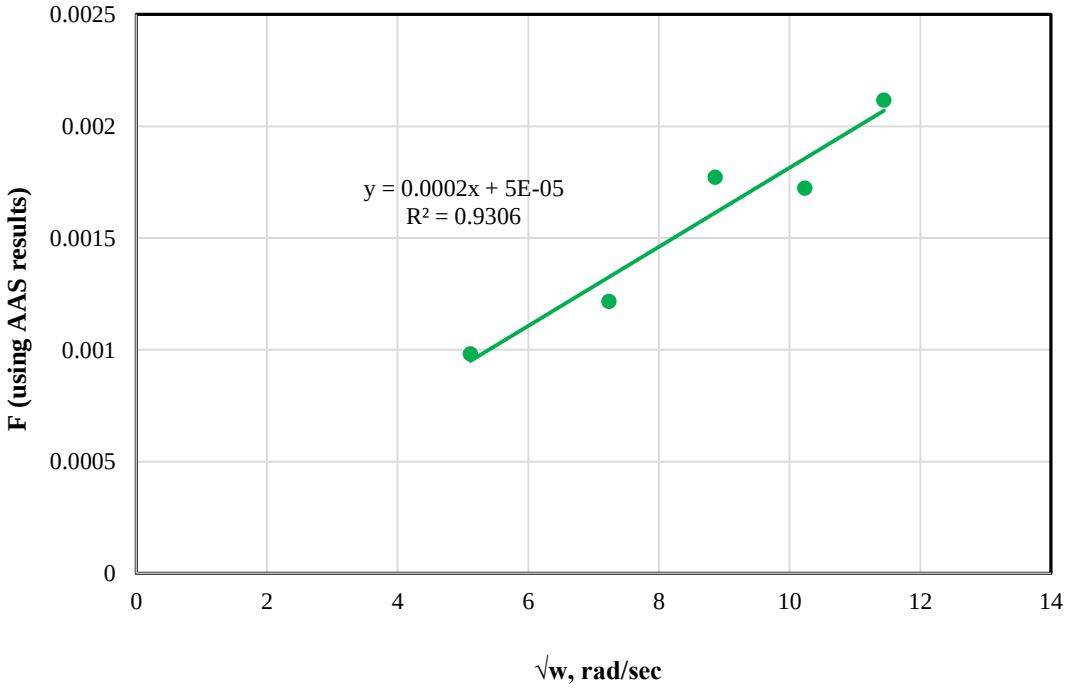

Figure 4.6: Diffusion Coefficient Graph (using AAS results), Guelph dolomite – 1000 psi

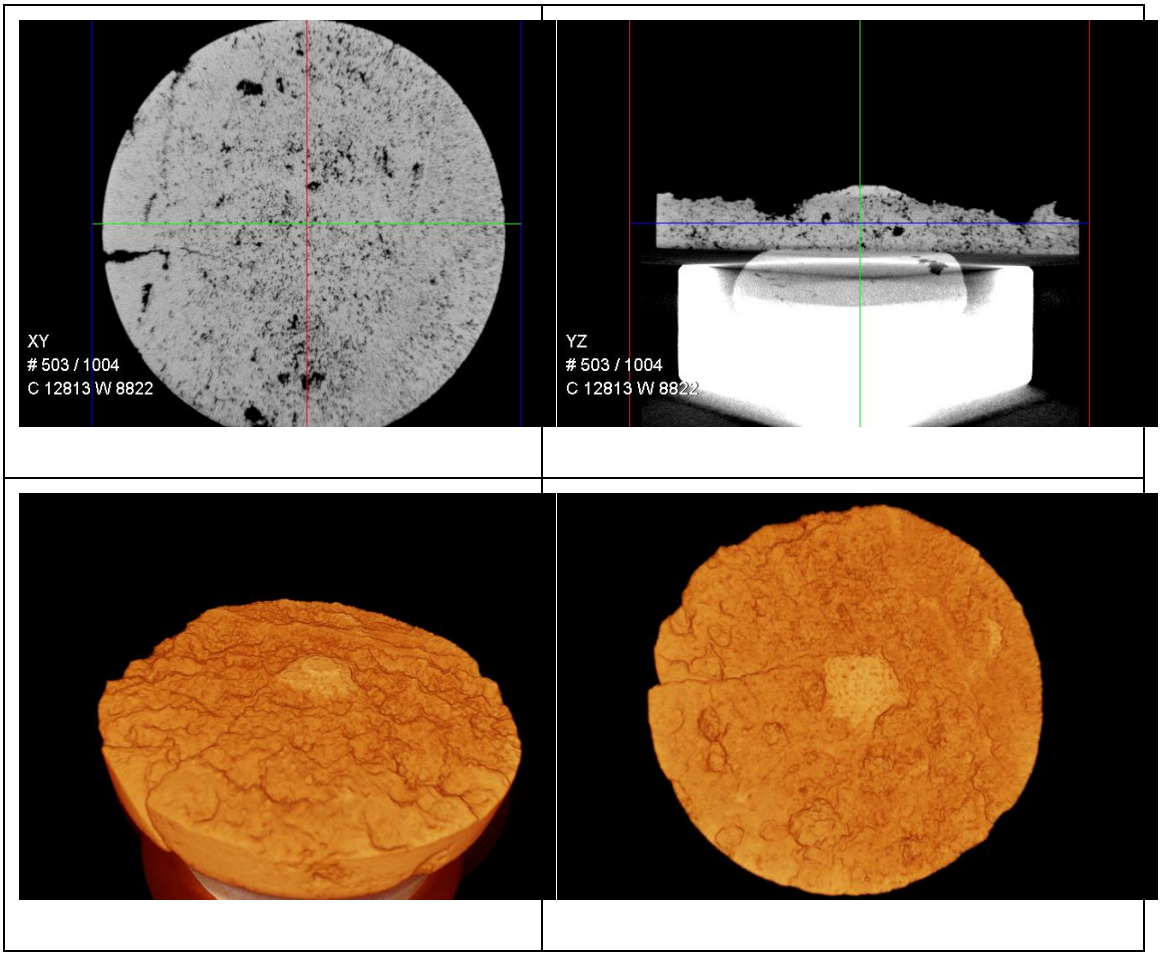

Figure 4.7: Micro XCT image of reacted disk at 500 rpm, Guelph dolomite – 1000 psi

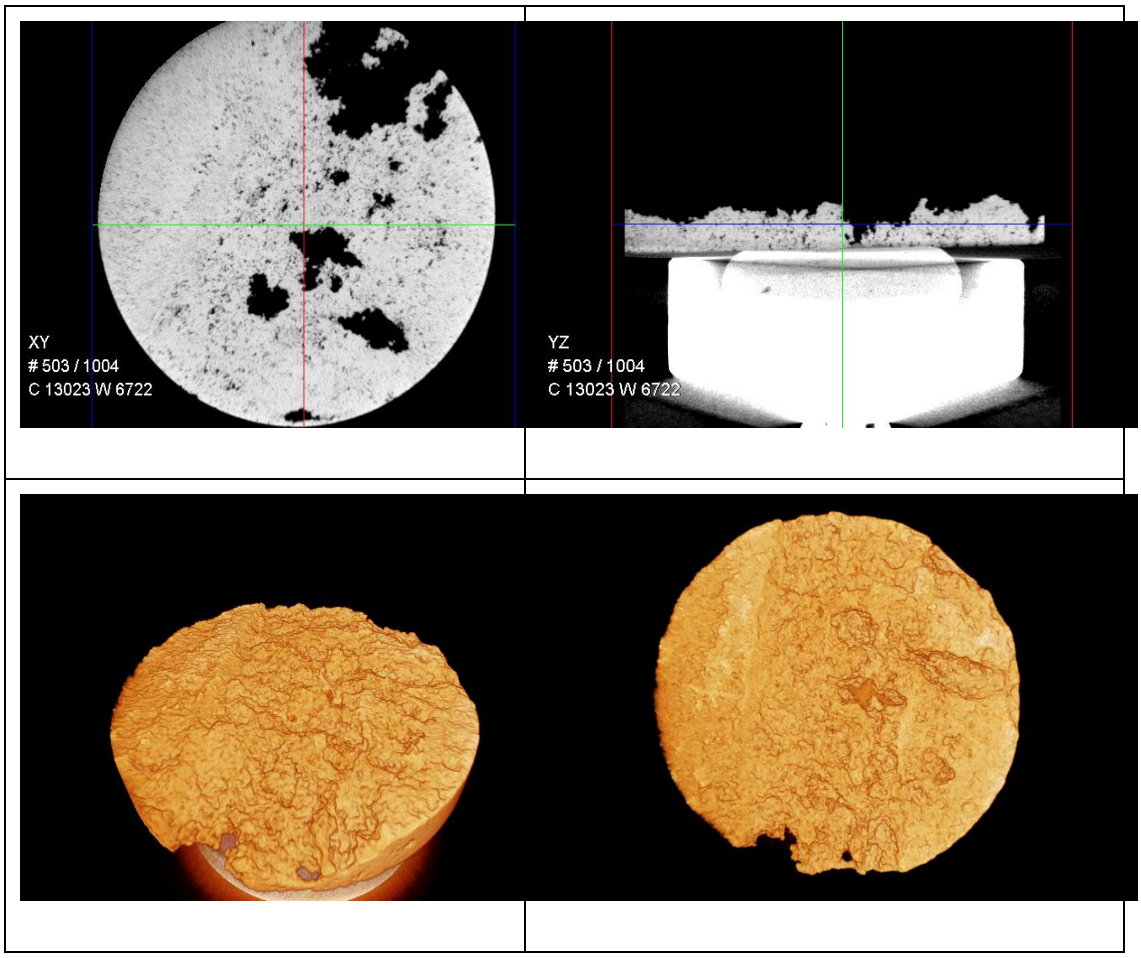

Figure 4.8: Micro XCT image of reacted disk at 1250 rpm, Guelph dolomite – 1000 psi

4.2 Silurian Dolomite at 1000 psi (15 wt. % HCl) Acid

The experimental parameters to conduct experiments for Silurian Dolomite at 1000 psi (15 wt. % HCl) Acid which will be referred to as Series # 02 are listed in Table 4.5. The second series experiments were conducted using Silurian Dolomite rock. Silurian dolomite does not contain any natural pores and fractures as compared to Guelph dolomite. The full core was 12" in length and 1.5" in diameter. Dolomite core were cut into disks that were approximately 1.5 inch in diameter and 0.27 inch in thickness. The pressure range for this series was 1000 psi. Total five experiments were conducted starting from low disk rotational speeds (250 rpm) to high disk rotational speed (1250 rpm). The Silurian dolomite porosity was measured and was found to be 10%. The following sections present the detailed result for series 02 experiments.

Table 4.5: Experimental conditions for series # 02 – 1000 psi – 15 wt. % acid

Experiment Parameters	
Rock Type	Dolomite
Core Type	Silurian Dolomite
Temperature, ˚C	65
Pressure, psi	1000
Acid Type	HCl
Concentration of HCl, wt. %	15
Disk Rotational Speeds, rpm	250, 500, 750, 1000, 1250

4.2.1 XRD Analysis of Silurian Dolomite

XRD was conducted to determine the purity of Silurian dolomite rock sample. The XRD results showed that the purity of the dolomite sample was approximately 99% with no traces of silica or clay. Figure 4.9 shows the measurement profile of the XRD conducted. Figure 4.10 shows the quantitative analysis report for Silurian dolomite phase identification. It was found that Silurian dolomite contained 99% dolomite content with minute traces of silicon oxide. The mineralogy of the rock was found to be similar as compared to Guelph dolomite rock.

4.2.2 Micro XCT of Silurian Dolomite (before experiment)

Silurian dolomite disks were prepared and scanned using Micro XCT to characterize the 3D image of the disks. Micro XCT equipment was operated at a voltage of 120kv and 10W power source. In addition, the scan time per dolomite disk was 90 minutes (approximately).

Figure 4.11 shows the Micro XCT image of the Silurian dolomite disk before conducting the reaction kinetics experiment. It can be analyzed after observing the micro XCT image of the disk that Silurian dolomite contains very less pores and natural fractures. Moreover, the rock surface is more uniform and even as compared to Guelph dolomite. The pores are compact which will restrict the rapid reaction of HCl acid with disk surface.

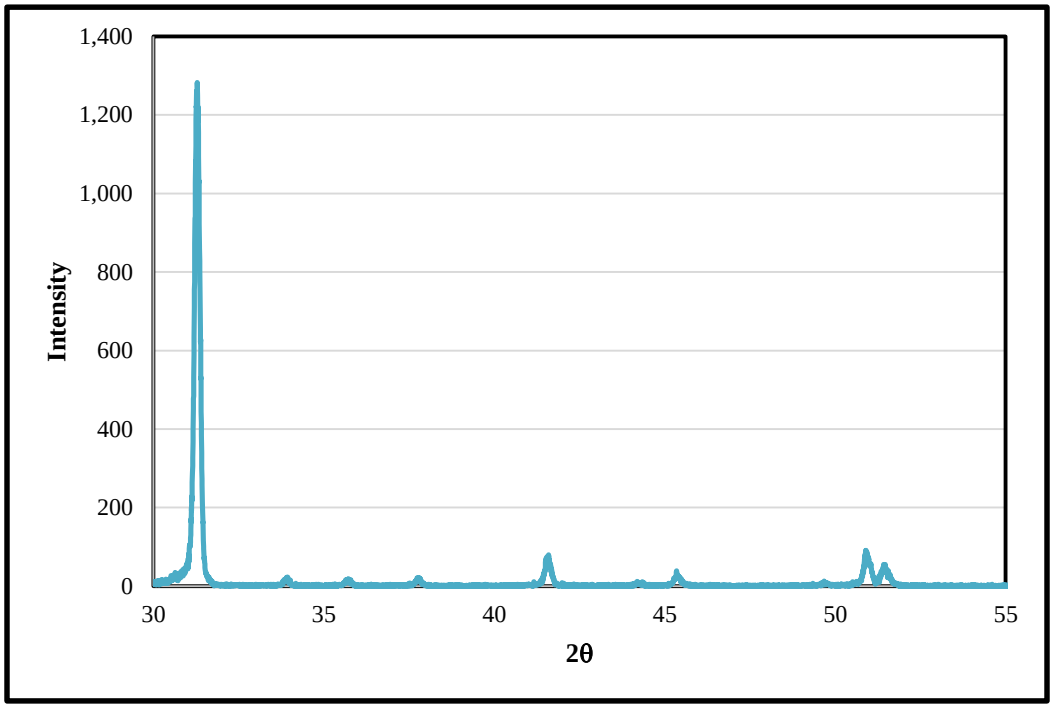

Figure 4.9: Measurement profile of Silurian dolomite XRD

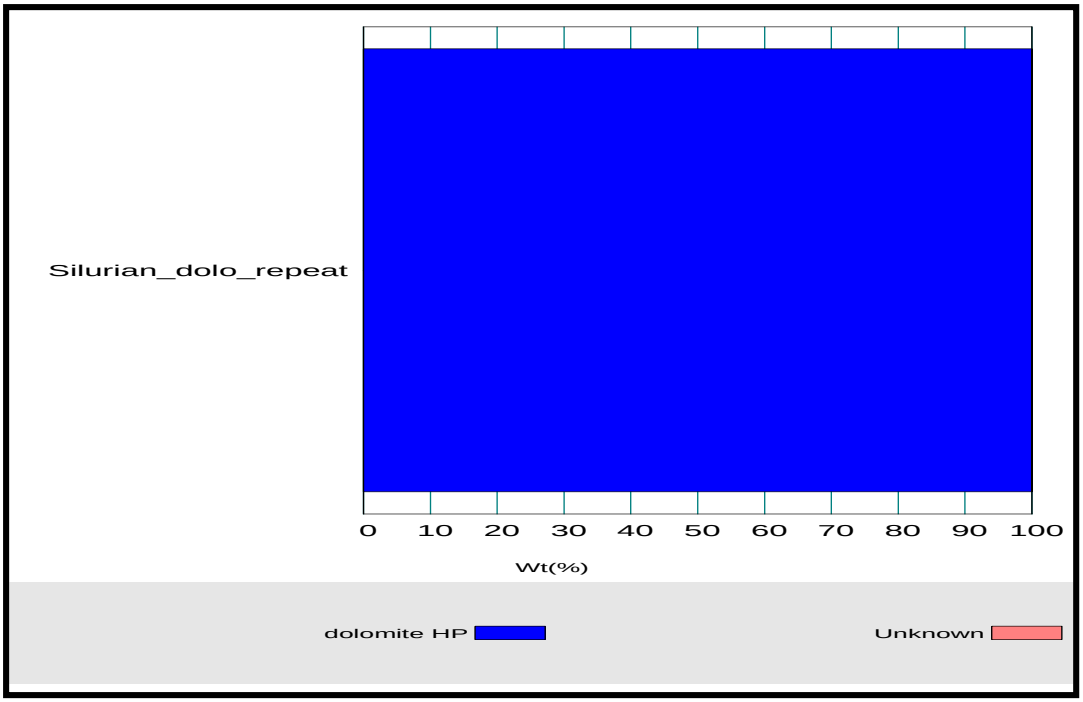

Figure 4.10: Quantitative analysis of Silurian Dolomite XRD

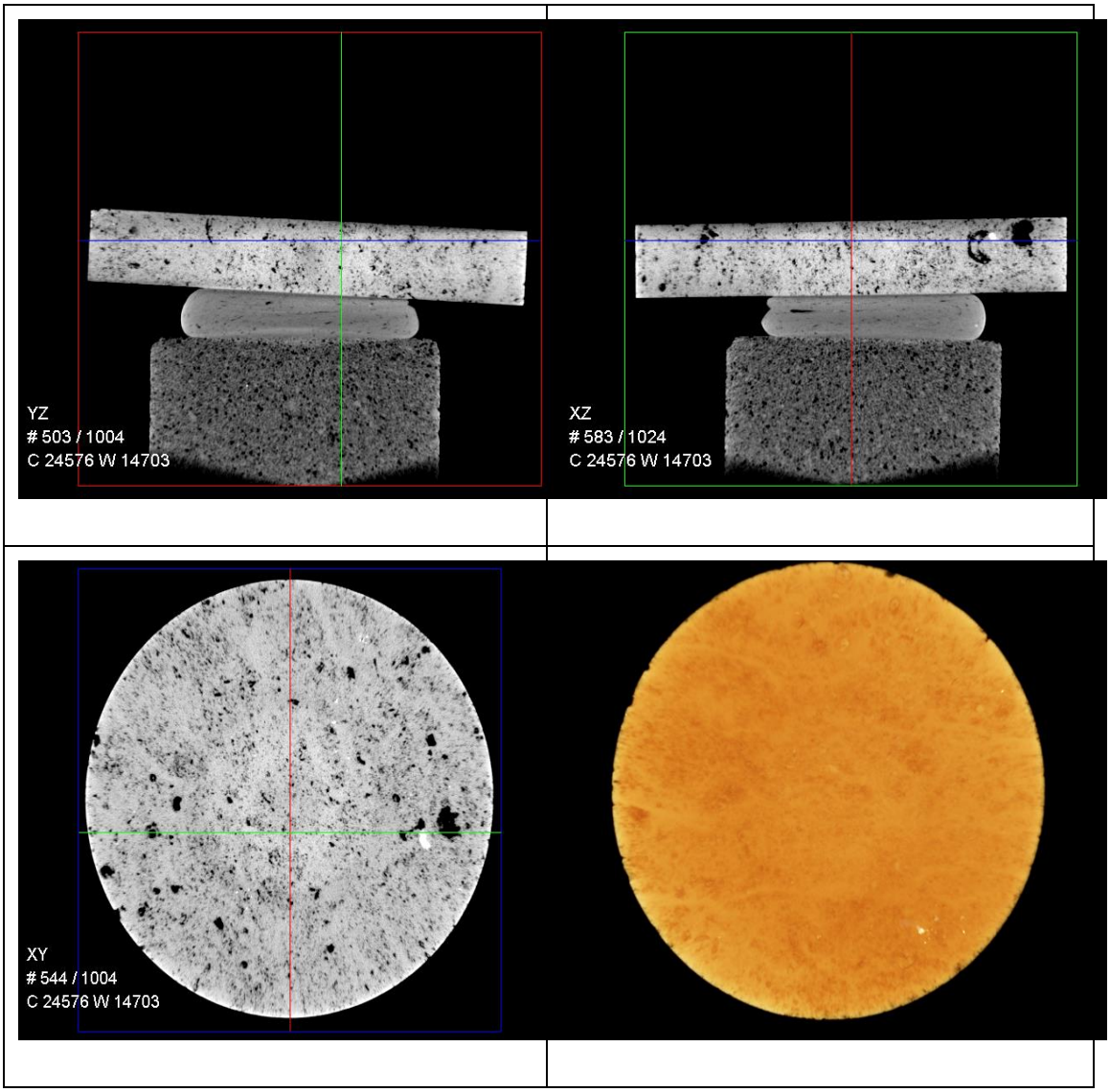

Figure 4.11: Micro XCT image of Silurian dolomite disk before reaction kinetics experiment

4.2.3 Preparation and standardization of 15 wt. % HCl acid

HCl acid was prepared to obtain 15 wt. % acid concentration which was used for reaction kinetics experiment. The molarity of fresh acid was determined using titration process and the average value was found to be 4.33 M.

4.2.4 Reaction Kinetics experiment

Rotating Disk Apparatus was used to conduct reaction kinetics measurement. A total of five experiments were conducted using Silurian dolomite disks starting from 250 rpm to 1250 rpm. The detailed procedure to conduct the experiment was described in chapter 03. The weight of the disks were measured before and after conducting each experiment which was used as a comparison for diffusion coefficient calculations. Table 4.6 shows the weight loss values for each experiment.

Table 4.6: Weight loss values for Silurian dolomite experiments - 1000 psi

Disk Rotational speed rpm	Weight of disk before experiment gm	Weight of disk after experiment gm	Weight loss (ΔW), gm
1250	19.8862	15.488	4.3982
1000	18.21	13.902	4.308
750	18.9	14.79	4.11
500	18.92	15.29	3.63
250	19.32	16.235	3.085

Figure 4.12 shows the graph between weight loss and disk rotational speeds. It can be observed from the above mentioned table that the weight loss increased as the disk rotational speed increased. However, when the disk rotational speed reached 1000 rpm, the increase in weight loss is very minimal and approximately the same. It can be analyzed that at higher rotational speeds, the reaction between Silurian dolomite and fresh acid at 1000 psi will become similar and higher disk rotation will make no difference in the rock dissolved i.e. weight loss.

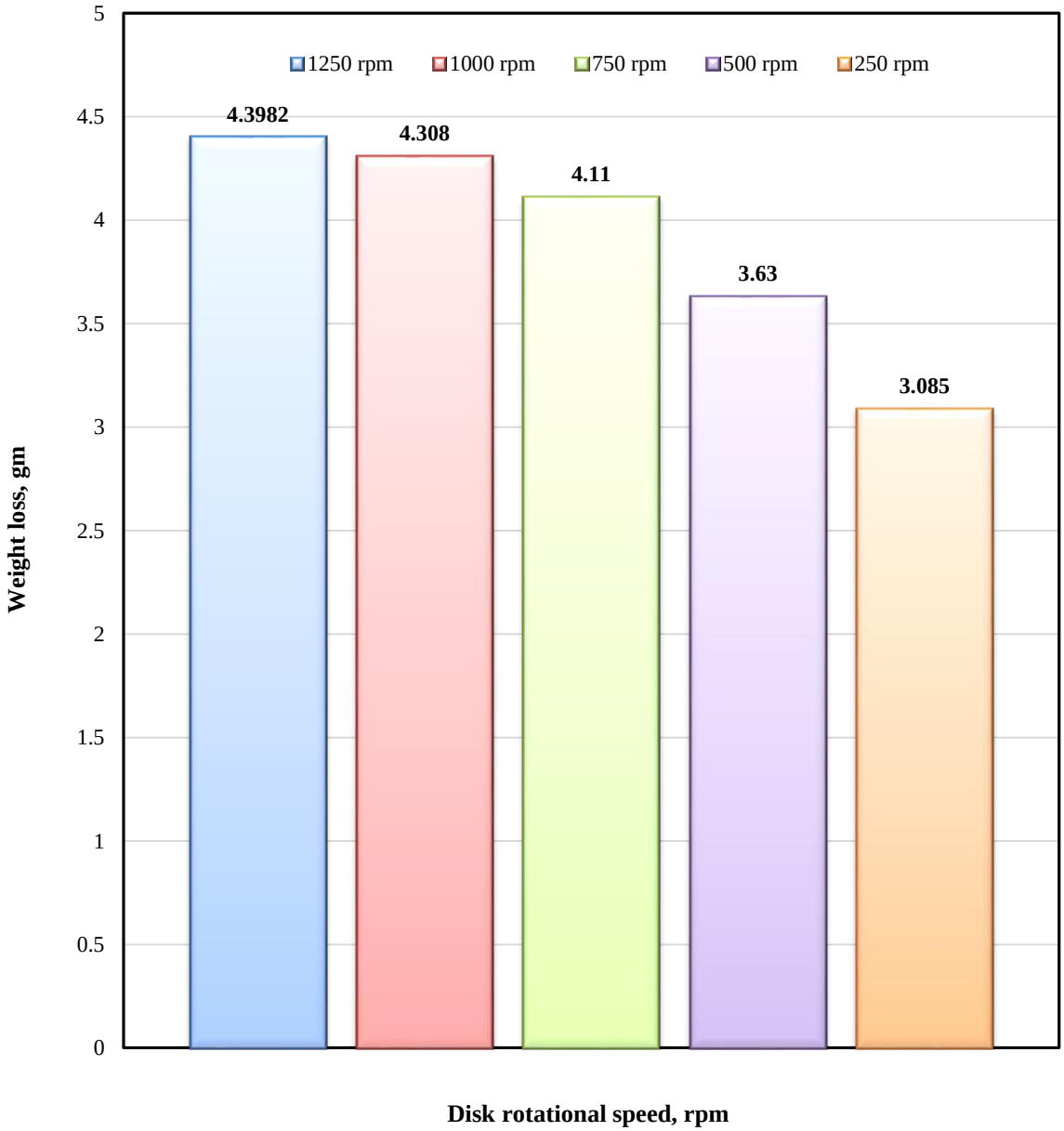

Figure 4.12: Weight loss of Silurian sample as function of RPM at 1000 psi

4.2.5 Diffusion Coefficient Analysis

The samples collected from the reaction kinetics experiment were then diluted and their calcium and magnesium concentrations were determined using AAS. The concentrations were then used to calculate dissolution rates as well as the diffusion coefficient. Table 4.7 shows the calculated values for dissolution rates and "F" function using weight loss results as well as using AAS results.

Table 4.7: Diffusion Coefficient Analysis calculations, Silurian dolomite – 1000 psi

Disk rotational speed rpm	$\sqrt{w}$ **rad/sec**	**Dissolution rates mole/s.cm^2**	**F (using weight loss results)**	**F (using AAS results)**
1250	11.4419	4.24834E-06	1.30E-03	1.30E-03
1000	10.2339	4.1723E-06	1.30E-03	1.30E-03
750	8.8628	3.94007E-06	1.24E-03	1.26E-03
500	7.2365	3.52387E-06	1.11E-03	1.11E-03
250	5.1170	3.00635E-06	9.44E-04	9.55E-04

Figure 4.13 and 4.14 shows the graph between "F" function vs. the square root of disk rotational speed using weight loss results and AAS results respectively. It can be observed from the Figures that reaction between Silurian dolomite and fresh acid at 1000 psi was mass transfer limited at low disk rotational speeds. However, the reaction was surface limited at high disk rotational speeds i.e. from 1000 rpm to 1250 rpm.

Using the slopes in Figure 4.13 and 4.14, diffusion coefficient was obtained. The diffusion coefficient obtained using weight loss and AAS results was **7.155×10^{-07} cm^2/sec**.

4.2.6 Micro XCT of dolomite disks (after experiment)

The reacted dolomite disks for 500 rpm and 1250 rpm were scanned using Micro XCT to characterize the nature of reaction and describe the pore structure. Figure 4.15 and 4.16 shows the Micro XCT images of the disk used in 500 rpm and 1250 rpm experiments, respectively. It can be observed that at 500 rpm, the dissolution of the disk was less. Reaction occurred only on the areas where the disk contain some small holes. In addition, the sides of the disk remain unreacted. However, 1250 rpm, the dissolution increased as compared to 500 rpm. The sides of the disk were also reacted with acid leading to a non-uniform reacted surface. Moreover, the entire surface of the disk was reacted.

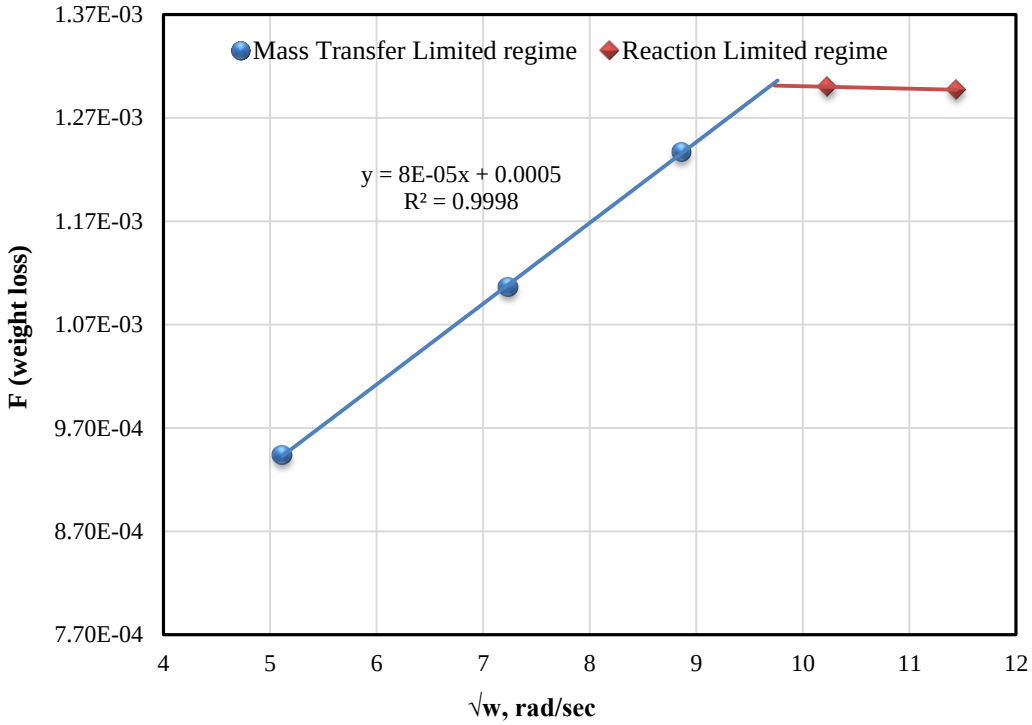

Figure 4.13: Diffusion Coefficient Graph (using weight loss results), Silurian dolomite – 1000 psi

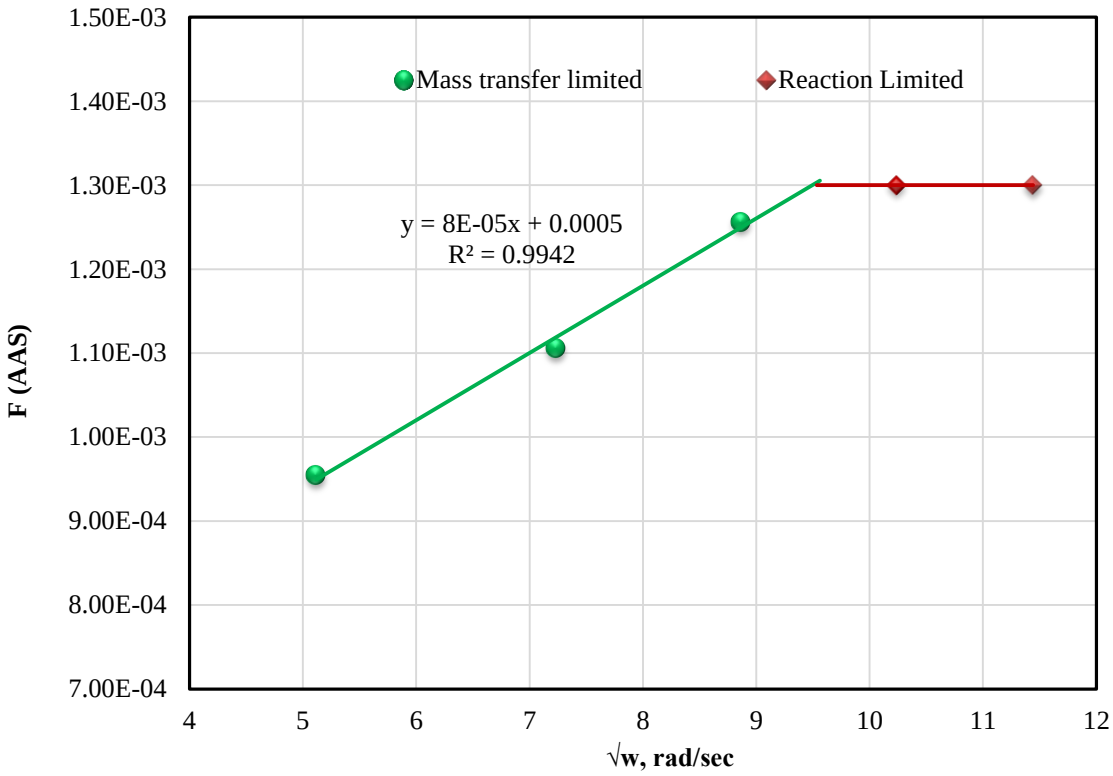

Figure 4.14: Diffusion Coefficient Graph (using AAS results), Silurian dolomite – 1000 psi

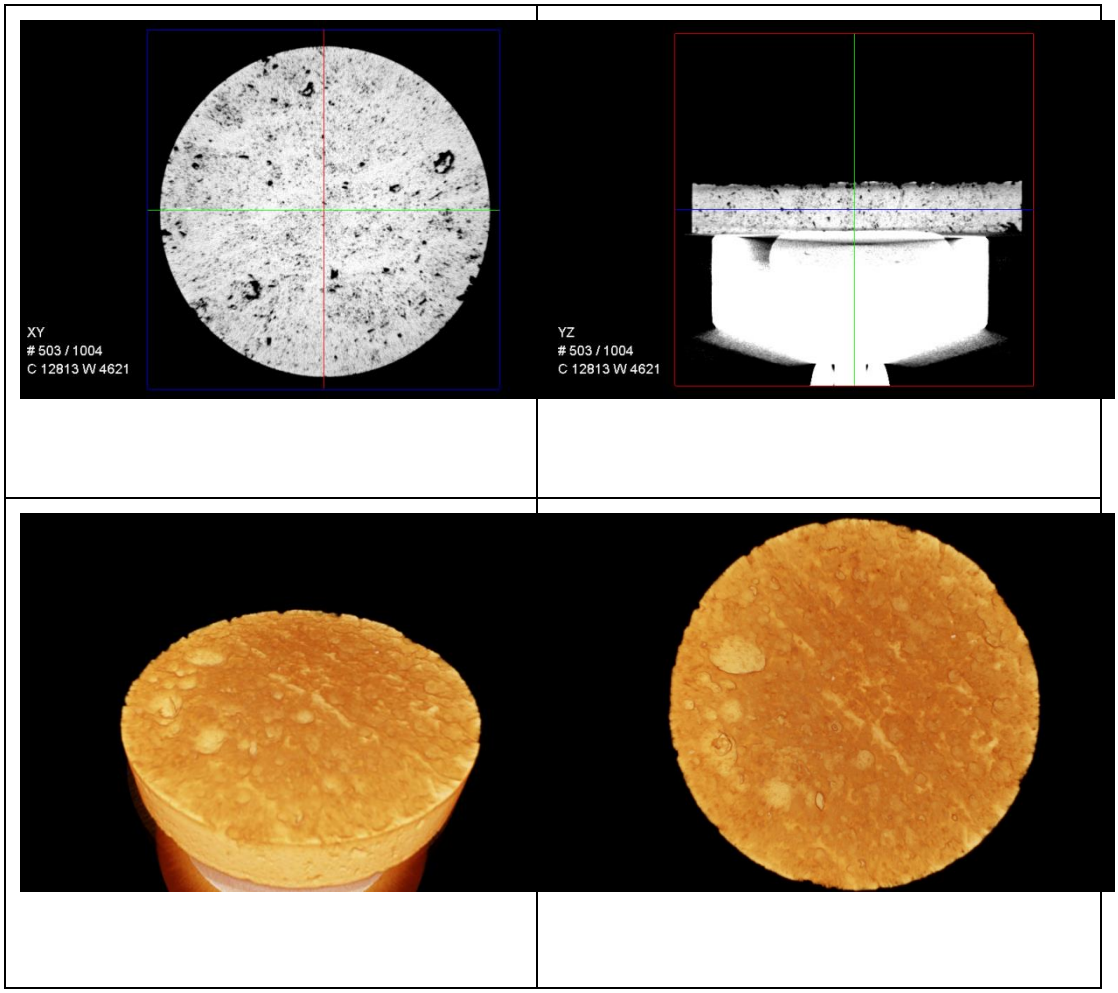

Figure 4.15: Micro XCT image of reacted disk at 500 rpm, Silurian dolomite – 1000 psi

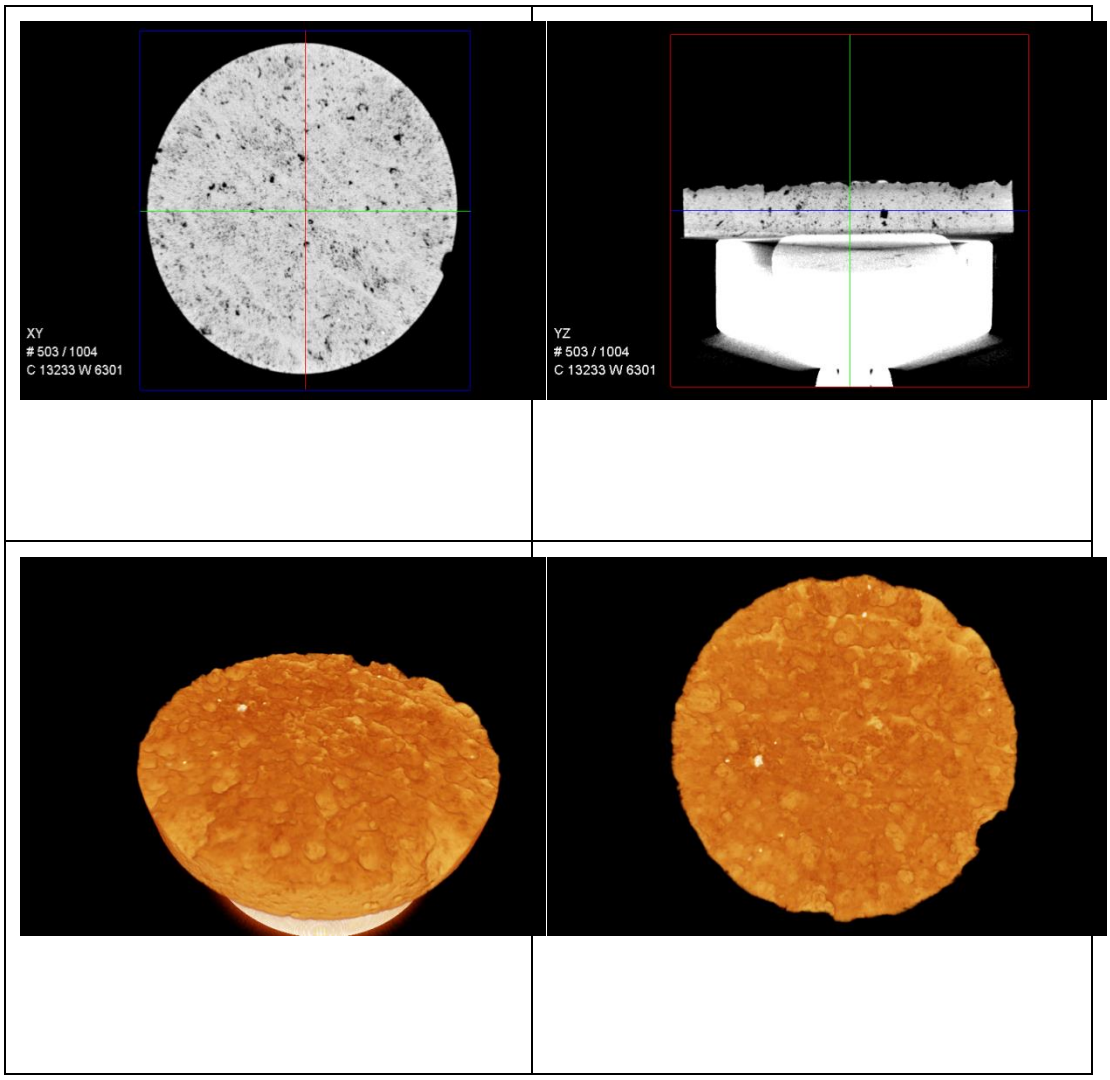

Figure 4.16: Micro XCT image of reacted disk at 1250 rpm, Silurian dolomite – 1000 psi

4.3 Silurian Dolomite at 3000 psi (15 wt. % HCl) Acid

The experimental parameters to conduct experiments for Silurian Dolomite at 3000 psi (15 wt. % HCl) Acid which will be referred to as Series # 03 are listed in Table 4.8.

The third series experiments were conducted using Silurian Dolomite rock; the same rock which was used to conduct experiments for 1000 psi (series # 02). Silurian dolomite used does not contain any natural pores and fractures as compared to Guelph dolomite. The core was 12" in length and 1.5" in diameter. Dolomite core were cut into disks that were approximately 1.5 inch in diameter and 0.27 inch in thickness. The pressure range for this series was 3000 psi. Total five experiments were conducted starting from low disk rotational speeds (250 rpm) to high disk rotational speed (1250 rpm). The Silurian dolomite porosity was measured and found to be 10%.

Table 4.8: Experimental conditions for series # 03 – 3000 psi – 15 wt. % acid

Experiment Parameters	
Rock Type	Dolomite
Core Type	Silurian Dolomite
Temperature, ˚C	65
Pressure, psi	3000
Acid Type	HCl
Concentration of HCl, wt. %	15
Disk Rotational Speeds, rpm	250, 500, 750, 1000, 1250

XRD results remain the same as discussed in series 02 results section. Moreover, the micro XCT result (before reaction kinetic experiments) for Silurian dolomite disk remain the same as discussed in series 02 results section. The following sections present the detailed results for series 03 experiments.

4.3.1 Preparation and standardization of 15 wt. % HCl acid

HCl acid was prepared to obtain 15 wt. % acid concentration which was used for reaction kinetics experiment. The molarity of fresh acid was determined using titration process and the average value was found to be 4.453 M.

4.3.2 Reaction Kinetics experiment

Rotating Disk Apparatus was used to conduct reaction kinetics measurement. A total of five experiments were conducted using Silurian dolomite disks starting from 250 rpm to 1250 rpm. The detailed procedure to conduct the experiment was described in chapter 03. The weight of the disks were measured before and after conducting each experiment which was used as a comparison for diffusion coefficient calculations. Table 4.9 shows the weight loss values for each experiment.

Figure 4.17 shows the graph between weight loss and disk rotational speeds. It can be observed that as the disk rotational speed increased, the weight loss values increased but at low disk rotational speeds i.e. until 750 rpm. However, when the disk rotational speed reached 1000 rpm, the weight loss value becomes constant and there was no further increment in it at 1250 rpm. In addition, at high disk rotational speeds the increase in weight loss becomes very less as compared to the increase in weight loss from 250 – 500 rpm and 500 – 750 rpm.

Table 4.9: Weight loss values for Silurian dolomite experiments - 3000 psi

Disk Rotational speed rpm	**Weight of disk before experiment gm**	**Weight of disk after experiment gm**	**Weight loss (ΔW), gm**
1250	19.57	15.99	3.58
1000	19.067	15.482	3.58
750	18.9986	15.883	3.1156
500	18.82	15.872	2.948
250	18.74	16.29	2.45

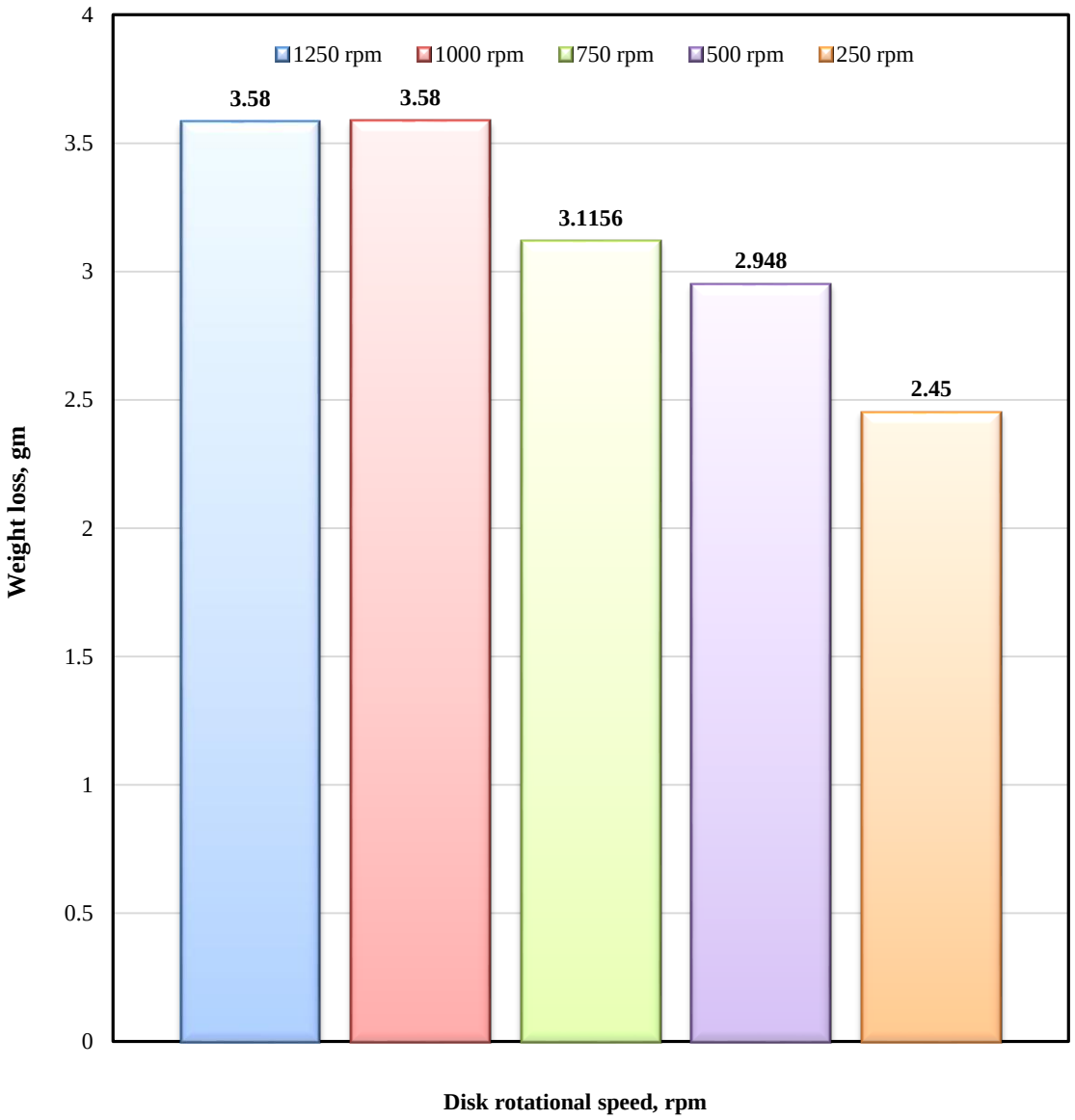

Figure 4.17: Weight loss values for Silurian sample as a function of RPM at 3000 psi

4.3.3 Diffusion Coefficient Analysis

The samples collected from the reaction kinetics experiment were then diluted and their calcium and magnesium concentrations were determined using AAS. The concentrations were then used to calculate dissolution rates as well as the diffusion coefficient. Table 4.10 shows the calculated values for dissolution rates and "F" function using weight loss results as well as using AAS results.

Figure 4.18 and Figure 4.19 shows the graph between "F" function vs. the square root of disk rotational speed using weight loss results and AAS results respectively. It was observed that at low disk rotational speeds, the reaction was mass transfer limited as the dissolution rates increased as a function of rpm until 750 rpm. However, at high disk rotational speeds, the reaction was limited by surface reaction rate.

Table 4.10: Diffusion Coefficient Analysis calculations, Silurian dolomite – 3000 psi

Disk rotational speed rpm	**$\sqrt{w}$ rad/sec**	**Dissolution rates mole/s.cm^2**	**F (using weight loss results)**	**F (using AAS results)**
1250	11.4419	3.46E-06	1.10E-03	1.10E-03
1000	10.2339	3.46E-06	1.10E-03	1.10E-03
750	8.8628	3.01E-06	9.20E-04	9.00E-04
500	7.2365	2.83653E-06	8.70E-04	8.40E-04
250	5.1170	2.36E-06	7.30E-04	7.02E-04

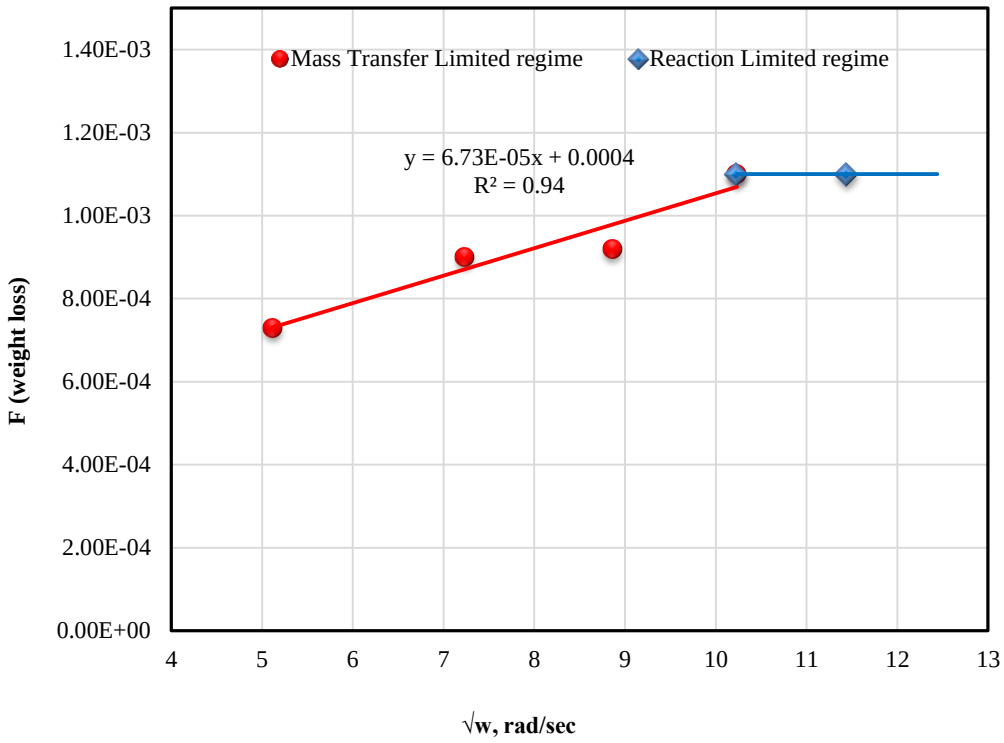

Figure 4.18: Diffusion Coefficient Graph (using weight loss results), Silurian dolomite – 3000 psi

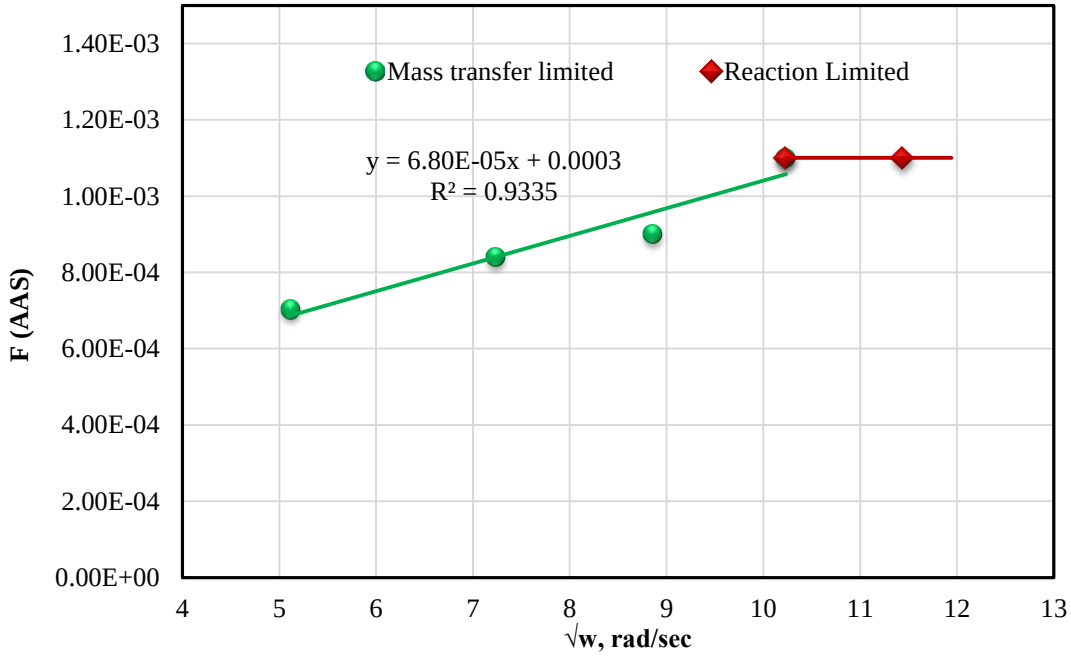

Figure 4.19: Diffusion Coefficient Graph (using AAS results), Silurian dolomite – 3000 psi

Using the slopes in Figure 4.18 and 4.19, diffusion coefficient was obtained. The diffusion coefficient values obtained from weight loss results was **5.521×10^{-07} cm^2/sec** and from AAS results was **5.61×10^{-07} cm^2/sec.**

4.3.4 Micro XCT of dolomite disks (after experiment):

The reacted dolomite disks for 500 rpm and 1250 rpm were scanned using Micro XCT to characterize the nature of reaction and describe the pore structure. Figure 4.20 and Figure 4.21 shows the Micro XCT images of the reacted disk used in 500 rpm and 1250 rpm experiments, respectively. At 500 rpm, the reaction between disk and acid is very minimal. However, at 1250 rpm, the dissolution increased. In addition, the reaction at the center of the disk was less as compared to the reaction taking place at the edges of the disk.

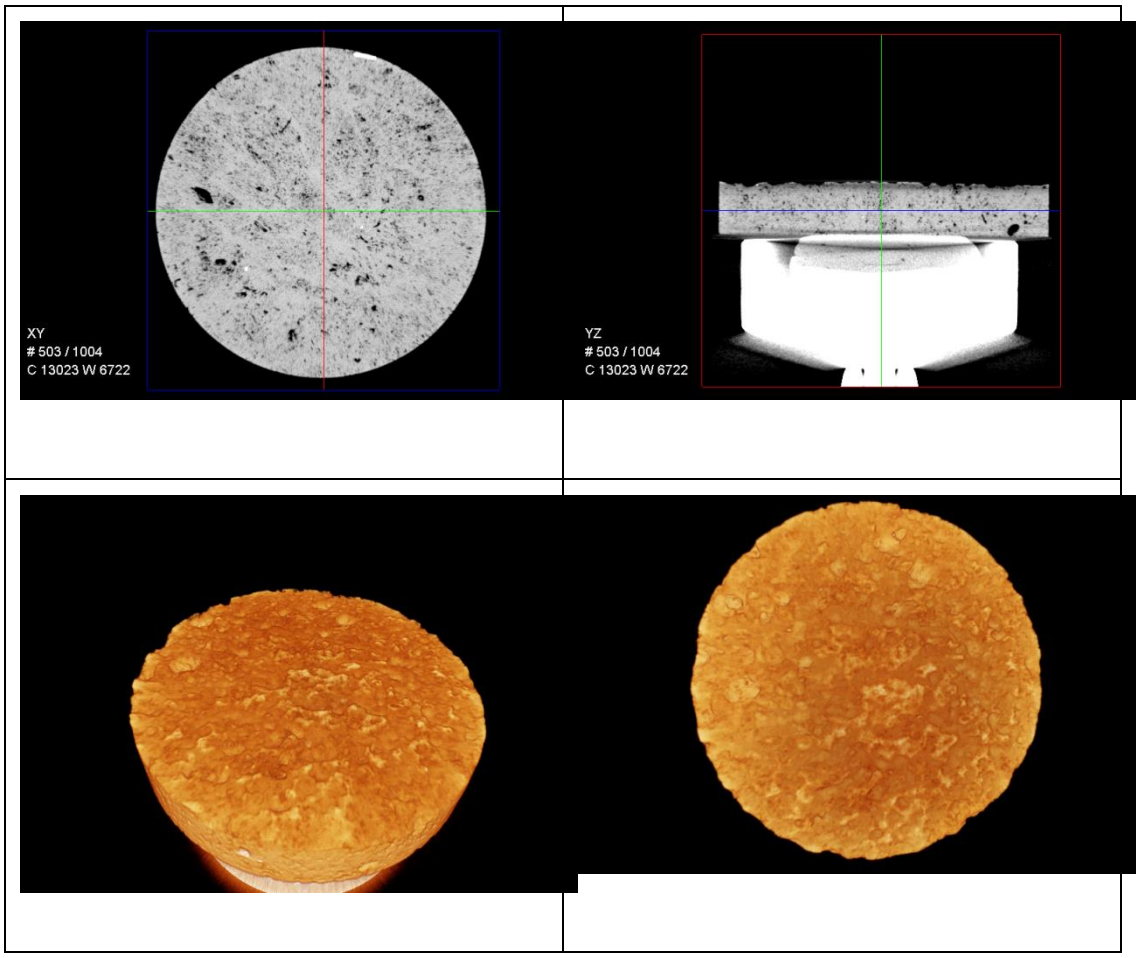

Figure 4.20: Micro XCT image of reacted disk at 500 rpm, Silurian dolomite – 3000 psi

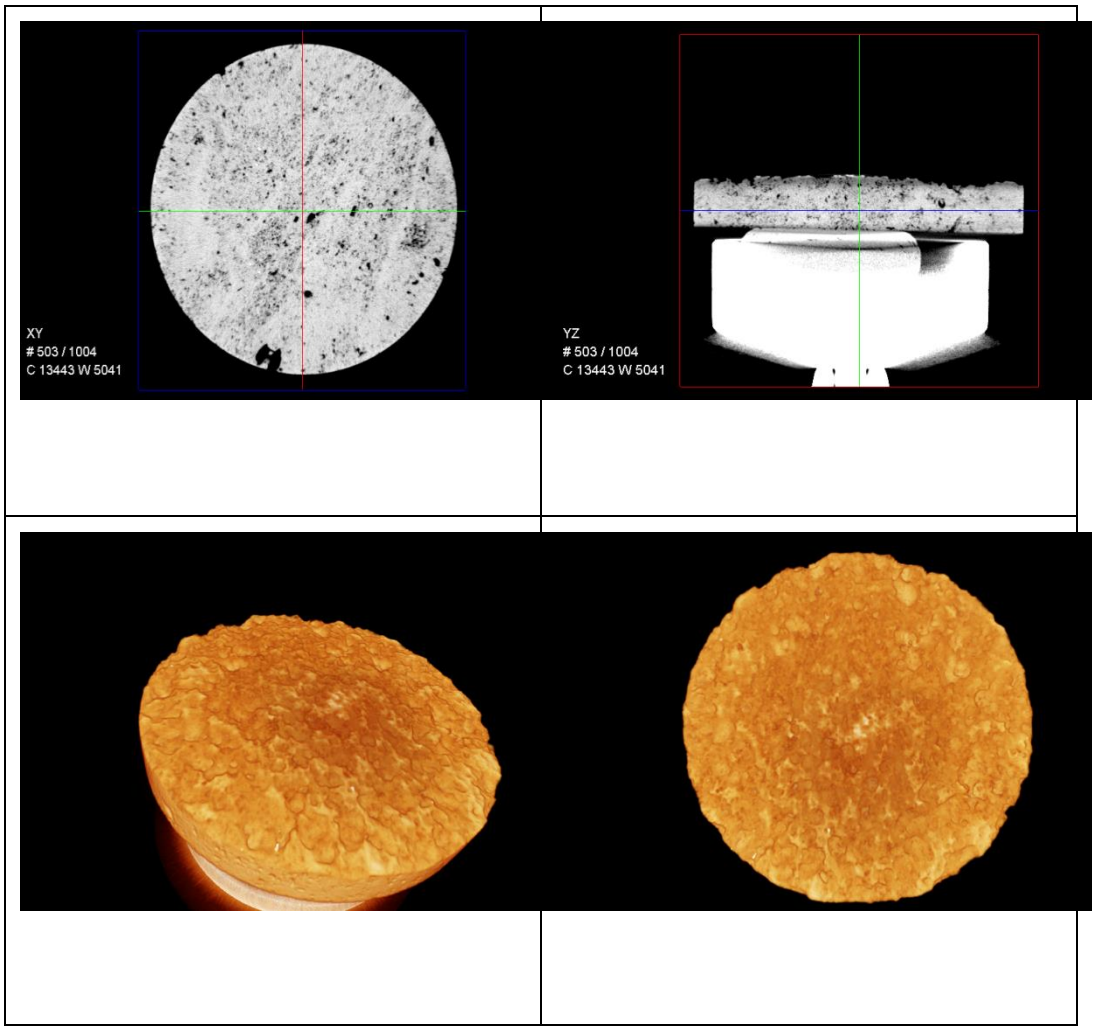

Figure 4.21: Micro XCT image of reacted disk at 1250 rpm, Silurian dolomite – 3000 psi

4.4 Discussion of Results

4.4.1 Effect of Pressure

The experiments conducted at 1000 psi and 3000 psi and their results gives clear indication of the significant impact of pressure on dissolution rates and diffusion coefficient. It can be observed that at low pressure, CO_2, which is produced by the reaction between HCl acid and dolomite rock, is present in gaseous phase. It enhances the mass transfer of hydrogen ions from the bulk solution to the surface of the rock/disk leading to an unending supply of fresh acid in the body of the disk until the experiment is finished. Hence it results in the overestimated values of reaction rates and diffusion coefficient. The mass transfer coefficient is thus significantly increased.

The experimental results demonstrate that 1000 psi is not sufficient to keep CO_2 in solution which is by no means representative of true reservoir conditions. Using reaction kinetics data obtained from low pressure in a wormhole design model may lead to an underestimation of wormhole penetration at pressures above 1000 psi.

However, at high pressure experiments i.e. 3000 psi , CO_2 is soluble in aqueous solution and tends to buffer the diffusion of hydrogen ions from the bulk solution to the rock surface leading to a lower reaction rate and diffusion coefficient.

The diffusion coefficient obtained using Silurian dolomite at low pressure was **7.155×10^{-07} cm^2/sec** and at high pressure was **5.610×10^{-07} cm^2/sec.** These results were in compliance with weight loss results and dissolution rates obtained at 1000 psi and 3000 psi. The weight loss and dissolution rates decreased as the pressure was elevated to 3000 psi. Micro XCT images also provided the confirmation regarding the impact of pressure discussed above. It can be analyzed through the images that at low pressure reaction rate increased leading

to more dissolution. However images obtained at 3000 psi depicts the decrease in reaction between acid and disk. Figure 4.22 shows the comparison of diffusion coefficients obtained at 1000 psi and 3000 psi experiments using Silurian dolomite rock. There was approximately 23% decrease in the diffusion coefficient value when compared with 1000 psi results. The decrease in the diffusion coefficient is not as significant as it would occurred in acid-calcite reaction. The reason being that dolomite rocks are less reactive in nature as compared to calcite rocks.

4.4.2 Effect of disk rotational speed (RPM)

Disk rotational speed also impacts the diffusion coefficient results. It was found that conducting experiments at 1000 psi using Guelph dolomite, the reaction was mass transfer limited. Reaction limited regime was not reached until 1250 rpm. The mass transfer coefficient was significantly increased as well as the diffusion coefficient.

On the other hand, conducting experiments at 1000 psi and 3000 psi using Silurian dolomite, two regimes occur because of the fluid/solid reaction. It was concluded that at low disk rotational speeds, the dissolution rate increased with the disk rotational speed. Hence the reaction was mass transfer limited till 750 rpm. The dissolution rate increased because the diffusion layer boundary of the rotating disk is large at low disk rotational speeds and therefore diffusion limits the reaction. However, at high rpms, the dissolution rate became constant and there was no further increase in the reaction rates. This occurred because the reaction rate in this regime is limited by the surface reaction rate. At high disk rotating speeds, the diffusion boundary layer is decreased and the mass transfer across the boundary layer no longer limits the rate of reaction.

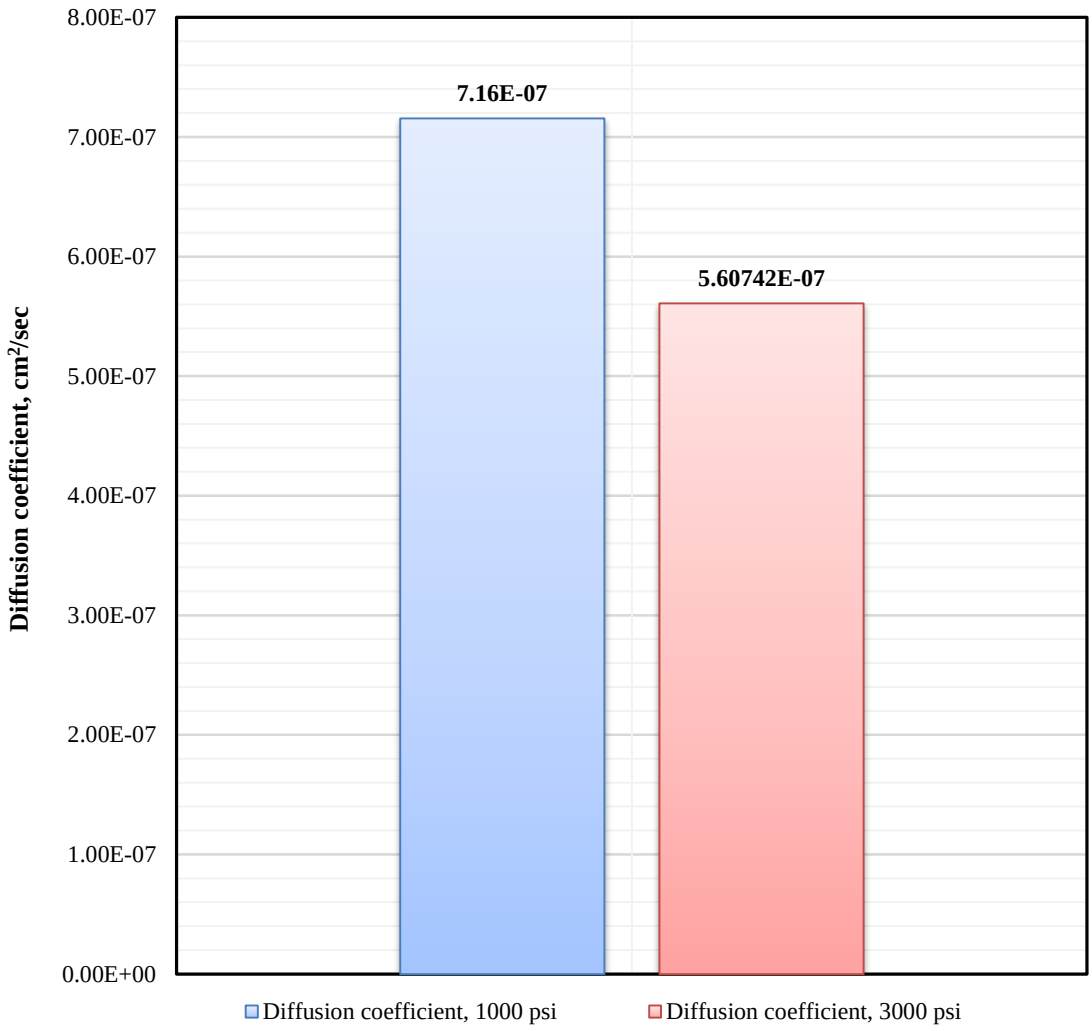

Figure 4.22: Comparison of computed diffusion coefficients at 1000 psi and 3000 psi

4.4.3 Effect of rock/disk surface

Two types of rock types were used to study the impact of low pressure conditions on dissolution rates and diffusion coefficient; Guelph and Silurian dolomite. The rock porosity was similar i.e. 10%. In addition, the XRD of the rocks showed similar dolomite content (99% purity). Figure 4.23 shows the comparison of XRD results for Guelph and Silurian dolomite rocks. It can be observed that both rocks showed the highest peak at the same two theta angle range i.e. 30 - 35.

However, the rocks differ in the shape of the surface or the channel through which acid flowed (i.e. rock morphology). It was observed from Micro XCT images of the rocks that Guelph dolomite rock surface contain small pores and natural fractures. The rock surface was also not uniform. However, Silurian dolomite had a uniform surface and does not contain fractures or holes inside it. The effect of the rock shape on diffusion coefficient results was significant. It can be observed that diffusion coefficient significantly increased when experiments were conducted using Guelph dolomite rock. However, there was a decrease in the diffusion coefficient result when Silurian dolomite was used to conduct the experiments. Similar observation was noted for weight loss values. The interesting point to note is that the rock porosity and pressure range was kept same.

The diffusion coefficient results were in compliance with micro XCT images obtained using two different rocks. It was observed that Guelph dolomite reacted very fast as compared to Silurian dolomite at 1000 psi pressure condition. In addition, acid penetrated deep inside the top surface of the disk resulting in holes as well as dissolution of small part of the disk at high disk rotational speeds. The dissolution was not uniform using Guelph

dolomite. On the other hand, Silurian dolomite showed uniformity in dissolution and no acid penetration was observed at high rotational speeds.

4.4.4 Weight Loss Analysis

The weight loss values for Guelph dolomite and Silurian dolomite experiments at high and low pressure were presented in the results section. It can be concluded that the weight loss percentage increased with increasing the disk rotational speed. In addition, the pressure did impact the weight loss percentage of the disk. It was found that at low pressure the weight loss values were high due to CO_2 in gaseous form. But the weight loss values decreased as the pressure reached 3000 psi as CO_2 was soluble in aqueous solution. Therefore, the reaction rate decreased at high pressure as compared to low pressure. Figure 4.24 shows comparison of weight loss values at 1000 and 3000 psi experiments.

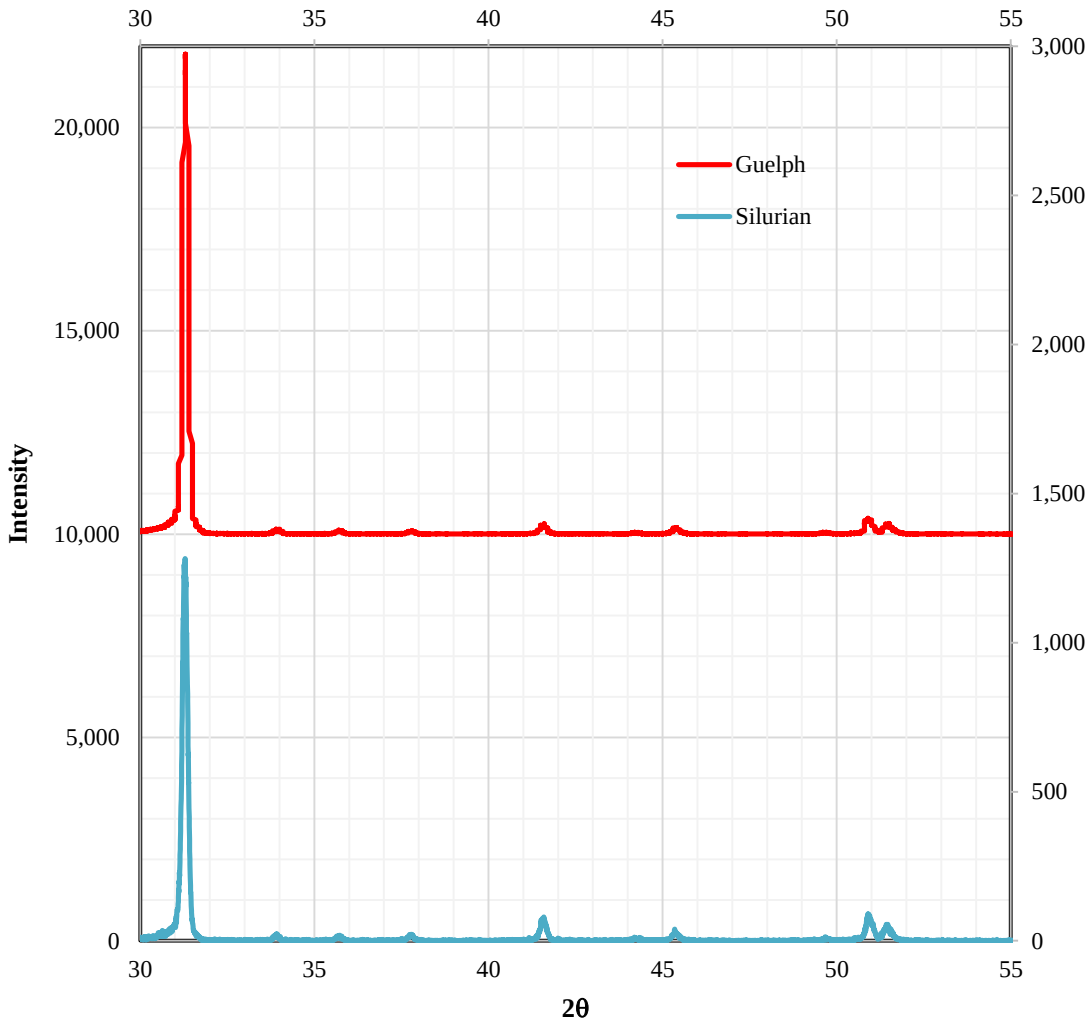

Figure 4.23: Comparison of XRD results for Guelph and Silurian dolomite rock

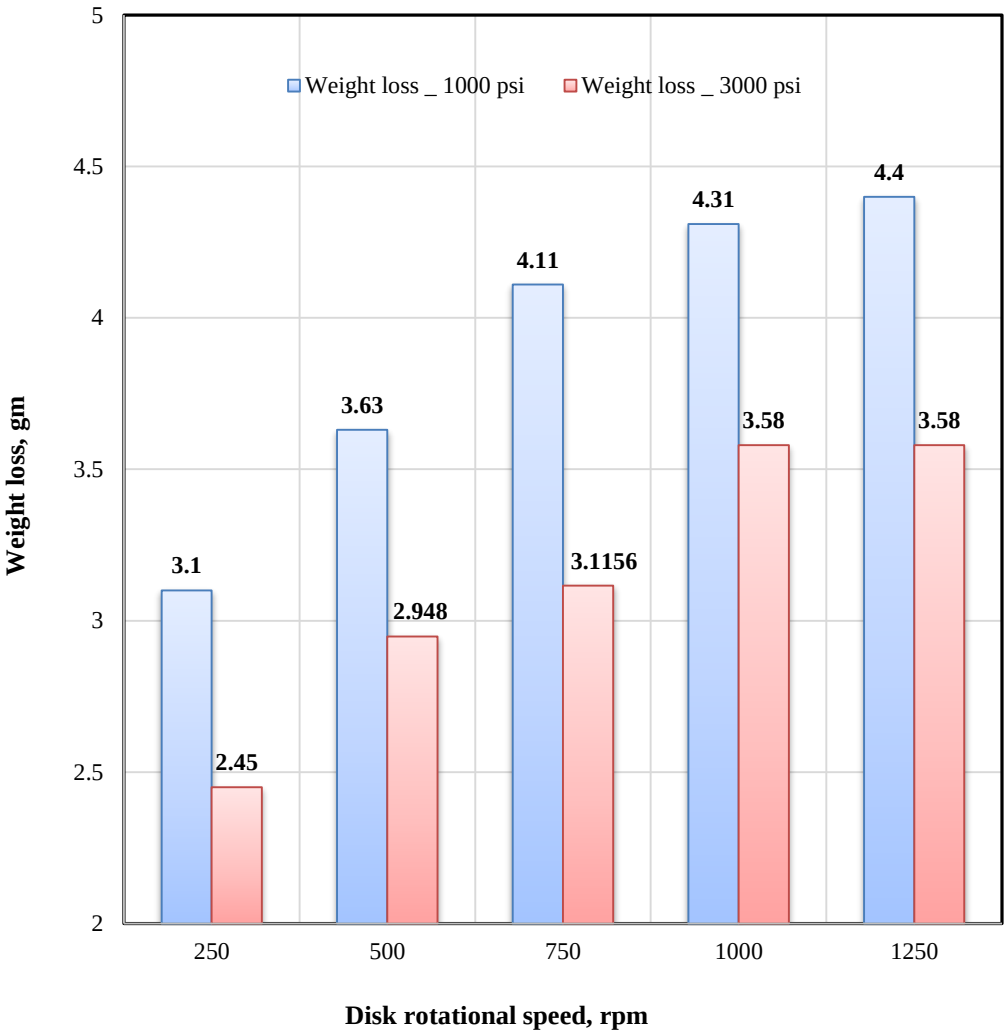

Figure 4.24: Comparison of computed weight loss values at 1000 psi and 3000 psi

4.4.5 Comparison of Diffusion Coefficient Results with Calcite

Qiu *et al.* (2014) studied the reaction kinetics of hydrochloric acid with calcite marble at the same experimental conditions as mentioned in this thesis work. The results are shown in the below mentioned table and compared with Dolomite study conducted in this thesis.

It can be observed that there was a significant decrease in diffusion coefficient of dolomite when compared with calcite. The reason being the slow reaction rate of dolomite which leads to the significant reduction in the results.

Pressure, psi	**Diffusion Coefficient, cm^2/sec**	
	Calcite	**Dolomite (Current Study)**
1000	6.48×10^{-05}	7.15×10^{-07}
3000	4.7×10^{-05}	5.52×10^{-07}

CHAPTER 5

EFFECT OF SPENT ACID ON DIFFUSION COEFFICIENT OF DOLOMITIC ROCK AT HIGH PRESSURE

The conventional wormhole models use the diffusion coefficient of fresh acid to predict the wormholing process. A fresh acid diffusion coefficient may be representative of the wormhole propagation close to the injection point but as the wormhole penetrates deeper into the formation, the tip of the wormhole contains predominantly spent acid. Using fresh acid reaction kinetics data can thereby overestimate the dissolution rate as it is not representative as the wormhole penetrates deeper into the formation. In order to properly quantify the acid penetration deep into the formation, a diffusion coefficient representing the level of acid spending at the tip should be employed.

Qiu *et al.* (2013) studied the impact of reaction products on reaction kinetics and described the laboratory procedures to obtain it. Rotating disk apparatus was used to compare the dissolution rate of a partially spent system- 15% HCl spent to 10% HCl- to a 10% fresh HCl solution using limestone core samples by varying disk rotational speeds. It was found that the reaction rate for the partially spent system was low as compared to fresh acid system. Moreover, diffusion coefficient of a spent acid system was significantly lower than the fresh acid system (30% less). The experiment also concluded that the reaction products (CO_2 and counterions) buffered the diffusion of H^+ ions in the spent acid mixture, decreasing the mass transfer coefficient which resulted in slower dissolution rates.

The second main objective of our research was to study the effect of spent acid on diffusion coefficient and reaction kinetics at elevated pressure of 3000 psi and temperature of 65°C using three different spent acid concentrations:

- 12.5 wt. %
- 10 wt. %
- 7.5 wt.%

In order to fulfill the above mentioned objective, fifteen experiments were conducted to study the impact of spent acid concentrations on the diffusion coefficient of dolomite rock at 3000 psi. The experiments were divided into three sets as shown in Table 5.1. The results for each of the three series of the experiments are described in the following sections.

Table 5.1: Experimental Layout for Spent acid – Dolomite

Pressure (psi)	**HCl concentration (wt. %)**	**Dolomite Used**	**Disk Rotational Speeds (rpm)**				
			250	**500**	**750**	**1000**	**1250**
3000	12.5	Silurian Dolomite	Exp 16	Exp 17	Exp 18	Exp 19	Exp 20
	10	Silurian Dolomite	Exp 21	Exp 22	Exp 23	Exp 24	Exp 25
	7.5	Silurian Dolomite	Exp 26	Exp 27	Exp 28	Exp 29	Exp 30

5.1 Silurian Dolomite at 3000 psi (12.5 wt. % spent HCl) Acid

The experimental parameters to conduct experiments for Silurian Dolomite at 3000 psi (12.5 wt. % spent HCl) Acid which will be referred as Series # 01 are listed in Table 5.2.

The first series experiments were conducted using Silurian Dolomite rock; the same rock which was used to conduct series # 02 and series # 03 experiments to study the impact of pressure. The core was 12" in length and 1.5" in diameter. Dolomite core were cut into disks that were 1.5 inch in diameter and 0.27 inch in thickness. The pressure range for this series was 3000 psi. Total five experiments were conducted starting from low disk rotational speeds (250 rpm) to high disk rotational speed (1250 rpm). The Silurian dolomite porosity was measured and found to be 10%.

Table 5.2: Experimental conditions for series # 01 – 3000 psi – 12.5 wt. % spent acid

Experiment Parameters	
Rock Type	Dolomite
Core Type	Silurian Dolomite
Temperature, ˚C	65
Pressure, psi	3000
Acid Type	HCl
Concentration of HCl, wt. %	12.5
Disk Rotational Speeds, rpm	250, 500, 750, 1000, 1250

XRD results remain the same as discussed in previous section (chapter 04). The purity of the dolomite used was approximately 99% with very less traces of silica and clay. Moreover, the micro XCT result (before reaction kinetic experiments) for Silurian dolomite disk also remain the same as discussed in previous section (chapter 04). The following sections present the detailed results for series # 01 experiments for spent acid 12.5 wt. %.

5.1.1 Preparation and standardization of 12.5 wt. % HCl acid

HCl acid (15 wt. %, 60 ml) was mixed with known quantity of dolomite powder (2.151 gm) at ambient conditions to prepare 12.5 wt. % acid concentration. The acid and powder was left to react until all the powder was dissolved. The resulting solution was then titrated to determine the molarity of the acid which was used in subsequent calculations of diffusion coefficient and dissolution rates. The molarity of 12.5 wt. % spent acid was found to be 3.69 M (average value).

5.1.2 Reaction Kinetics experiment

Rotating Disk Apparatus was used to conduct reaction kinetics measurement. A total of five experiments were conducted using Silurian dolomite disks starting from 250 rpm to 1250 rpm. The detailed procedure to conduct the experiment was described in chapter 03. The amount of dolomite powder used in the experiments was 21.51 gm dissolved in 600 ml 15 wt. % HCl acid to obtain 12.5 wt. % acid concentration during the experiment. The duration of conducting experiments were increased in order to completely dissolve the dolomite powder in acid. Since dolomite is also slow in reaction, it takes longer time to completely dissolve with acid. The weight of the disks were measured before and after

conducting each experiment which was used as a comparison for diffusion coefficient calculations. Table 5.3 shows the weight loss values for each experiment.

Table 5.3: Weight loss values for Silurian dolomite experiments – 12.5 wt. %, 3000 psi

Disk Rotational speed rpm	Weight of disk before experiment gm	Weight of disk after experiment gm	Weight loss (ΔW), gm
1250	19.152	16.1663	3.0
1000	19.606	16.477	3.0
750	19.674	17.01	2.664
500	18.574	16.29	2.28
250	19.424	17.37	2.054

Figure 5.1 shows the graph between weight loss and disk rotational speeds. It can be observed that as the disk rotational speed increased, the weight loss values increased but at low disk rotational speeds i.e. until 750 rpm. However, when the disk rotational speed reached 1000 rpm, the weight loss value becomes constant and there was no further increment in it at 1250 rpm. In addition, the increase in weight loss from 250 – 750 rpm lied in the range from 2.1 – 2.6 gm. However, as soon as disk rotational speed reached 1000 rpm, the weight loss increased to 3 gm.

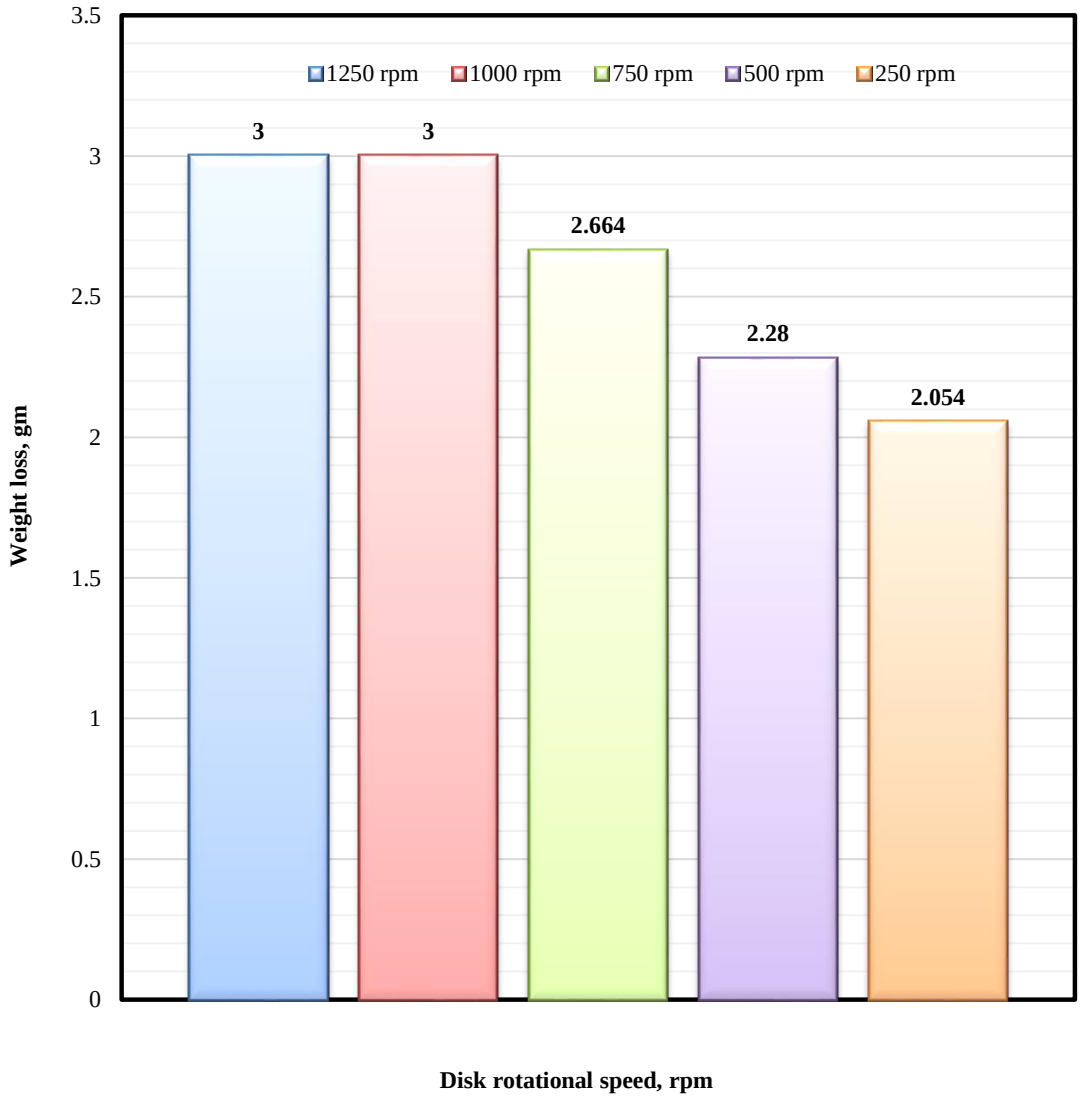

Figure 5.1: Weight loss for Silurian sample as a function of RPM for 12.5 wt. % spent acid at 3000 psi

5.1.3 Diffusion Coefficient Analysis

The samples collected from the reaction kinetics experiment were then diluted and their calcium and magnesium concentrations were determined using AAS. The concentrations were then used to calculate dissolution rates as well as the diffusion coefficient. Table 5.4 shows the calculated values for dissolution rates and "F" function using weight loss results as well as using AAS results.

Figure 5.2 and 5.3 shows the graph between "F" function vs. the square root of disk rotational speed using weight loss results and AAS results respectively. It was observed that at low disk rotational speeds (i.e. until 750 rpm), the reaction was mass transfer limited. However, at high disk rotational speeds, the reaction was surface reaction limited.

Table 5.4: Diffusion Coefficient Analysis calculations, Silurian dolomite – 12.5 wt. %, 3000 psi

Disk rotational speed rpm	$\sqrt{w}$ **rad/sec**	**Dissolution rates mole/s.cm^2**	**F (using weight loss results)**	**F (using AAS results)**
1250	11.4419	2.90E-06	1.06E-03	1.07E-03
1000	10.2339	2.90E-06	1.06E-03	1.07E-03
750	8.8628	2.59E-06	9.10E-04	9.10E-04
500	7.2365	2.22E-06	8.15E-04	8.00E-04
250	5.1170	1.99E-06	7.32E-04	7.42E-04

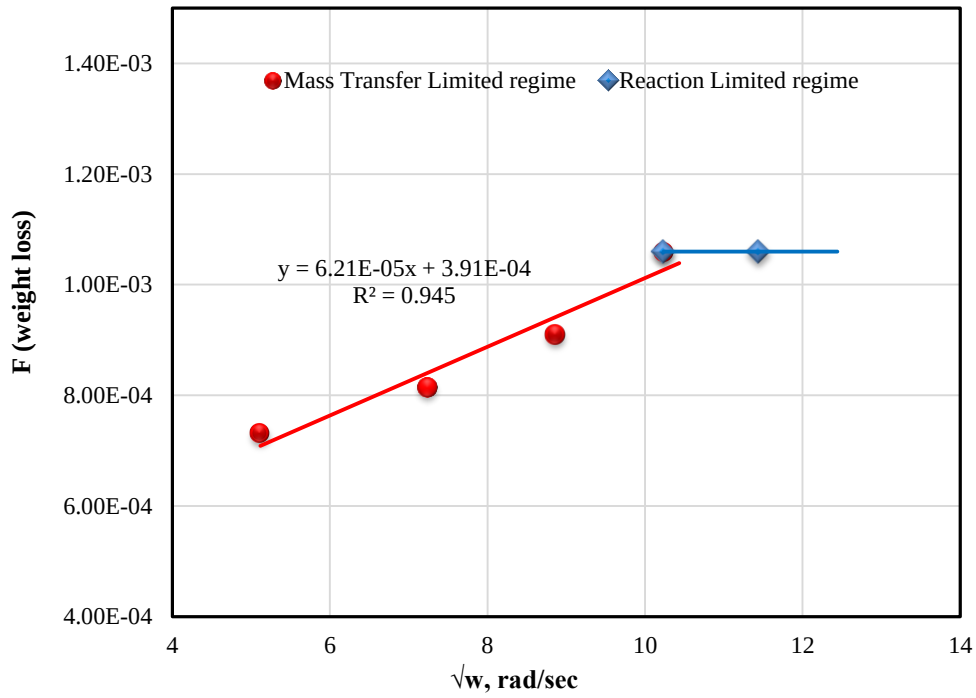

Figure 5.2: Diffusion Coefficient Graph (using weight loss results), Silurian dolomite – 12.5 wt. %, 3000 psi

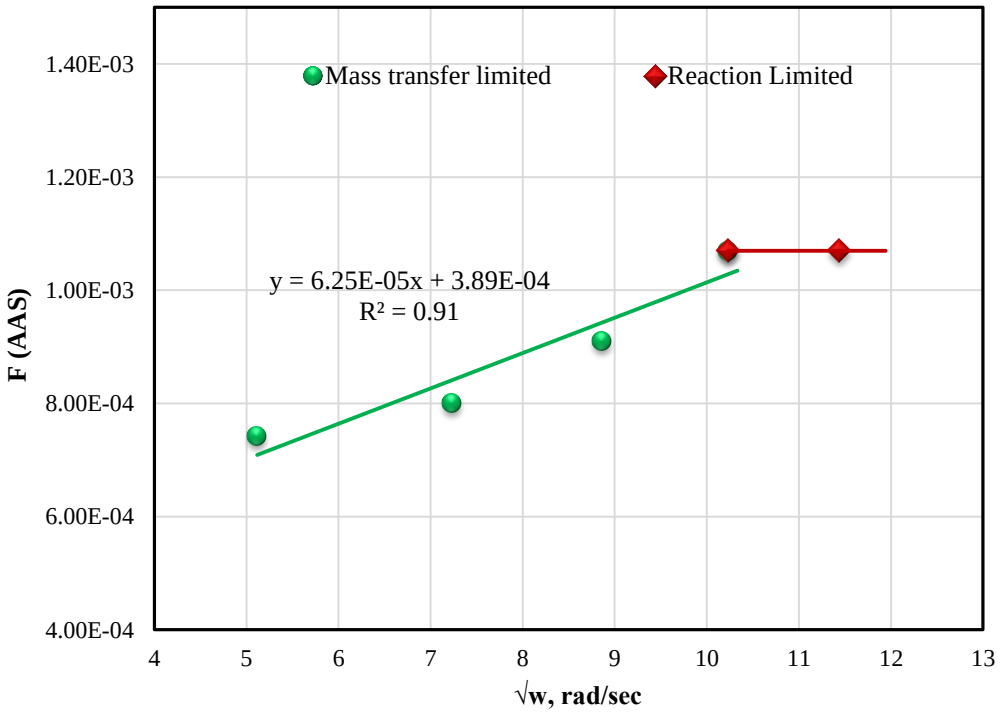

Figure 5.3: Diffusion Coefficient Graph (using AAS results), Silurian dolomite – 12.5 wt. %, 3000 psi

Using the slopes in Figure 5.2 and 5.3, diffusion coefficient values were obtained. The diffusion coefficient value obtained using weight loss results was **4.89×10^{-07} cm^2/sec** and using AAS results was **4.941×10^{-07} cm^2/sec.**

5.1.4 Micro XCT of dolomite disks (after experiment)

The reacted dolomite disks for 500 rpm and 1250 rpm were scanned using Micro XCT to characterize the nature of reaction and describe the pore structure. Figures 5.4 and 5.5 shows the Micro XCT images of the disk used in 500 rpm and 1250 rpm experiments, respectively. At 500 rpm, the dissolution was found to be less. Reaction only occurred at places where the disk originally contain some small holes and spots. However, at 1250 rpm, dissolution of the disk by acid was increased as compared to 500 rpm. In addition, the edges of the disk were also dissolved by the acid.

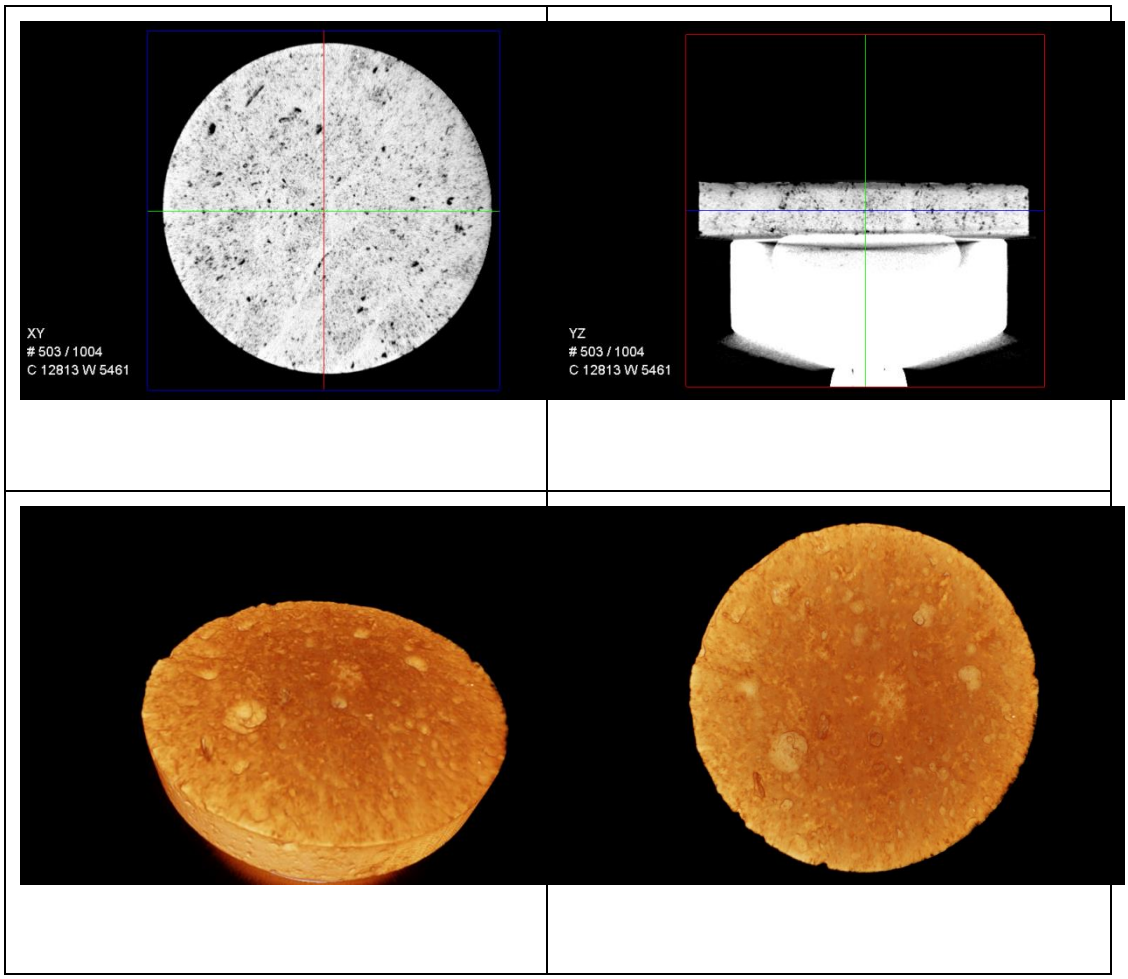

Figure 5.4: Micro XCT image of reacted disk at 500 rpm, Silurian dolomite – 12.5 wt. %, 3000 psi

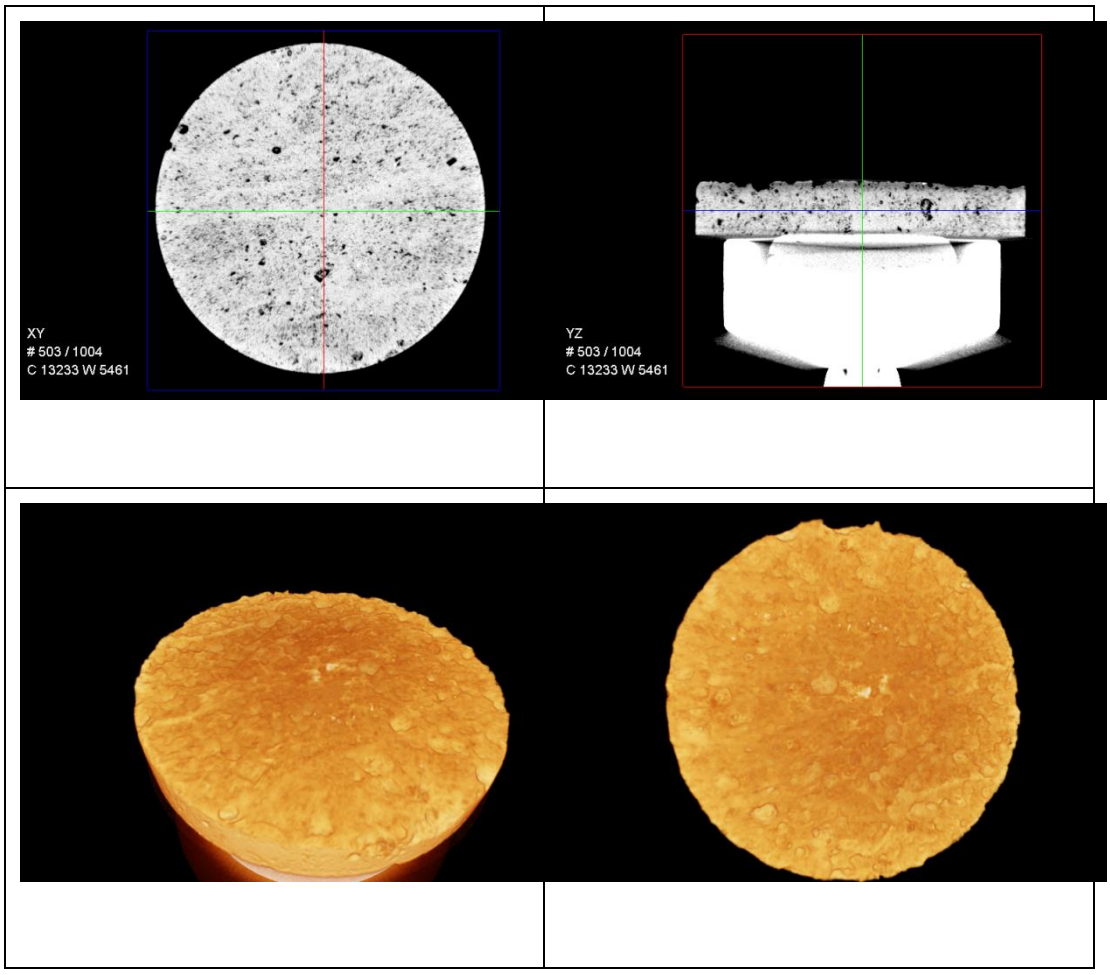

Figure 5.5: Micro XCT image of reacted disk at 1250 rpm, Silurian dolomite – 12.5 wt. %, 3000 psi

5.2 Silurian Dolomite at 3000 psi (10 wt. % spent HCl) Acid

The experimental parameters to conduct experiments for Silurian Dolomite at 3000 psi (10 wt. % spent HCl) Acid which will be referred as Series # 02 are listed in Table 5.5. The second series experiments for spent 10 wt. % were conducted using Silurian Dolomite rock. The core was 12" in length and 1.5" in diameter. The pressure range for this series was 3000 psi. Total five experiments were conducted starting from low disk rotational speeds (250 rpm) to high disk rotational speed (1250 rpm). A new Silurian dolomite core was used to prepare disks. The Silurian dolomite porosity was measured and found to be 13% as compared to the previous core porosity which was 10%. The following sections present the detailed results for series # 02 experiments for spent acid 10 wt. %.

Table 5.5: Experimental conditions for series # 02 – 3000 psi – 10 wt. % spent acid

Experiment Parameters	
Rock Type	Dolomite
Core Type	Silurian Dolomite
Temperature, ˚C	65
Pressure, psi	3000
Acid Type	HCl
Concentration of HCl, wt. %	10
Disk Rotational Speeds, rpm	250, 500, 750, 1000, 1250

5.2.1 Preparation and standardization of 10 wt. % HCl acid

HCl acid (15 wt. %, 60 ml) was mixed with known quantity of dolomite powder (4.232 gm) at ambient conditions to prepare 10 wt. % acid concentration. The acid and powder was left to react until all the powder was dissolved. The resulting solution was then titrated to determine the molarity of the acid which was used in subsequent calculations of diffusion coefficient and dissolution rates. The molarity of 10 wt. % spent acid was found to be 2.896 M (average value).

5.2.2 Reaction Kinetics experiment

Rotating Disk Apparatus was used to conduct reaction kinetics measurement. A total of five experiments were conducted using Silurian dolomite disks starting from 250 rpm to 1250 rpm. The detailed procedure to conduct the experiment was described in chapter 03. The amount of dolomite powder used in the experiments was 42.52 gm dissolved in 600 ml of 15 wt. % HCl acid to obtain 10 wt. % acid concentration during the experiment. The duration of conducting experiments were increased in order to completely dissolve the dolomite powder in acid. Since dolomite is also slow in reaction, it takes longer time to completely dissolve with acid. The weight of the disks were measured before and after conducting each experiment which was used as a comparison for diffusion coefficient calculations. Table 5.6 shows the weight loss values for each experiment.

Table 5.6: Weight loss values for Silurian dolomite experiments – 10 wt. %, 3000 psi

Disk Rotational speed rpm	Weight of disk before experiment gm	Weight of disk after experiment gm	Weight loss (ΔW), gm
1250	20.2398	16.937	3.3028
1000	19.754	16.9768	2.7772
750	19.734	17.19	2.544
500	19.6873	17.323	2.36
250	20.08	17.792	2.288

Figure 5.6 shows the graph between weight loss and disk rotational speeds. It can be observed that as the disk rotational speed increased, the percentage weight loss also increased. The weight loss values lied in the range from 2.3 – 2.77 gm when experiments were conducted from 250 rpm to 1000 rpm. However, when the disk rotational speed increased to 1250 rpm, there was a significant increase in weight loss i.e. 3.3 gm. It was also observed at high disk rotational speeds that the weight loss values were not constant as observed for 12.5 wt. % experiments.

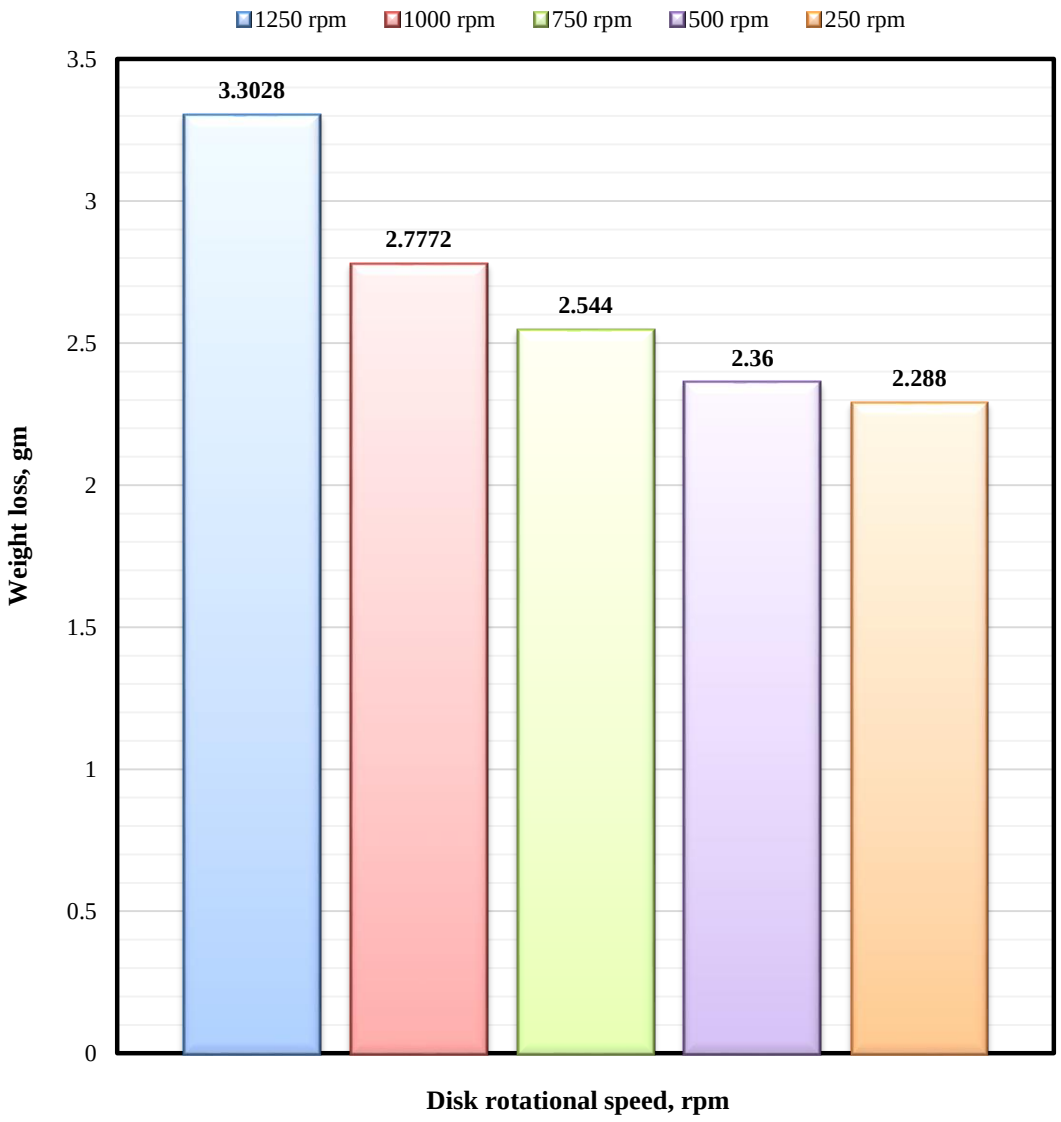

Figure 5.6: Weight loss for Silurian sample as a function of RPM for spent 10 wt. % acid at 3000 psi

5.2.3 Diffusion Coefficient Analysis

The samples collected from the reaction kinetics experiment were then diluted and their calcium and magnesium concentrations were determined using AAS. The concentrations were then used to calculate dissolution rates as well as the diffusion coefficient. Table 5.7 shows the calculated values for dissolution rates and "F" function using weight loss results as well as using AAS results.

Table 5.7: Diffusion Coefficient Analysis calculations, Silurian dolomite – 10 wt. %, 3000 psi

Disk rotational speed rpm	$\sqrt{w}$ **rad/sec**	**Dissolution rates mole/s.cm^2**	**F (using weight loss results)**	**F (using AAS results)**
1250	11.4419	2.81E-06	1.52E-03	1.50E-03
1000	10.2339	2.35E-06	1.30E-03	1.36E-03
750	8.8628	2.17E-06	1.20E-03	1.30E-03
500	7.2365	2.01E-06	1.09E-03	1.09E-03
250	5.1170	1.94E-06	1.01E-03	1.49E-03

Figures 5.7 and 5.8 shows the graph between "F" function vs. the square root of disk rotational speed using weight loss results and AAS results respectively. It was observed that the reaction was controlled by mas transfer limited regime. Surface limited regime was not observed spent 10 wt. % experiments. The slope obtained using both weight loss and AAS results was 9.83×10^{-05} and 9.39×10^{-05} respectively. In addition, the dissolution rate and "F" value obtained at 250 rpm experiment was not considered to calculate the diffusion coefficient. The reason being that around 3 gm. of the dolomite powder remain undissolved at the end of the experiment and 10 wt. % acid concentration was not achieved. Hence the results for 250 rpm experiment were not in acceptable range.

Using the slopes in Figure 5.7 and 5.8, diffusion coefficient was obtained. The diffusion coefficient value obtained using weight loss results was **9.75×10^{-07} cm^2/sec** and using AAS results was **9.099×10^{-07} cm^2/sec.**

5.2.4 Micro XCT of dolomite disks (after experiment)

The reacted dolomite disks for 500 rpm and 1250 rpm were scanned using Micro XCT to characterize the nature of reaction and describe the pore structure. Figure 5.9 and 5.10 shows the Micro XCT images of the disk used in 500 rpm and 1250 rpm experiments, respectively. It was observed that the dissolution of the acid by rock was increased for both 500 and 1250 rpm experiments. At 500 rpm, the surface of the disk was relatively smooth when compared with 1250 rpm. Small amount of acid also penetrated at the edge of the disk. On the other hand, dissolution was increased at 1250 rpm and the edges of the disk came in contact with the acid. The disk surface was non-uniform in shape after reaction.

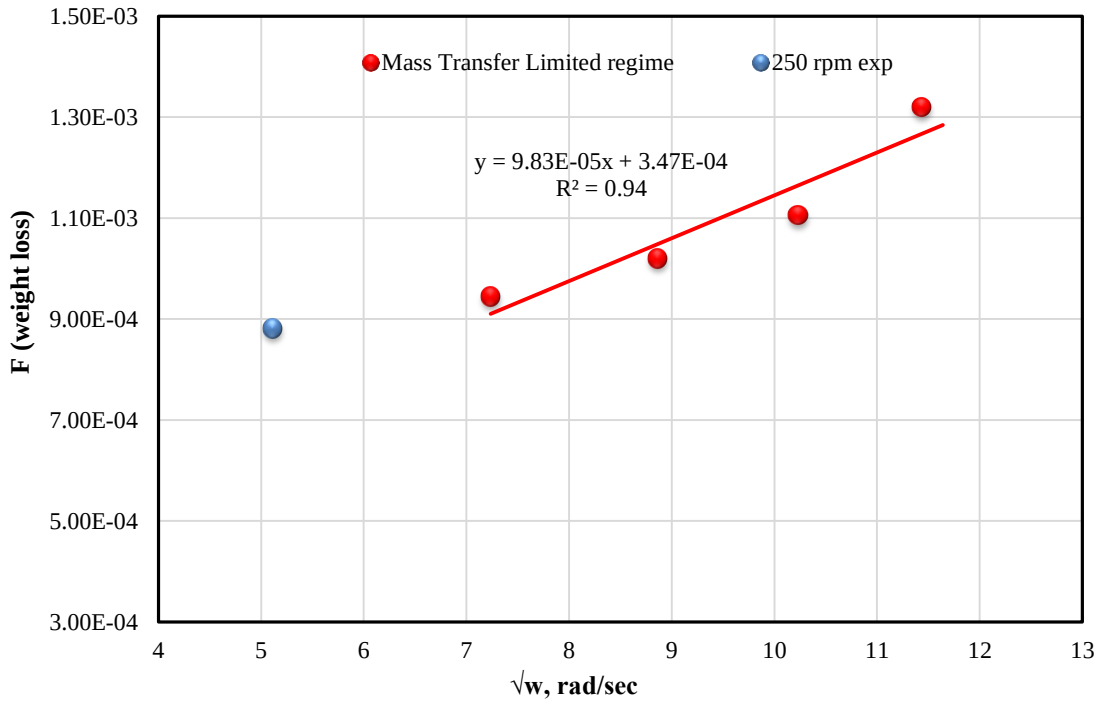

Figure 5.7: Diffusion Coefficient Graph (using weight loss results), Silurian dolomite – 10 wt. %, 3000 psi

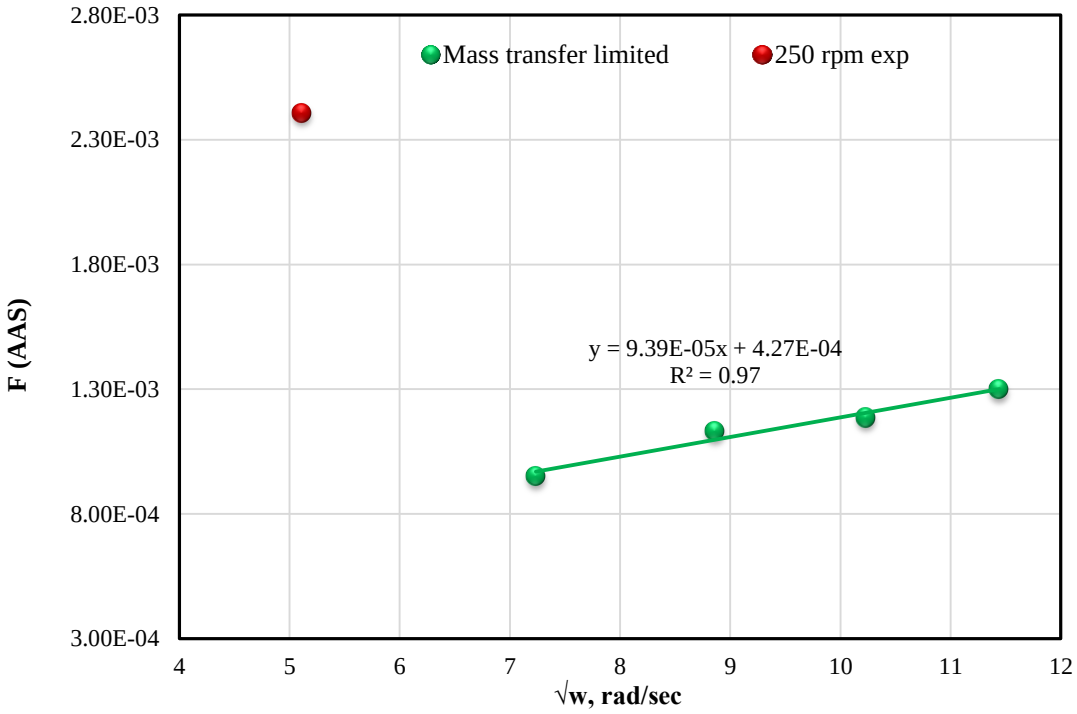

Figure 5.8: Diffusion Coefficient Graph (using AAS results), Silurian dolomite – 10 wt. %, 3000 psi

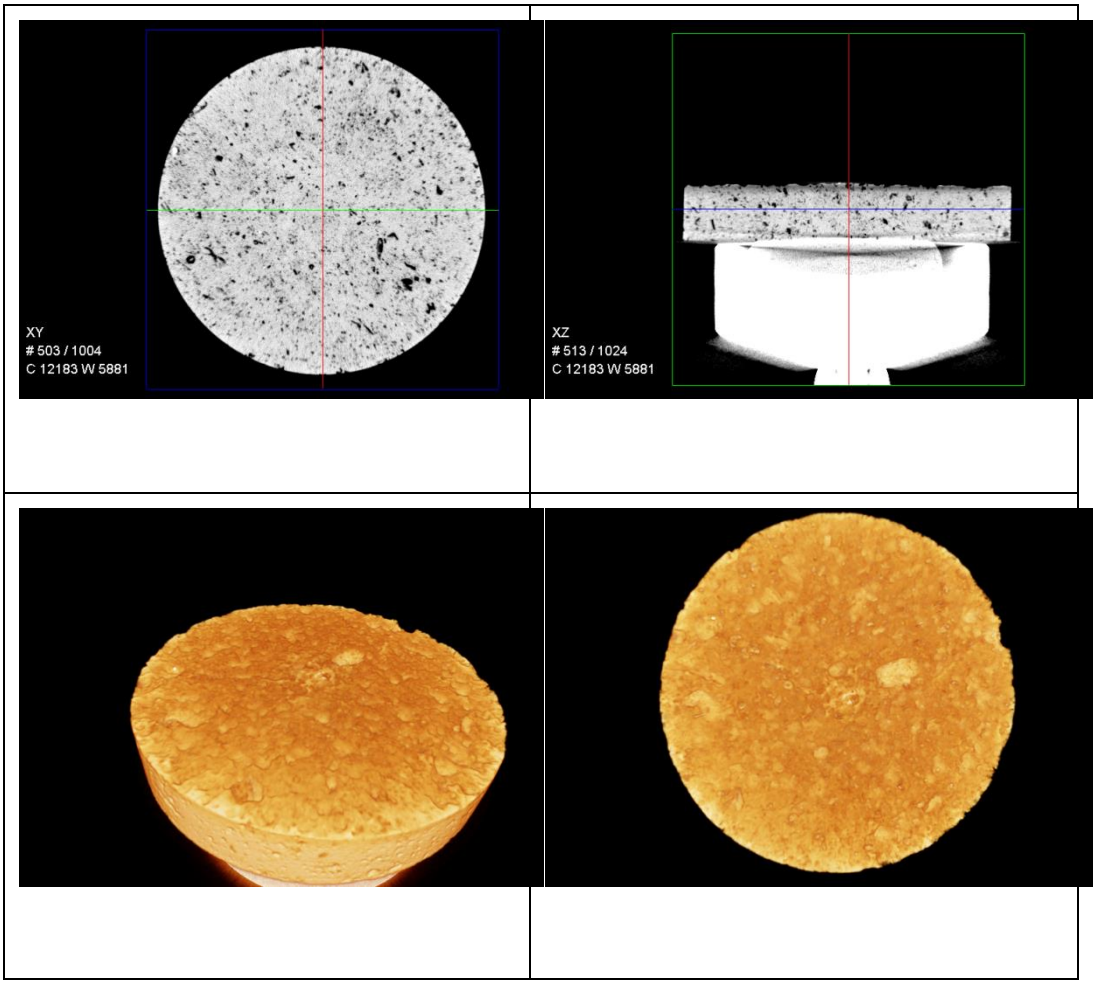

Figure 5.9: Micro XCT image of reacted disk at 500 rpm, Silurian dolomite – 10 wt. %, 3000 psi

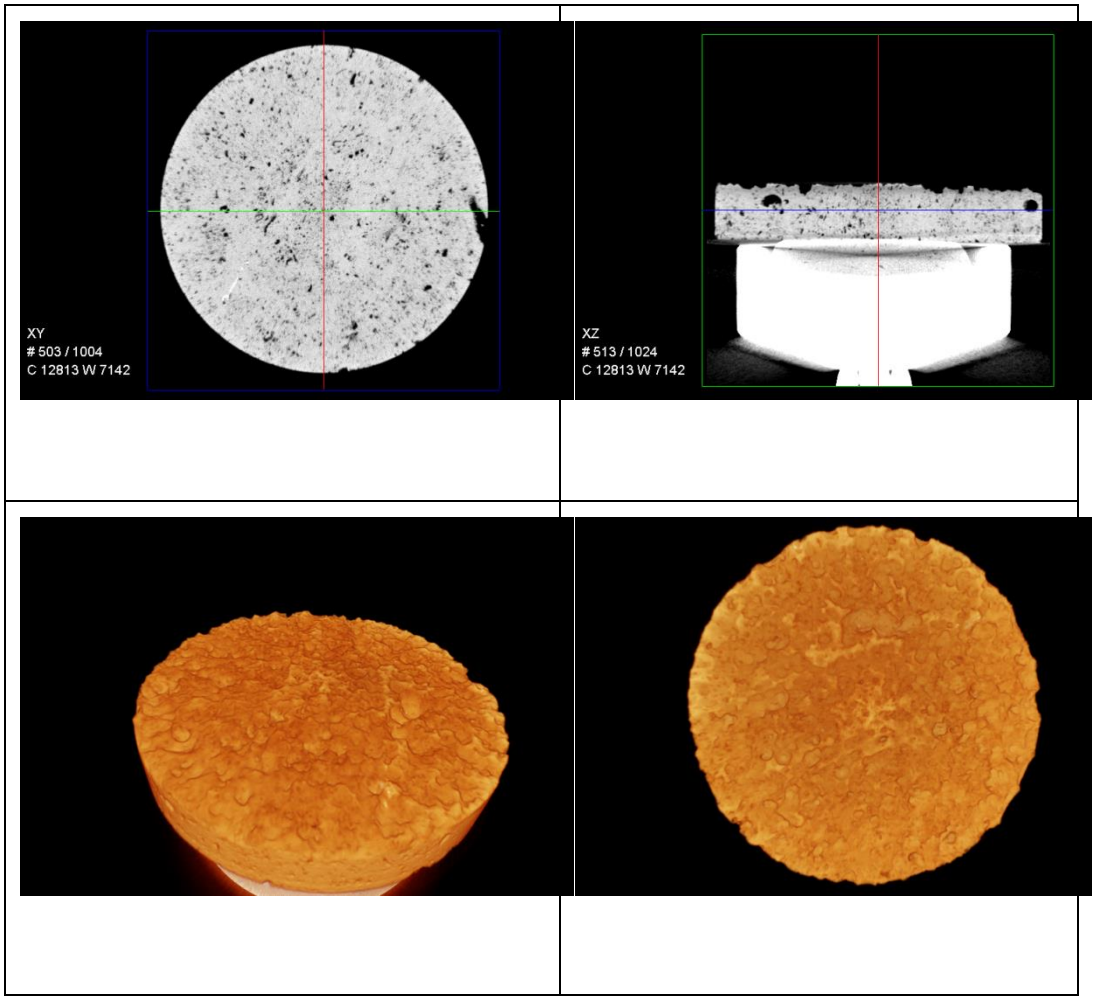

Figure 5.10: Micro XCT image of reacted disk at 1250 rpm, Silurian dolomite – 10 wt. %, 3000 psi

Two additional experiments were conducted at 1000 and 1250 rpm using the Silurian dolomite disk used for spent 12.5 wt. % spent acid experiments (series # 01). The core porosity was 10 % as compared to the new core porosity which was 13 %. It was found that the weight loss values decreased significantly when old disks were used to conduct the experiments. The weight loss values for 1000 rpm and 1250 rpm experiment were 2.46 gm. and 2.34 gm. respectively. It was evident that less amount of dolomite was dissolved while using the same acid concentration i.e. 10 wt. %. Moreover, Micro XCT was performed on the reacted disk at 1250 rpm to study the dissolution. Figure 5.11 shows the Micro XCT image for the reacted disk. It can be inferred that the dissolution was less as compared to the 13% porosity disk. The edges of the disk were relatively smooth and the surface of the disk was still uniform. However, the reacted disk at 13% porosity (same experimental conditions) showed major increase in dolomite dissolution.

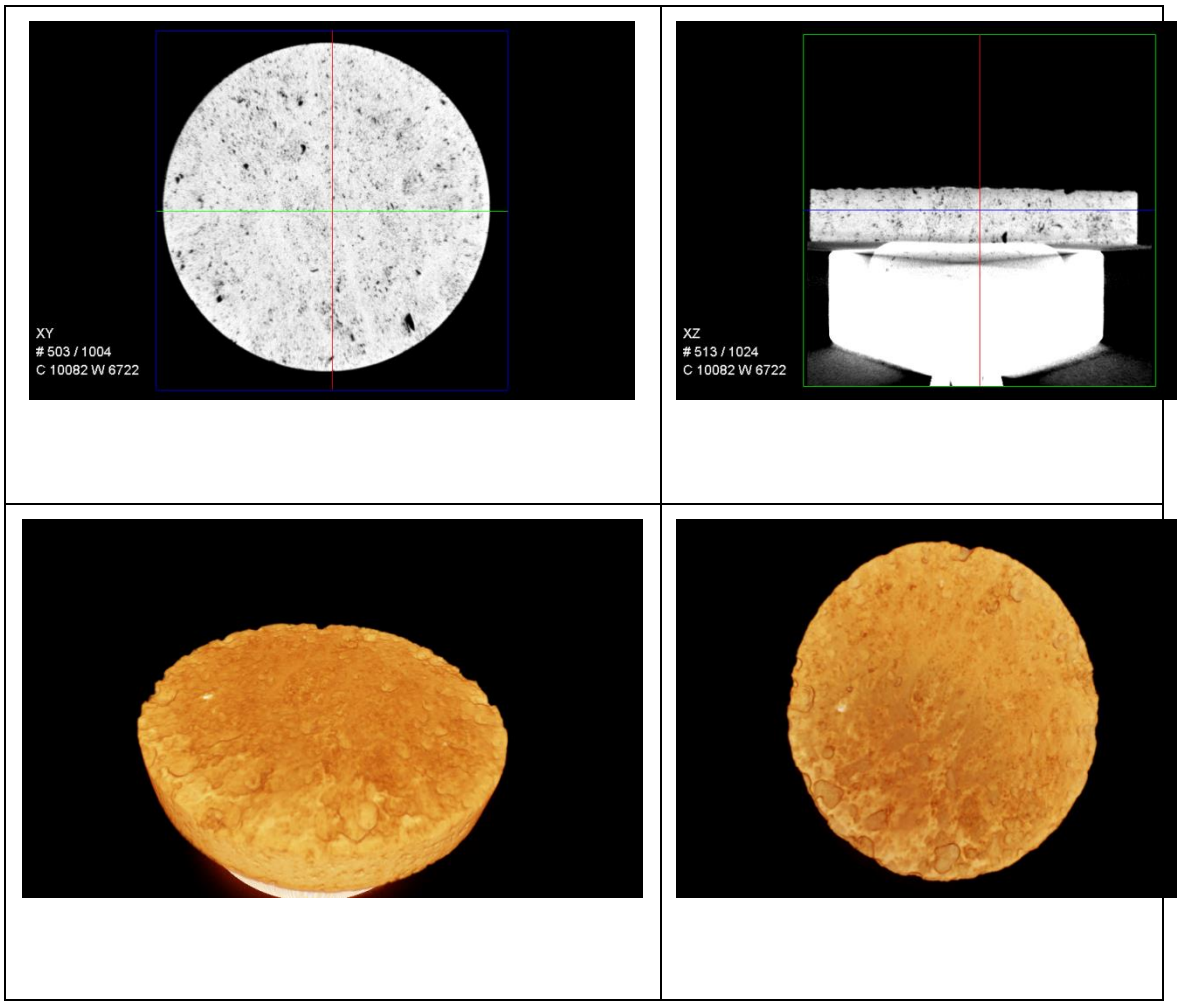

Figure 5.11: Micro XCT image of reacted disk at 1250 rpm, spent 10 wt. % and 10% porosity

5.3 Silurian Dolomite at 3000 psi (7.5 wt. % spent HCl) Acid

The experimental parameters to conduct experiments for Silurian Dolomite at 3000 psi (7.5 wt. % spent HCl) Acid which will be referred as Series # 03 are listed in Table 5.8. The third series experiments for spent 7.5 wt. % were conducted using new Silurian Dolomite rock. The core was 12" in length and 1.5" in diameter. The pressure range for this series was 3000 psi. Total five experiments were conducted starting from low disk rotational speeds (250 rpm) to high disk rotational speed (1250 rpm). A new Silurian dolomite core was used to prepare disks. The Silurian dolomite porosity was measured and found to be 17% as compared to the previous core porosities which were 10% and 13%. The following sections present the detailed results for series # 03 experiments for spent acid 7.5 wt. %.

Table 5.8: Experimental conditions for series # 03 – 3000 psi – 7.5 wt. % spent acid

Experiment Parameters	
Rock Type	Dolomite
Core Type	Silurian Dolomite
Temperature, ˚C	65
Pressure, psi	3000
Acid Type	HCl
Concentration of HCl, wt. %	7.5
Disk Rotational Speeds, rpm	250, 500, 750, 1000, 1250

5.3.1 Micro XCT of Silurian Dolomite (before experiment)

Silurian dolomite disks were prepared and scanned using Micro XCT to characterize the 3D image of the disks before conducting the reaction kinetics experiment. Micro XCT equipment was operated at a voltage of 120kv and 10W power source. In addition, the scan time per dolomite disk was 90 minutes (approximately).

Figure 5.12 shows the Micro XCT image of the Silurian dolomite disk before conducting the reaction kinetics experiment. It can be observed from the image that the disk is significantly porous. Moreover, the disk surface is not smooth. It can be inferred that the reaction rate will increase due to the high porosity.

5.3.2 Preparation and standardization of 7.5 wt. % HCl acid

HCl acid (15 wt. %, 60 ml) was mixed with known quantity of dolomite powder (6.31 gm) at ambient conditions to prepare 7.5 wt. % acid concentration. The acid and powder was left to react until all the powder was dissolved. The resulting solution was then titrated to determine the molarity of the acid which was used in subsequent calculations of diffusion coefficient and dissolution rates. The molarity of 7.5 wt. % spent acid was found to be 2.166 M (average value).

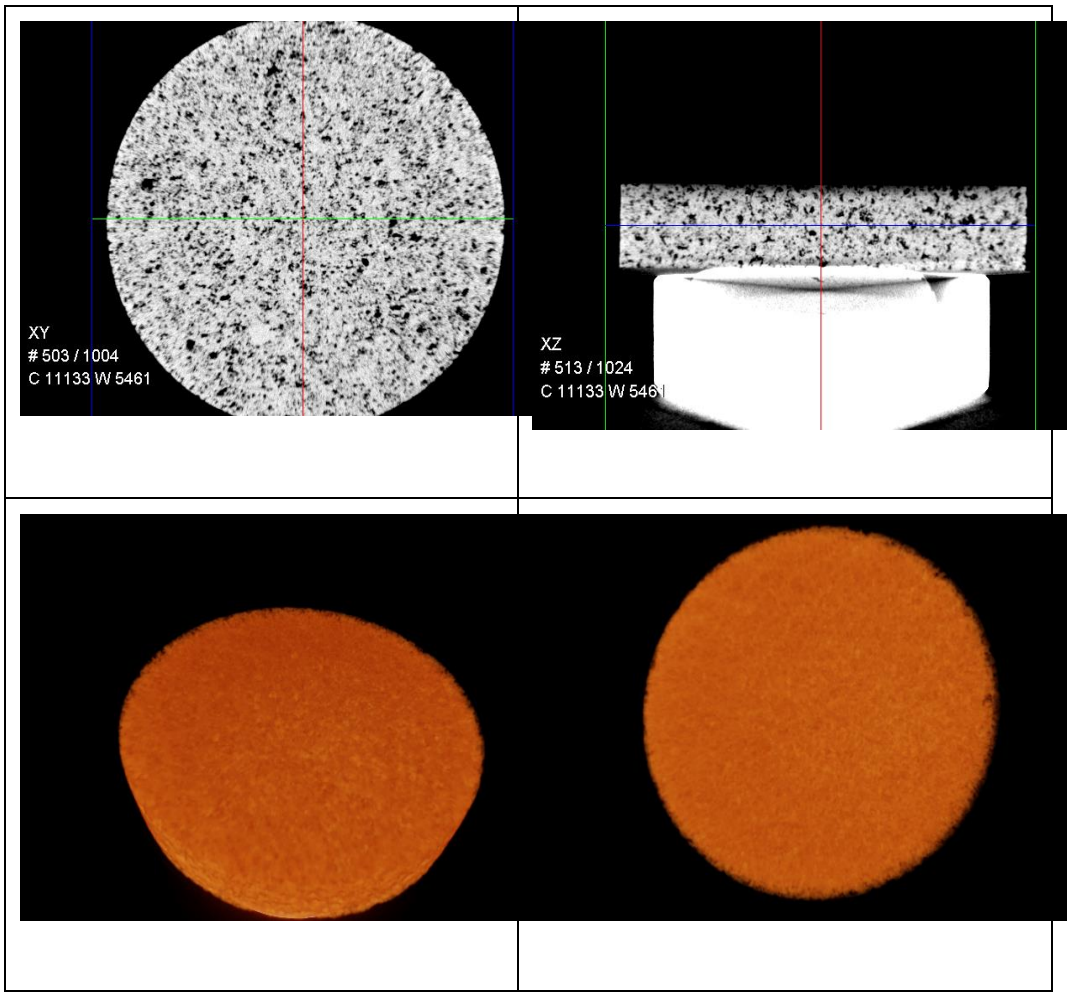

Figure 5.12: Micro XCT image of Silurian dolomite disk before reaction kinetics experiment – 7.5 wt. %

5.3.3 Reaction Kinetics experiment

Rotating Disk Apparatus was used to conduct reaction kinetics measurement. A total of five experiments were conducted using Silurian dolomite disks starting from 250 rpm to 1250 rpm. The detailed procedure to conduct the experiment was described in chapter 03. The amount of dolomite powder used in the experiments was 63.08 gm dissolved in 600 ml of 15 wt. % HCl acid to obtain 7.5 wt. % acid concentration during the experiment. The duration of conducting experiments was increased in order to completely dissolve the dolomite powder in acid. Since dolomite is also slow in reaction, it takes longer time to completely dissolve with acid. The weight of the disks were measured before and after conducting each experiment which was used as a comparison for diffusion coefficient calculations. Table 5.9 shows the weight loss values for each experiment.

Table 5.9: Weight loss values for Silurian dolomite experiments – 7.5 wt. %, 3000 psi

Disk Rotational speed rpm	Weight of disk before experiment gm	Weight of disk after experiment gm	Weight loss (ΔW), gm
1250	19.694	16.318	3.376
1000	20.081	16.822	3.26
750	20.02	17.492	2.528
500	19.7806	17.5404	2.2402
250	19.7417	18.01	1.731

Figure 5.13 shows the graph between weight loss and disk rotational speeds. It can be observed that as the disk rotational speed increased, the percentage weight loss also increased. The weight loss values lied in the range from 2.0 – 2.5 gm when experiments were conducted from 250 rpm to 750 rpm. However, when the disk rotational speed increased to 1000 rpm, there was a significant increase in weight loss value i.e. 3.26 gm. However, at 1250 rpm, there was a small increase in weight loss as compared to 1000 rpm. It was also observed at high disk rotational speeds that the weight loss values were not constant as observed for spent 12.5 wt. % experiments.

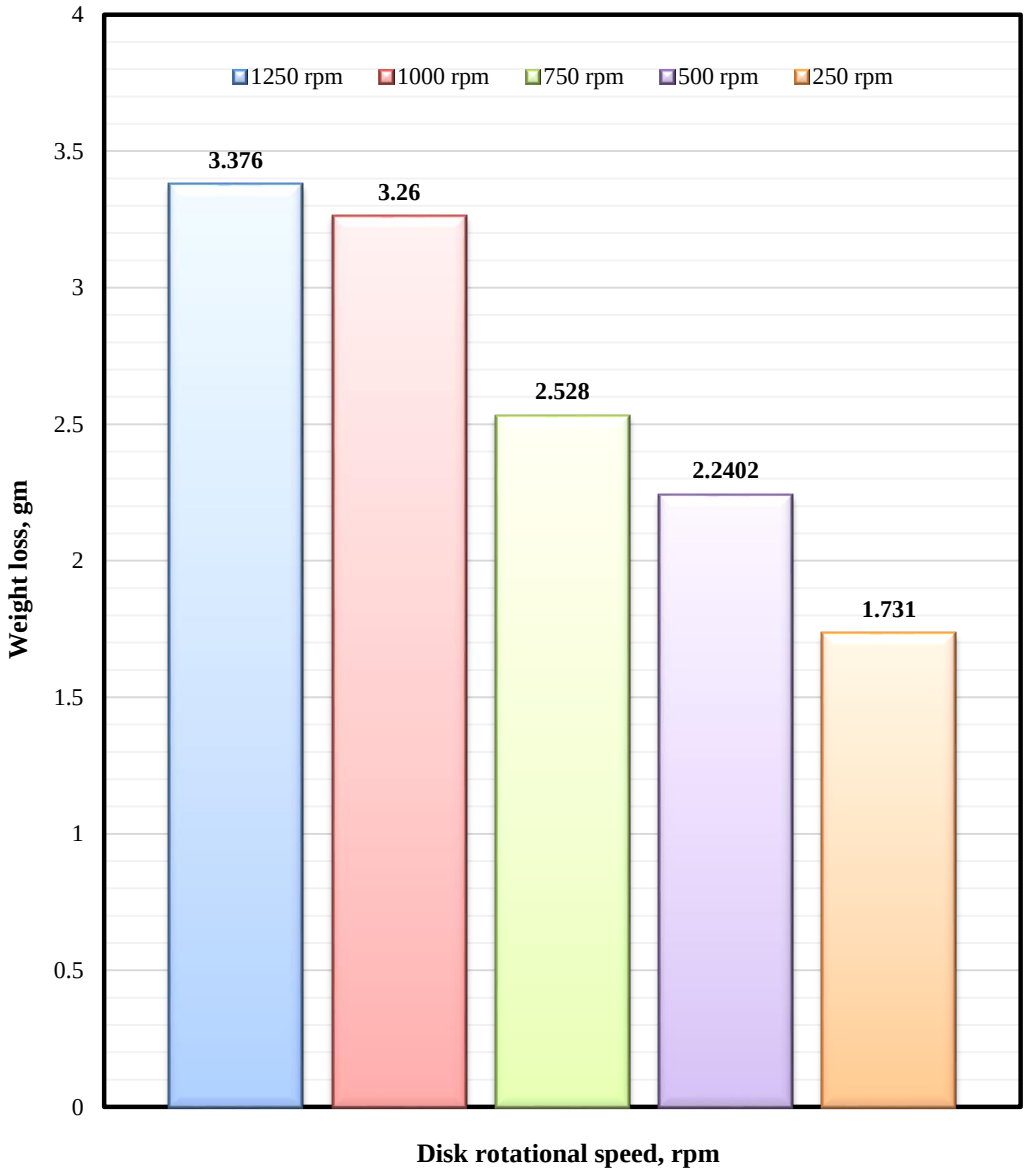

Figure 5.13: Weight loss for Silurian sample as a function of RPM for spent 7.5 wt. % acid at 3000 psi

5.3.4 Diffusion Coefficient Analysis

The samples collected from the reaction kinetics experiment were then diluted and their calcium and magnesium concentrations were determined using AAS. The concentrations were then used to calculate dissolution rates as well as the diffusion coefficient. Table 5.10 shows the calculated values for dissolution rates and "F" function using weight loss results as well as using AAS results.

Table 5.10: Diffusion Coefficient Analysis calculations, Silurian dolomite – 7.5 wt. %, 3000 psi

Disk rotational speed rpm	**$\sqrt{w}$ rad/sec**	**Dissolution rates mole/s.cm^2**	**F (using weight loss results)**	**F (using AAS results)**
1250	11.4419	3.192E-06	2.00E-03	1.18E-03
1000	10.2339	3.084E-06	1.94E-03	1.48E-03
750	8.8628	2.325E-06	1.46E-03	1.60E-03
500	7.2365	2.134E-06	1.34E-03	2.02E-03
250	5.1170	1.655E-06	1.04E-03	2.50E-03

Figure 5.14 and 5.15 shows the graph between "F" function vs. the square root of disk rotational speed using weight loss results and AAS results respectively. It was observed that the reaction was controlled by mas transfer limited regime. Surface limited regime was not observed for spent 7.5 wt. % experiments. The slope obtained using both weight loss and AAS results were 1.6×10^{-04} and 2.0×10^{-04} respectively.

Using the slopes in Figure 5.14 and 5.15, diffusion coefficient was obtained. The diffusion coefficient values obtained using weight loss results was **2.02×10^{-06} cm^2/sec** and using AAS results was **2.83×10^{-06} cm^2/sec.**

5.3.5 Micro XCT of dolomite disks (after experiment)

The reacted dolomite disks for 500 rpm and 1250 rpm were scanned using Micro XCT to characterize the nature of reaction and describe the pore structure. Figure 5.16 and 5.17 shows the Micro XCT images of the reacted disk used in 500 rpm and 1250 rpm experiments, respectively. It was observed that the dissolution of the acid by rock was increased for both 500 and 1250 rpm experiments. At 500 rpm, the center of the disk was not reacted with the acid but the remaining part of the disk was reacted significantly. The edges of the disk were also reacted. However, at 1250 rpm, the entire surface of the disk was reacted significantly by the acid. The reacted disk surface was non uniform in its profile.

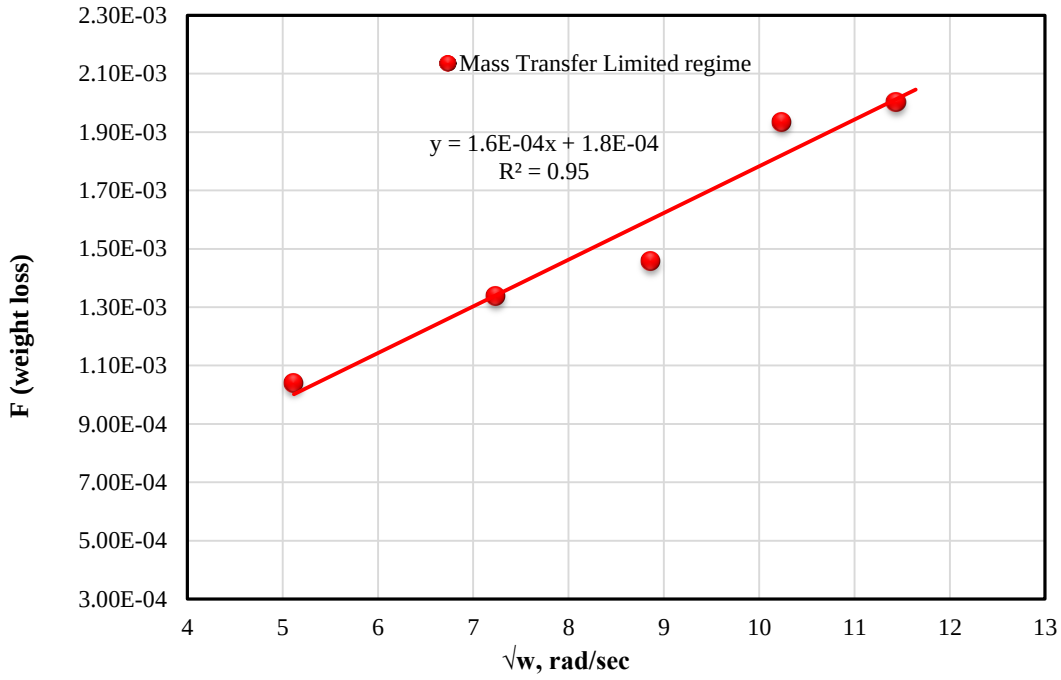

Figure 5.14: Diffusion Coefficient Graph (using weight loss results), Silurian dolomite – 7.5 wt. %, 3000 psi

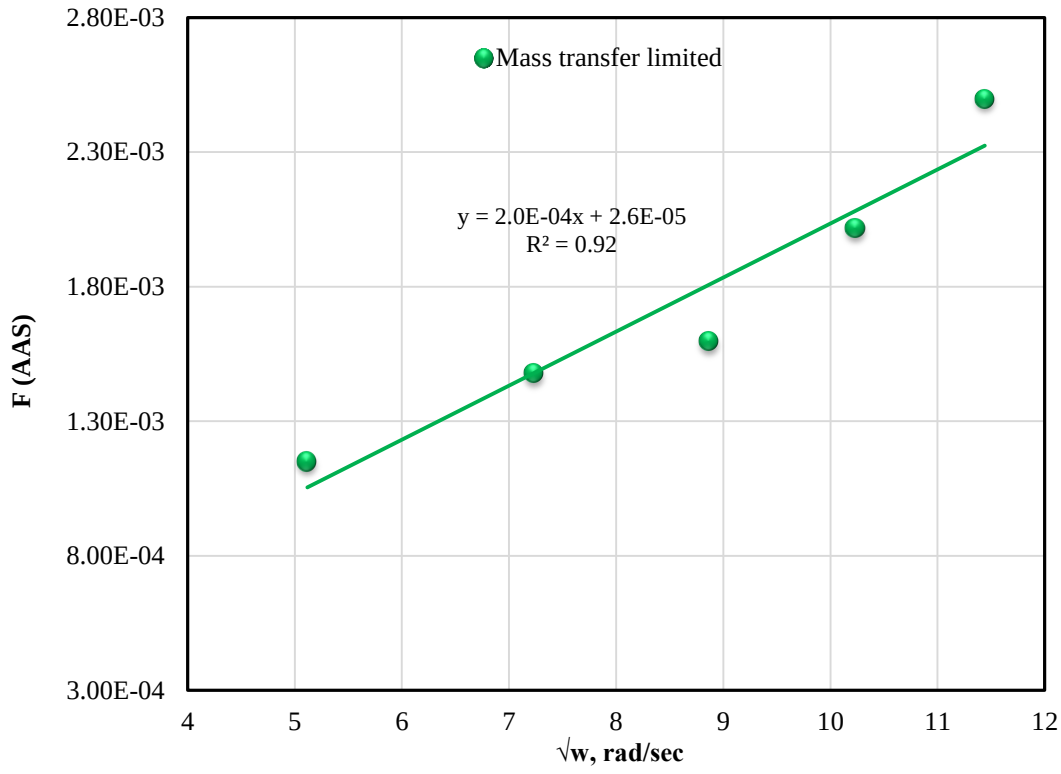

Figure 5.15: Diffusion Coefficient Graph (using AAS results), Silurian dolomite – 7.5 wt. %, 3000 psi

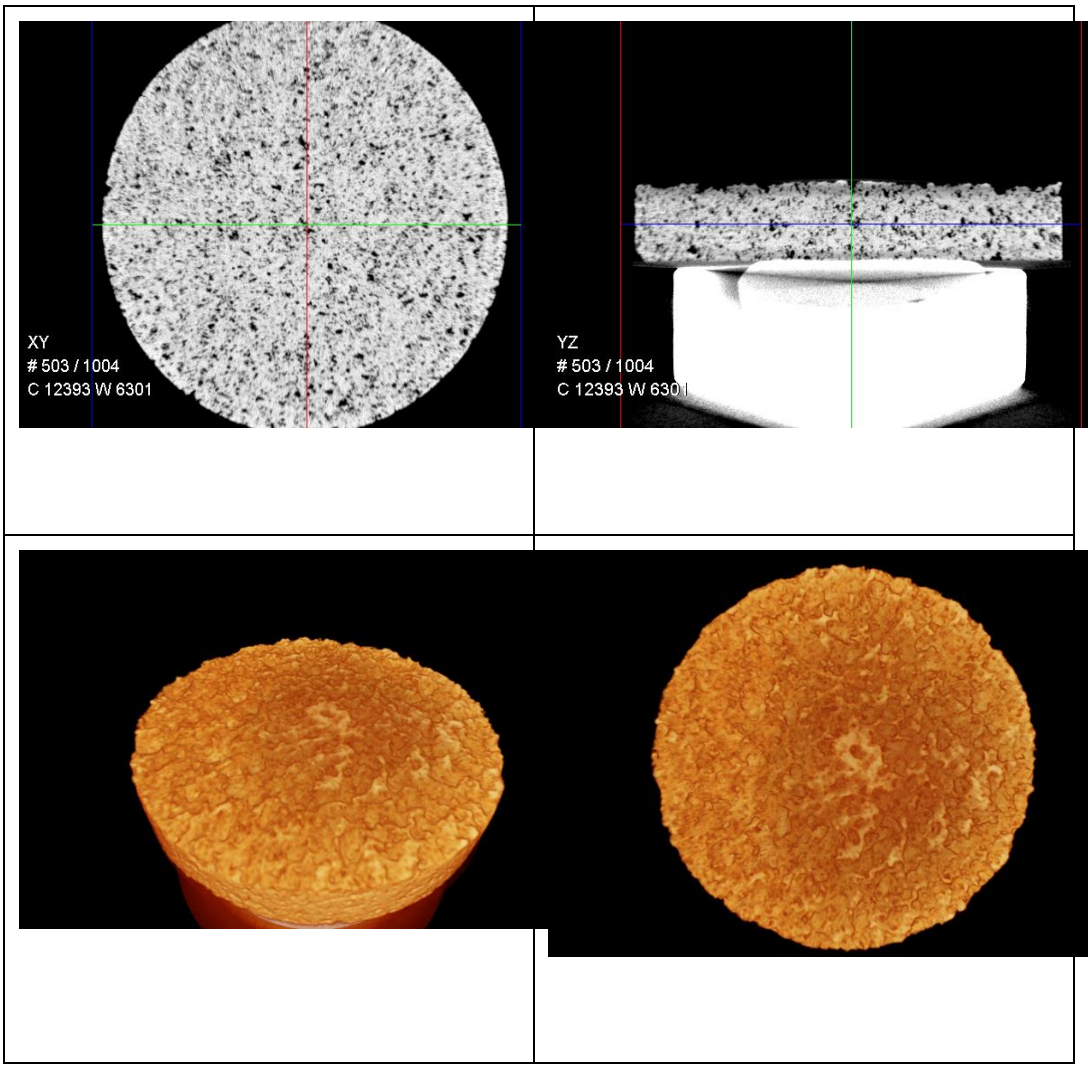

Figure 5.16: Micro XCT image of reacted disk at 500 rpm, Silurian dolomite – 7.5 wt. %, 3000 psi

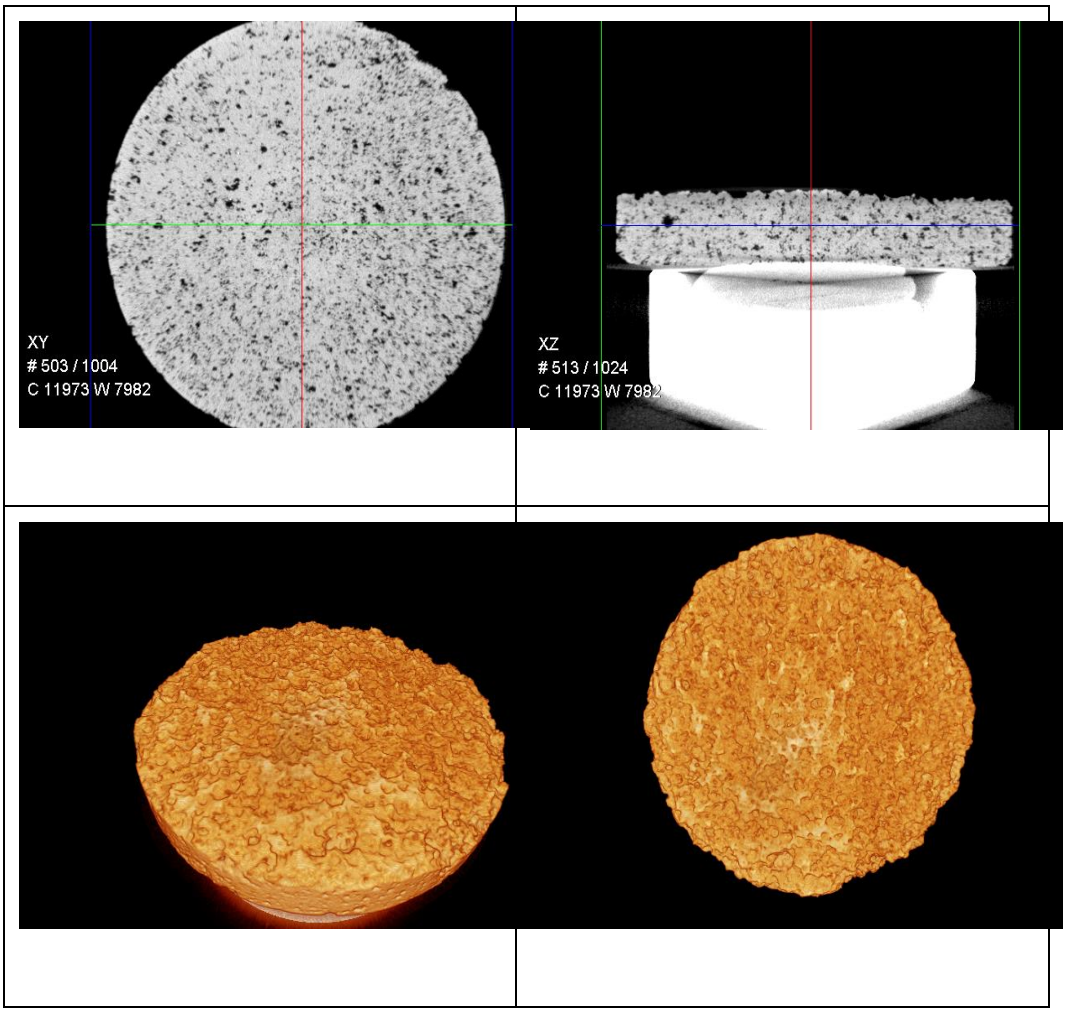

Figure 5.17: Micro XCT image of reacted disk at 1250 rpm, Silurian dolomite – 7.5 wt. %, 3000 psi

5.4 Discussion of Results

5.4.1 Effect of Spent acid concentrations

Experiments were conducted for three different spent acid concentrations i.e. 12.5, 10 and 7.5 wt. %. It was observed that when the fresh acid (15 wt. %) was spent to 12.5 wt. % concentration, the percentage weight loss and dissolution rates both decreased. In addition, there was a 12% decrease in the diffusion coefficient of spent 12.5 wt. % system. Figure 5.18 shows the comparison of weight loss values for fresh acid and spent 12.5 wt. % system. The diffusion coefficient obtained using fresh acid at 3000 psi was **5.60×10^{-07} cm^2/sec**. However, the diffusion coefficient obtained using spent 12.5 wt. % at 3000 psi was **4.941×10^{-07} cm^2/sec.**

It can be analyzed that there was a decrease in the dissolution rates as well as in diffusion coefficient calculation but the decrease was not significant owing to two major reasons. Firstly, reaction rate of dolomite is very slow. The reason being that the ionic radii of Mg is smaller than Ca, hence the Mg-O bond possess high degree of covalency than the Ca-O bond in dolomite rock. Owing to smaller bond length and increase in covalency, the dipole moment of the Mg-O bond is less than that Ca-O bond. Thus, Ca-O bonds in dolomite are broken easily and the rate determining step is the rate of breakage of Mg-O bonds. In addition, the gravimetric dissolving power for dolomite is found to be less i.e. 1.27 (for 100% strength acid). Though the acid concentration decreased to 12.5 wt. %, but due to the slow reaction of dolomite, the difference in the diffusion coefficient was not substantial.

On the other hand, when the experiments were conducted using calcite at same experimental conditions (Qiu *et al.,* 2013), the diffusion of H^+ ions was buffered by the action of CO_2 and counter ions in the spent acid mixture. The mass transfer coefficient was significantly reduced as well as the diffusion coefficient (order of 30 to 50 % lower). However in our research with dolomite, the percentage decrease was around 12 %.

When the fresh acid was spent to 10 wt. %, new Silurian dolomite core was used to prepare the disks. The porosity value increased to 13%. It was observed that there was an increase in the weight loss, dissolution rates and diffusion coefficient values. The diffusion coefficient obtained using spent 10 wt. % system was 9.746×10^{-07} cm^2/sec. There was a 5% decrease in the acid concentration but the diffusion coefficient still increased.

Similarly, when the fresh acid was spent to 7.5 wt. %, a new Silurian dolomite core was used to prepare the disks having porosity value of 17%. It was observed that the dissolution rates as well as diffusion coefficient increased. The diffusion coefficient obtained using spent 7.5 wt. % system was **2.20×10^{-06} cm^2/sec**.

Figure 5.19 shows the comparison of diffusion coefficient results for spent acid experiments. It can be concluded that as the acid was spent to 10 and 7.5 wt. %, porosity played a dominant effect in increasing the dissolution rates and diffusion coefficient. Figure 5.20 shows the high resolution images (3.5 micron image resolution) obtained using Micro XCT that showed compliance with the diffusion coefficient results for spent acid experiments.

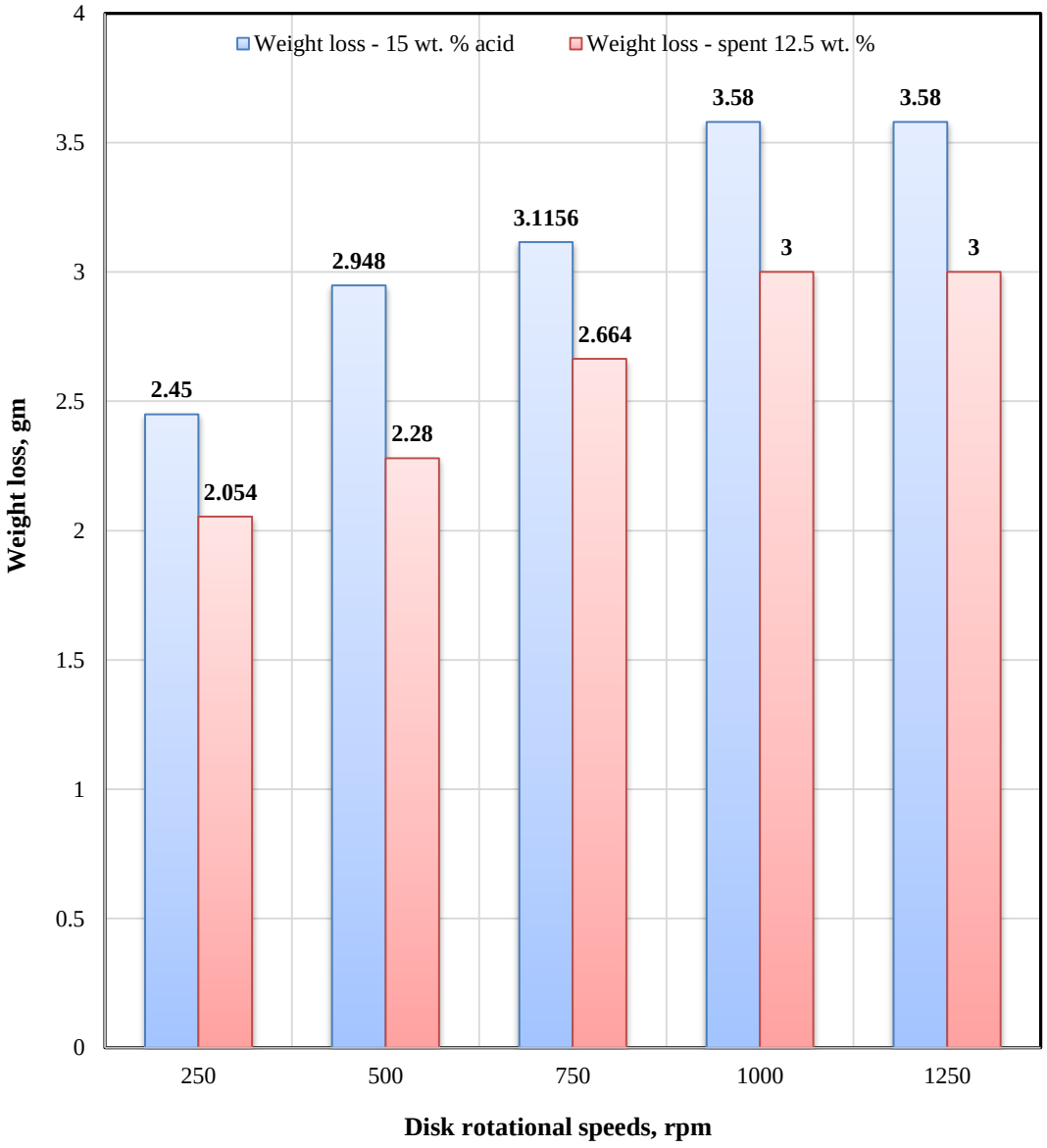

Figure 5.18: Comparison of computed weight loss values for 15 wt. % and spent 12.5 wt. % acid

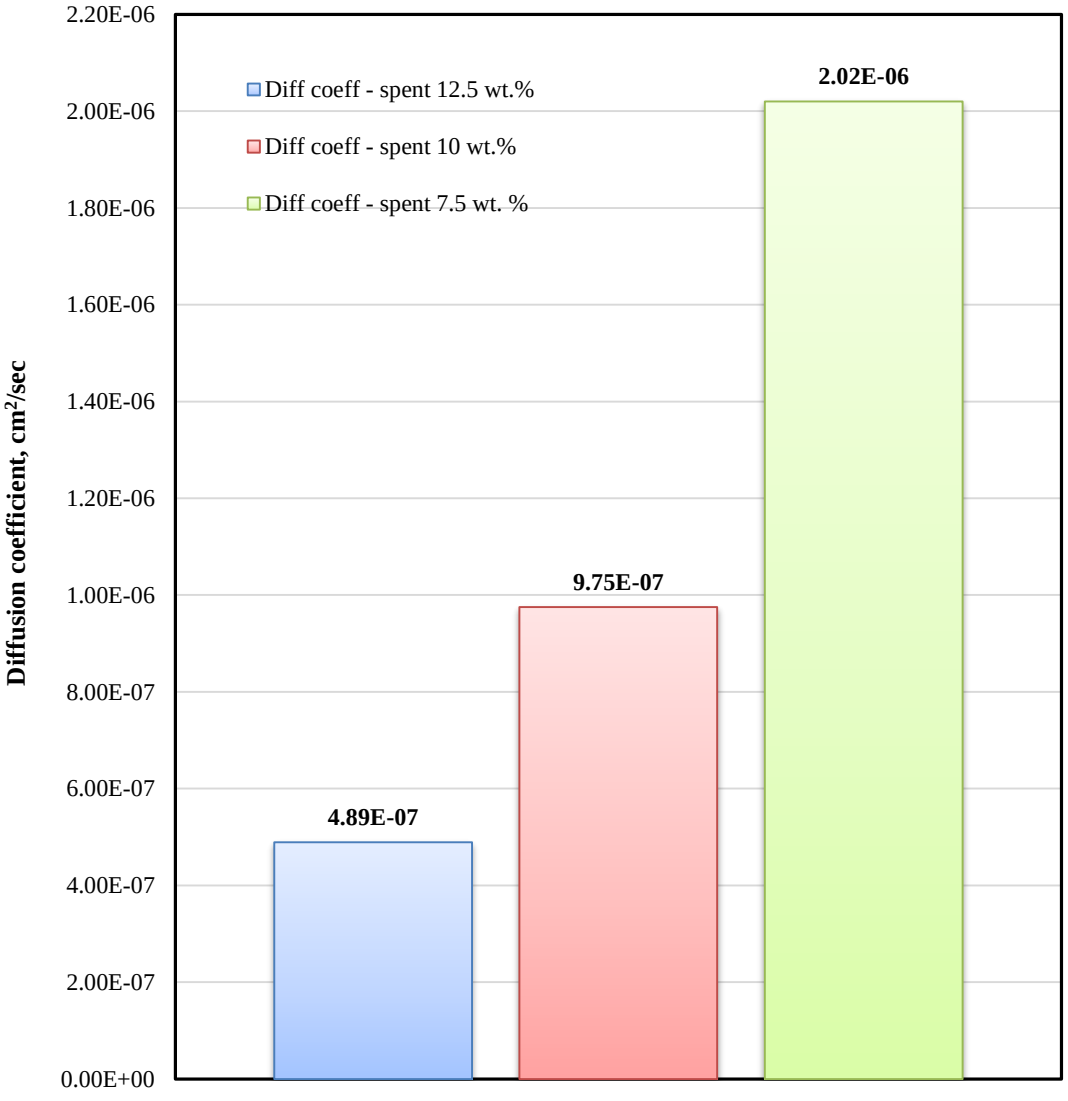

Figure 5.19: Comparison of computed diffusion coefficient values for spent acid experiments

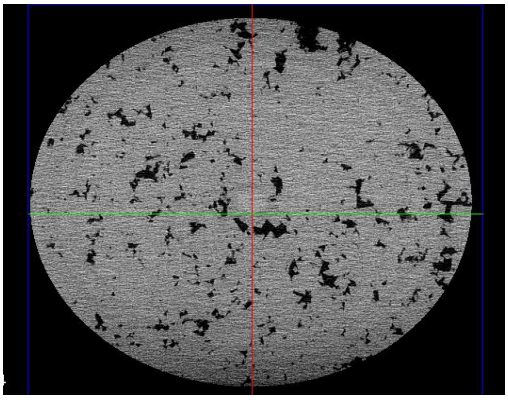

Spent 12.5 wt. % and Φ = 10%

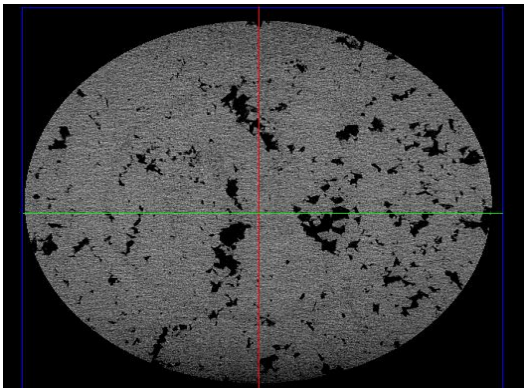

Spent 10 wt. % and Φ = 13%

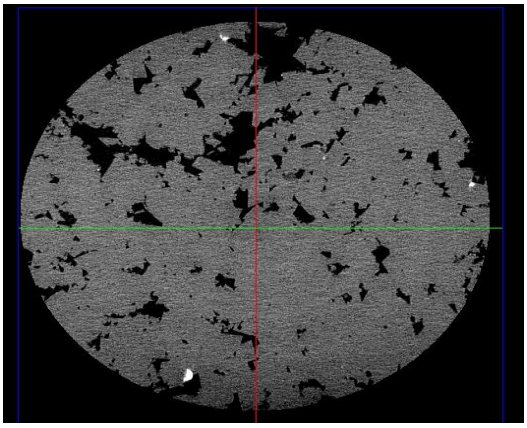

Spent 7.5 wt. % and Φ = 17%

Figure 5.20: Comparison of High Resolution Micro XCT Images for spent 12.5, 10 and 7.5 wt. % system

5.4.2 Effect of Rock Porosity (ϕ)

Rock porosity had a significant effect on the reaction kinetic measurements as observed in our research. Three Silurian dolomite cores were used to complete the experimental work having porosity values of 10 %, 13 % and 17 %. It was observed that as the rock porosity increased, the acid reaction rates also increased significantly. High porosity tends to increase the surface area of the reacting rock disk. Because the acid dissolution rate depends on the surface area of the disk, the dissolution rate will appear to increase as the porosity of the rock increases.

As the rock porosity increased, the diffusion coefficient values for spent 12.5, 10 and 7.5 wt. % were also increased. Though the acid concentration had decreased but porosity i.e. increase in reaction surface area, played an important part in increasing the dissolution rates and diffusion coefficient values.

The porosity increase effect was also observed in Micro XCT images which facilitated in describing the dissolution of reacted disks. It can be inferred that when the disk porosity was low, the dissolution rate of the disk was also less. The center of the disk had negligible reaction as compared to the edges of the disk. Figure 5.21 shows the top view image of the surface of the disk for 10% porosity. On the other hand, as the disk porosity increased from 10% to 13%, it significantly affected the dissolution rate of the disk. Acid penetration inside the disk was increased. Moreover, the edges and center of the disk both reacted with the acid. Figure 5.22 shows the top view image of the surface of the disk for 13% porosity.

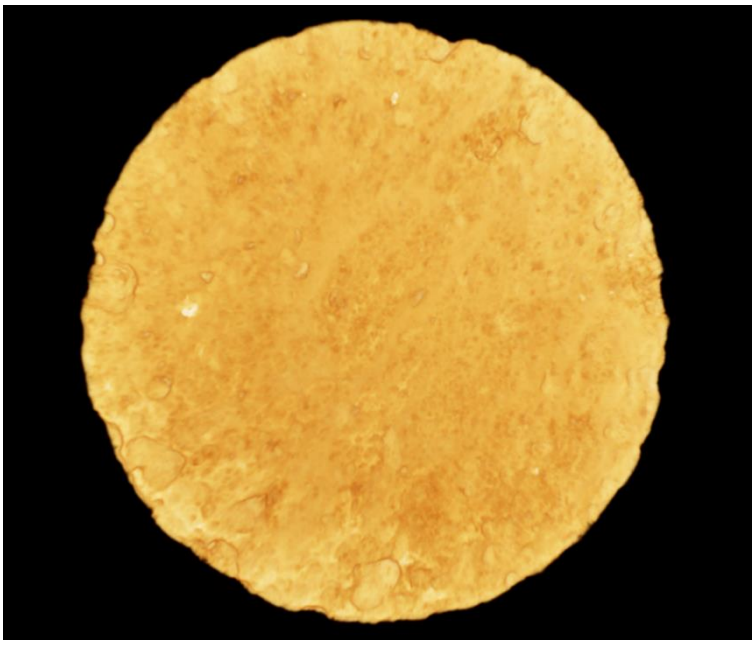

Figure 5.21: Micro XCT image of top surface of disk – Spent 10 wt. % and 10% porosity

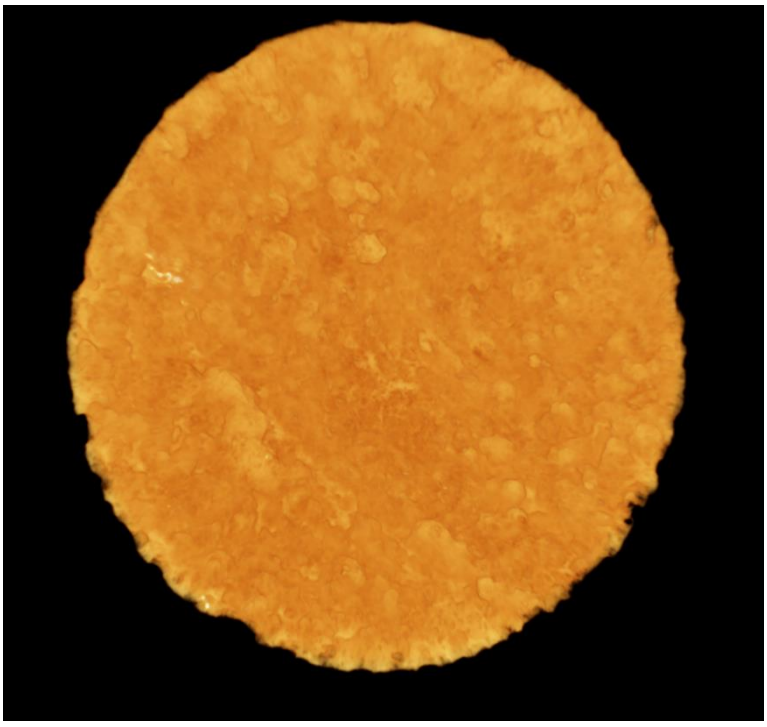

Figure 5.22: Micro XCT image of top surface of disk – Spent 10 wt. % and 13% porosity

Additional (four) experiments were conducted to determine the effect of porosity on the diffusion coefficient results by keeping all the other parameters constant. The dolomite disks used had porosity value of 17%. The experimental parameters are mentioned below.

Experiment Parameters	
Rock Type	Dolomite
Core Type	Silurian Dolomite
Temperature, ˚C	65
Pressure, psi	3000
Acid Type	HCl
Concentration of HCl, wt. %	15
Disk Rotational Speeds, rpm	250, 750, 1000, 1250

HCl acid was prepared to obtain 15 wt. % acid concentration which was used for reaction kinetics experiment. The molarity of fresh acid was determined using titration process and the average value was found to be 4.422 M.

Rotating Disk Apparatus was used to conduct the experiments. Table 5.11 shows the detailed results for weight loss, dissolution rates and F function.

Figure 5.23 shows the graph between “F” function vs. the square root of disk rotational speed. It was observed the reaction was mass transfer limited for the entire disk speeds

until 1250 rpm. Surface reaction limited regime was not observed. In addition, using the slope in the equation, diffusion coefficient value was obtained i.e. **4.12×10^{-06} cm^2/sec.**

Table 5.11: Diffusion Coefficient Analysis calculations, 15 wt. % acid and 17% porosity

Disk rotational speed rpm	$\sqrt{w}$ **rad/sec**	**Weight loss gm**	**Dissolution rates mole/s.cm^2**	**F (using weight loss results)**
1250	11.4419	9.025	8.47E-06	2.60E-03
1000	10.2339	7.148	6.73E-06	2.07E-03
750	8.8628	5.91	5.57E-06	1.71E-03
250	5.1170	3.13	2.93E-06	9.00E-04

Figure 5.24 shows the comparison of reaction regimes between 10% and 17% porosity experiments using 15 wt. % acid concentration. It was observed that at low porosity, mass transfer limited regime was obtained at low rpms. However, at high rpms, the reaction was surface reaction limited. On the other hand, when the disk porosity was increased to 17%, the reaction was mass transfer limited until 1250 rpm. Reaction limited regime was not observed.

Figure 5.25 shows the comparison of the diffusion coefficient values for 10% and 17% porosity experiments using 15 wt. % acid concentration. A significant increase in diffusion coefficient was observed for high porosity experiments (8.5 times increase) as compared to low porosity.

The high porosity reacted disk at 1000 rpm was scanned using Micro XCT. The image resolution was 3.5 micron. The results were compared with the low porosity reacted disk at 1000 rpm. The acid concentration was 15 wt. %. It was observed that rock porosity significantly affected the dissolution rate. At low porosity, the dissolution of rock by acid was less. However, as the disk porosity increased, the dissolution rate was also increased leading to significant increase in the diffusion coefficient results. Figure 5.26 and 5.27 shows the high resolution images for reacted disks at two different porosity.

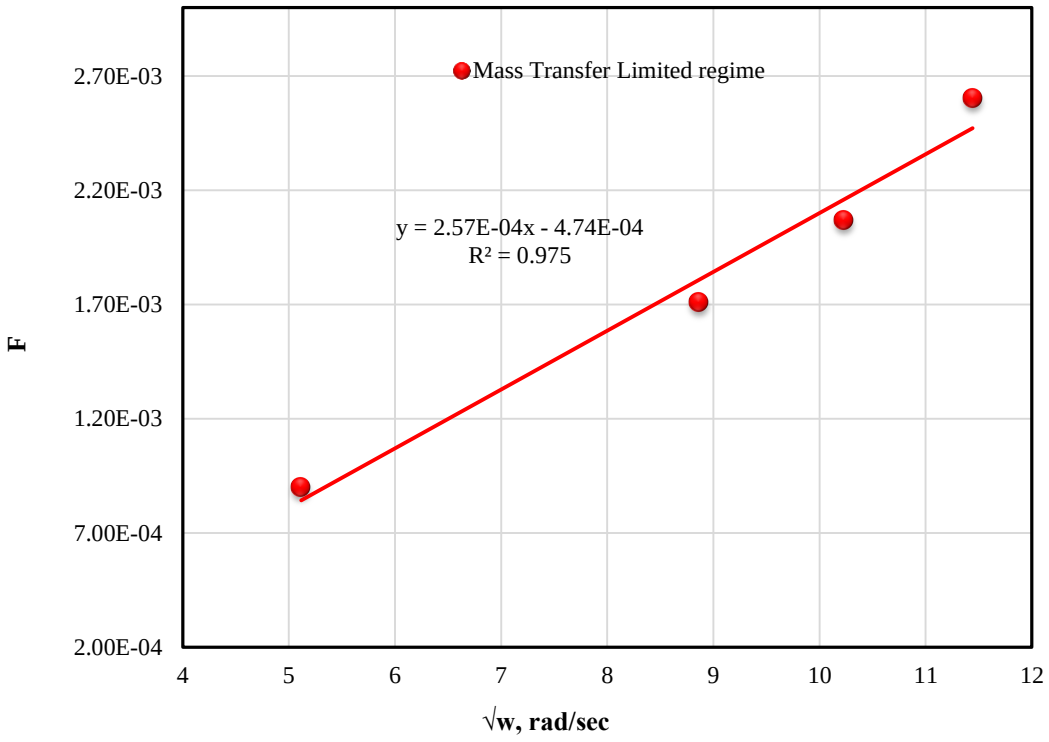

Figure 5.23: Diffusion Coefficient Graph – 15 wt. % acid and 17% porosity

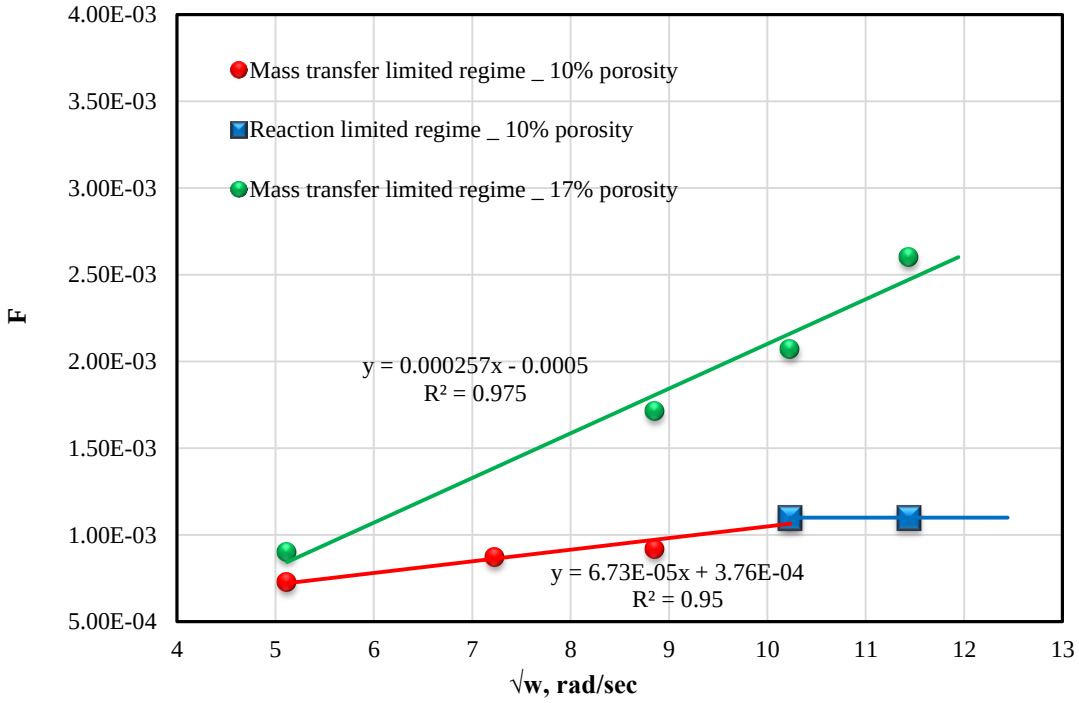

Figure 5.24: Comparison of Reaction regimes for 10% and 17% porosity

Figure 5.25: Comparison of computed diffusion coefficient values for 10% and 17% porosity

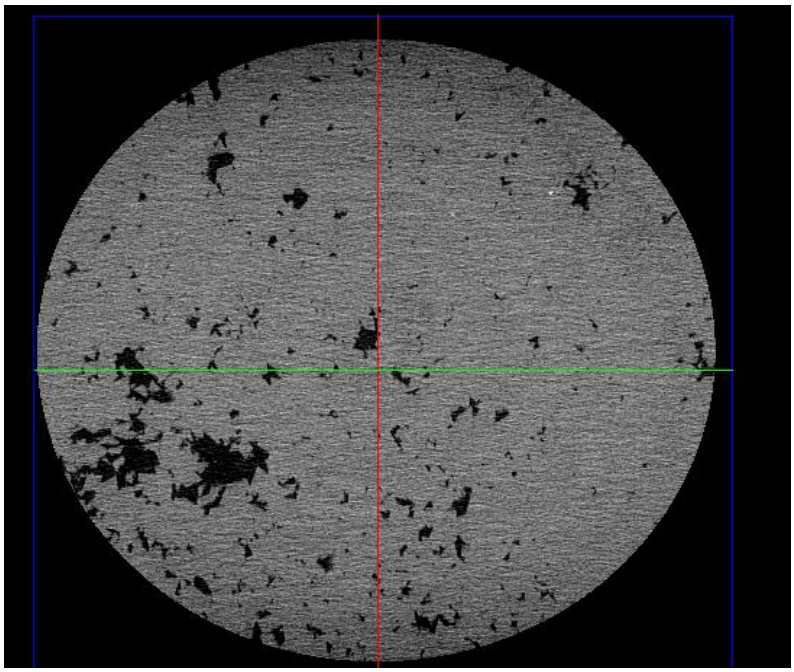

Figure 5.26: Focused Micro XCT image of reacted disk – 10% porosity and 1000 rpm

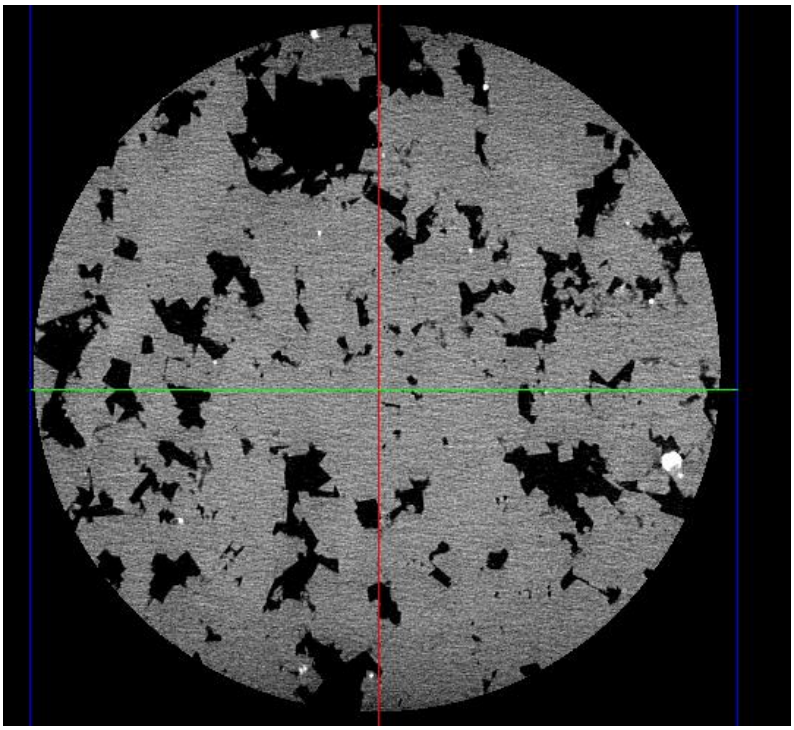

Figure 5.27: Focused Micro XCT image of reacted disk – 17% porosity and 1000 rpm

5.4.3 Effect of disk rotational speeds (RPM)

Disk rotational speed had a significant effect on the reaction regime of dolomite and spent acid concentrations. For spent 12.5 wt. %, dissolution rates increased as the disk rotational speed increased till 750 rpm. Hence at low disk rotational speeds, the reaction was found to be mass transfer limited. However at high disk rotational speeds, the acid dissolution rate was constant and the reaction in this regime was controlled by surface reaction rate.

For spent 10 wt. % experiments, the dissolution rate increased as the disk rotational speed was increased to 1250 rpm. Hence the reaction regime was found to be mass transfer limited. As compared to spent 12.5 wt. % experiments, reaction limited regime was not encountered for high rotational speeds. Similarly for spent 7.5 wt. % experiments, the reaction regime was mass transfer limited.

The two reaction regimes can be explained clearly by the Boundary Layer Theory proposed by Fogler (2005). Fluid/solid reactions can be described by the sequence of adsorption, surface reaction and desorption. The slowest step is considered to be the rate determining step. If the slowest step is the adsorption or desorption of reactants and products to and from the rock surface, the reaction is considered as mass transfer limited. If the slowest step is the surface reaction itself, then the reaction is surface reaction limited. Therefore, at low disk rotational speeds, the dissolution rate increases with disk rotational speed which is the mass transfer limited regime. The dissolution rate increases because the diffusion layer boundary of the rotating disk decreases at high disk rotational speeds. At high disk rotational speeds, the dissolution rate is constant. This occurs because the reaction rate is limited by the surface reaction rate.

It was also observed for spent 10 wt. % experiment that as the disk rotational speed was increased to 1250 rpm, the percentage weight loss as well as the dissolution rate increased significantly. Similar behavior was also observed for spent 7.5 wt. % experiment when the disk rotational speed was increased to 1000 rpm i.e. the increase in weight loss and dissolution rates. There are two major reasons for it. Firstly, at high rpms, the effect of increase in porosity is more substantial because the rotation is increased, hence more acid penetrated inside the disk leading to significant dissolution of the rock by acid. The second reason can be explained efficiently by the aid of Two Film Theory proposed by Lewis & Whitman (1924) and the Penetration Theory proposed by Higbie (1935). At low disk rotational speeds, there exists a stagnant layer or thin film of gas (CO_2) produced by the reaction of dolomite rock and HCl acid at the disk interface. There is equilibrium condition at the interface. Mass transfer by convection is insignificant and transport of H^+ ions is achieved by steady state diffusion. The concentration difference represents the potential or driving force for diffusion to take place. However at high disk rotational speeds (1000 and 1250 rpm), the stagnant layer of gas film is removed by the turbulent eddies which are supposed to penetrate towards the interface and becomes diffused in solution. Moreover, the disk surface is being renewed by fresh liquid after small time intervals. Mass transfer of H^+ ions takes place by unsteady molecular diffusion.

In simple words, the CO_2 that is generated at disk surface, being gaseous, tends to disrupt the boundary layer liquid which contains higher concentrations of reaction products than the main fluid solution/stream. Thus at high disk rotational speeds, the boundary layer fluid is forced to mix more than the usual with main stream fluid. Consequently, acid from the

main stream is transported more efficiently to the disk surface leading to increase in dissolution rates.

CHAPTER 6

CONCLUSIONS & RECOMMENDATIONS

The ultimate objective of the research thesis was to understand the reaction kinetics of carbonate formations which will help in improving the acid stimulation job design and will be of great worth to the Middle East. The novel set of reaction kinetics data obtained for both fresh acid and spent acid concentrations at high pressure conditions with pure dolomite disks will be implemented in a two scale continuum model to predict rock dissolved at any point in a 3D porosity field, wormhole morphology and penetration velocity. Simulation results of fluid flow coupled with reaction provide new insights on how acidizing design models should be improved to more accurately quantify wormhole penetration which then leads to more accurate production forecasts. Additionally, acid reaction studies will present the vital role elevated pressure has in reducing the kinetics of acid as they react with dolomite disks. Therefore, this thesis will be a significant step to enhance the capability of the wormholing model for heterogeneous carbonate formations.

Rotating disk apparatus was used to study the reaction kinetics of fresh acid (15 wt. %) and various spent acid concentrations (12.5, 10 and 7.5 wt. %) with dolomite rock of varying porosity at a temperature of 65ºC and pressure ranges of 1000 psi and 3000 psi by varying the disk rotational speeds from 250 rpm to 1250 rpm. The results from experiments which were discussed in detail in chapter 04, lead us to the following conclusions:

1. At low pressure condition, dissolution rates and diffusion coefficient were increased because CO_2 was present in gaseous state which tends to increase the transport of hydrogen ions from bulk solution to the surface of the disk.
2. At high pressure condition, CO_2 is soluble in aqueous solution and tends to buffer the diffusion of hydrogen ions leading to a lower reaction rate.
3. Rock surface containing natural fractures and holes played a significant role in increasing the dissolution rate as discussed for Guelph dolomite. Diffusion coefficient was significantly increased as compared to Silurian dolomite results at 1000 psi pressure condition.
4. Reaction rate experiments showed that the diffusion coefficient for spent 12.5 wt. % was slightly lower than that of the fresh acid at same pressure condition.
5. Rock porosity significantly affected the reaction kinetics measurement. High porosity tends to increase the surface area of the reacting disk which cause increase in the dissolution rates.
6. The reaction was mass transfer limited at low disk rotational speeds and reaction limited at high disk rotational speeds for low pressure and high pressure experiments using Silurian dolomite. Similar behavior was also observed for spent 12.5 wt. % experiments.
7. The reaction was mass transfer limited over the entire range of disk rotational speeds for spent 10 wt. % and spent 7.5 wt. % experiments.
8. Micro XCT was performed to support the experimental results as well as obtain 3D images of the reacted and unreacted dolomite disks to facilitate the quantitative measurements.

Based on the observations and conclusions of this research, the following recommendations are suggested for future work in this area.

1. Rock used for experiments must have similar porosity values to effectively study the effect of CO_2 and counterions for spent acid experiments. Dolomite marbles can be used to eliminate the effects of rock porosity, permeability and mineralogy.
2. For spent acid concentrations (10 and 7.5 wt. %), the experiments must be conducted for higher disk rotational speeds (higher than 1250 rpm) to determine the reaction limited regime.
3. The same study should be conducted using emulsified acids and organic acids to study the impact of pressure and spent acid concentrations on diffusion coefficient results.
4. Experimental setup can be modified in such a way that reaction kinetics measurement are conducted while performing Micro XCT to characterize and visualize the 3D image of the reaction phenomena during the experiment.

APPENDICES

APPENDIX A: Summary of Reaction Kinetics Literature Review

Paper Ref No	Year	Rock/Core	Length of core	Diameter of core	Acid	Temperature	Pressure	Disk Rotational Speed	Disk diameter	Disk thickness
			inch	inch		°F	psi	rev/min	inch	inch
SPE-151815-PA-P	2013	Dolomite	6	1.5	Emulsified Acid (15 wt% HCl & 0.7 acid volume fraction)	230	1100	100 - 1500	1.5	0.75
SPE-164110-MS-P	2013	Indiana limestone	0.75	1.5	Organic Acid (10 wt%)	150-250	1500	100-1500	1.5	0.75 (length given)
SPE-164480-MS-P	2013	Dolomite	-	-	0.866N Organic acid (acetic & formic acids) and Chelating agent (GLDA)	250		100-1500	1.5	0.7
SPE-164245-MS-P	2013	Calcium carbonate	Rotating disk experimental conditions are not available but theoritical concepts related to rotating disk exp are discussed. Moreover, core flood exp conditions are present.							
SPE-165120-MS-P	2013	Limestone	6	1.5	Emulsified GLDA (EGLDA)	230	1100	100-1500	1.5	0.75
SPE-151062-PA-P	2012	Indiana limestone	-	-	Emulsified Acid (15 wt% HCl & 0.7 acid volume fraction)	230	1100	100-1500	1.5	0.75
SPE-140138-PA-P	2012	Pink Desert limestone	-	-	In-situ-gelled HCl/formic acid blends	250	1200	100 and 1000	1.5	0.65
SPE-151061-MS-P	2012	Limestone	6	-	Emulsified Acid (diesel and acid solution of HCl & water)	230	1100	100-1500	1.5	0.75 (length)
SPE-140167-MS-P	2011	Indiana limestone	1	1.5	Lactic acid (1, 5 & 10 wt%)	80-250	>1000	100-1800	1.5	0.65
SPE-139816-MS-P	2011	Pink Desert limestone	0.65	1.5	GLDA (Chelating agent)	150, 220 & 300	>1000	100-1800	1.5	1
SPE-133501-MS-P	2010	Austin Chalk, Edward Limestone & Pink Dessert Limestone	1	1.5	In-situ-gelled acid (5 wt%)	150, 200 & 250	1500	100-1800	1.5	1
PETSOC-09-06-66-P	2009	Calcite & Dolomite	5	1.5	HCl	23 & 85 (in °C)	6.9 (Mpa)	-	1.5	0.5
SPE-107451-PA-P	2009	$CaCO_3$ (named as Acqua Bianca)	-	-	Surfactant-based acid solution	25 (in °C)	1000	200-1000	1.5	0.65
SPE-118724-MS-P	2009	$CaCO_3$ (named as Acqua Bianca)	-	-	Citric Acid (1 - 7.5 wt%)	25, 40 & 50 (in °C)	1000	100-1000	1.5	0.65
SPE-103979-PA-P	2008	Calcite	-	-	Gelled acids	25-65 (in °C)	1000	100-1000	1.5	0.65
SPE-102838-MS-P	2006	$CaCO_3$ (named as Acqua Bianca)	-	-	Surfactant-based acid solution (0-7 wt%)	25-80 (in °C)	1000	0-1000	1.5	0.65
PETSOC-04-10-05-P	2004	Dolomite	5	1.5	HCl (0.2-17 wt%)	room temp to 85 °C	-	100-1000	1.5	0.5
SPE-80256-PA	2004	Calcite (Acqua Bianca) & Dolomite (Crystallina)	-	-	HCl	23 & 50 (in °C)	1000	100-1000	1.5	1.1
SPE-68924	2001	Calcite	-	-	EDTA & HEDTA fluids	65 to >200	600	-	1	0.25

APPENDIX B: Detailed Titration Results for Fresh Acid Standardization

Series # 01: Guelph Dolomite at 1000 psi (15 wt. % HCl acid)

Titration 01	
Initial NaOH burette reading	0 ml
Final NaOH burette reading	13.9 ml
Initial HCl burette reading	0 ml
Final HCl burette reading	15 ml
Concentration of HCl	$(C_1V_1)_{NaOH} = (C_2V_2)_{HCl}$ $0.0956\ x\ 13.9 = C_2\ x\ 15$ $C_2 = \frac{1.32884}{15}$ $C_2 = 0.0885\ M$
Molarity of HCl	$0.0885\ x\ 50 = \mathbf{4.425\ M}$

Titration 02	
Initial NaOH burette reading	0 ml
Final NaOH burette reading	13.7 ml
Initial HCl burette reading	0 ml
Final HCl burette reading	15 ml
Concentration of HCl	$(C_1V_1)_{NaOH} = (C_2V_2)_{HCl}$ $0.0956\ x\ 13.7 = C_2\ x\ 15$ $C_2 = \frac{1.30972}{15}$ $C_2 = 0.0873\ M$
Molarity of HCl	$0.0873\ x\ 50 = \mathbf{4.36\ M}$

Titration 03	
Initial NaOH burette reading	0 ml
Final NaOH burette reading	13.7 ml
Initial HCl burette reading	0 ml
Final HCl burette reading	15 ml
Concentration of HCl	$(C_1V_1)_{NaOH} = (C_2V_2)_{HCl}$ $0.0956\ x\ 13.7 = C_2\ x\ 15$ $C_2 = \frac{0.0873}{15}$ $C_2 = 0.0885\ M$
Molarity of HCl	$0.0873\ x\ 50 = \mathbf{4.36\ M}$

Series # 02: Silurian Dolomite at 1000 psi (15 wt. % HCl acid)

Titration 01	
Initial NaOH burette reading	0 ml
Final NaOH burette reading	13.6 ml
Initial HCl burette reading	0 ml
Final HCl burette reading	15 ml
Concentration of HCl	$(C_1V_1)_{NaOH} = (C_2V_2)_{HCl}$ $0.0956\ x\ 13.6 = C_2\ x\ 15$ $C_2 = \frac{1.3007}{15}$ $C_2 = 0.0866\ M$
Molarity of HCl	$0.0866\ x\ 50 = \mathbf{4.33\ M}$

Titration 02	
Initial NaOH burette reading	0 ml
Final NaOH burette reading	13.3 ml
Initial HCl burette reading	0 ml
Final HCl burette reading	15 ml
Concentration of HCl	$(C_1V_1)_{NaOH} = (C_2V_2)_{HCl}$ $0.0956\ x\ 13.3 = C_2\ x\ 15$ $C_2 = \frac{1.27148}{15}$ $C_2 = 0.0847\ M$
Molarity of HCl	$0.0847\ x\ 50 = \mathbf{4.23\ M}$

Titration 03	
Initial NaOH burette reading	0 ml
Final NaOH burette reading	13.6 ml
Initial HCl burette reading	0 ml
Final HCl burette reading	15 ml
Concentration of HCl	$(C_1V_1)_{NaOH} = (C_2V_2)_{HCl}$ $0.0956\ x\ 13.6 = C_2\ x\ 15$ $C_2 = \frac{1.3007}{15}$ $C_2 = 0.0866\ M$
Molarity of HCl	$0.0866\ x\ 50 = \mathbf{4.36\ M}$

Series # 03: Silurian Dolomite at 3000 psi (15 wt. % HCl acid)

Titration 01	
Initial NaOH burette reading	0 ml
Final NaOH burette reading	13.6 ml
Initial HCl burette reading	0 ml
Final HCl burette reading	15 ml
Concentration of HCl	$(C_1V_1)_{NaOH} = (C_2V_2)_{HCl}$ $0.09765\ x\ 13.6 = C_2\ x\ 15$ $C_2 = \frac{1.32804}{15}$ $C_2 = 0.0885\ M$
Molarity of HCl	$0.0885\ x\ 50 = \mathbf{4.42\ M}$

Titration 02	
Initial NaOH burette reading	0 ml
Final NaOH burette reading	13.8 ml
Initial HCl burette reading	0 ml
Final HCl burette reading	15 ml
Concentration of HCl	$(C_1V_1)_{NaOH} = (C_2V_2)_{HCl}$ $0.09765\ x\ 13.8 = C_2\ x\ 15$ $C_2 = \frac{1.34757}{15}$ $C_2 = 0.089838\ M$
Molarity of HCl	$0.089838\ x\ 50 = \mathbf{4.49\ M}$

Titration 03	
Initial NaOH burette reading	0 ml
Final NaOH burette reading	13.7 ml
Initial HCl burette reading	0 ml
Final HCl burette reading	15 ml
Concentration of HCl	$(C_1V_1)_{NaOH} = (C_2V_2)_{HCl}$ $0.09765\ x\ 13.7 = C_2\ x\ 15$ $C_2 = \frac{1.337805}{15}$ $C_2 = 0.089187\ M$
Molarity of HCl	$0.089187\ x\ 50 = \mathbf{4.45\ M}$

APPENDIX C: Detailed Titration Results for Spent Acid Standardization

Series # 01: Silurian Dolomite at 3000 psi (12.5 wt. % HCl acid)

Titration 01	
Initial NaOH burette reading	0 ml
Final NaOH burette reading	11.4 ml
Initial HCl burette reading	0 ml
Final HCl burette reading	15 ml
Concentration of HCl	$(C_1V_1)_{NaOH} = (C_2V_2)_{HCl}$ $0.09765\ x\ 11.4 = C_2\ x\ 15$ $C_2 = \frac{1.11321}{15}$ $C_2 = 0.074214\ M$
Molarity of HCl	$0.074214\ x\ 50 = \mathbf{3.71\ M}$

Titration 02	
Initial NaOH burette reading	0 ml
Final NaOH burette reading	11.4 ml
Initial HCl burette reading	0 ml
Final HCl burette reading	15 ml
Concentration of HCl	$(C_1V_1)_{NaOH} = (C_2V_2)_{HCl}$ $0.09765\ x\ 11.4 = C_2\ x\ 15$ $C_2 = \frac{1.11321}{15}$ $C_2 = 0.074214\ M$
Molarity of HCl	$0.074214\ x\ 50 = \mathbf{3.71\ M}$

Titration 03	
Initial NaOH burette reading	0 ml
Final NaOH burette reading	11.3 ml
Initial HCl burette reading	0 ml
Final HCl burette reading	15 ml
Concentration of HCl	$(C_1V_1)_{NaOH} = (C_2V_2)_{HCl}$ $0.09765\ x\ 11.3 = C_2\ x\ 15$ $C_2 = \frac{1.103445}{15}$ $C_2 = 0.073563\ M$
Molarity of HCl	$0.073563\ x\ 50 = \mathbf{3.678\ M}$

Series # 02: Silurian Dolomite at 3000 psi (10 wt. % HCl acid)

Titration 01	
Initial NaOH burette reading	0 ml
Final NaOH burette reading	9.0 ml
Initial HCl burette reading	0 ml
Final HCl burette reading	15 ml
Concentration of HCl	$(C_1V_1)_{NaOH} = (C_2V_2)_{HCl}$ $0.09765\ x\ 9 = C_2\ x\ 15$ $C_2 = \frac{0.87885}{15}$ $C_2 = 0.05859\ M$
Molarity of HCl	$0.05859\ x\ 50 = \mathbf{2.929\ M}$

Titration 02	
Initial NaOH burette reading	0 ml
Final NaOH burette reading	8.9 ml
Initial HCl burette reading	0 ml
Final HCl burette reading	15 ml
Concentration of HCl	$(C_1V_1)_{NaOH} = (C_2V_2)_{HCl}$ $0.09765\ x\ 8.9 = C_2\ x\ 15$ $C_2 = \frac{0.869085}{15}$ $C_2 = 0.057939\ M$
Molarity of HCl	$0.057939\ x\ 50 = \mathbf{2.896\ M}$

Titration 03	
Initial NaOH burette reading	0 ml
Final NaOH burette reading	8.8 ml
Initial HCl burette reading	0 ml
Final HCl burette reading	15 ml
Concentration of HCl	$(C_1V_1)_{NaOH} = (C_2V_2)_{HCl}$ $0.09765\ x\ 8.8 = C_2\ x\ 15$ $C_2 = \frac{0.85932}{15}$ $C_2 = 0.057288\ M$
Molarity of HCl	$0.057288\ x\ 50 = \mathbf{2.864\ M}$

Series # 03: Silurian Dolomite at 3000 psi (7.5 wt. % HCl acid)

Titration 01	
Initial NaOH burette reading	0 ml
Final NaOH burette reading	6.9 ml
Initial HCl burette reading	0 ml
Final HCl burette reading	15 ml
Concentration of HCl	$(C_1V_1)_{NaOH} = (C_2V_2)_{HCl}$ $0.09557\ x\ 6.9 = C_2\ x\ 15$ $C_2 = \frac{0.659433}{15}$ $C_2 = 0.0439622\ M$
Molarity of HCl	$0.0439622\ x\ 50 = \mathbf{2.198\ M}$

Titration 02	
Initial NaOH burette reading	0 ml
Final NaOH burette reading	6.8 ml
Initial HCl burette reading	0 ml
Final HCl burette reading	15 ml
Concentration of HCl	$(C_1V_1)_{NaOH} = (C_2V_2)_{HCl}$ $0.09557\ x\ 6.8 = C_2\ x\ 15$ $C_2 = \frac{0.649876}{15}$ $C_2 = 0.043325\ M$
Molarity of HCl	$0.043325\ x\ 50 = \mathbf{2.166\ M}$

Titration 03	
Initial NaOH burette reading	0 ml
Final NaOH burette reading	6.8 ml
Initial HCl burette reading	0 ml
Final HCl burette reading	15 ml
Concentration of HCl	$(C_1V_1)_{NaOH} = (C_2V_2)_{HCl}$ $0.09557\ x\ 6.8 = C_2\ x\ 15$ $C_2 = \frac{0.649876}{15}$ $C_2 = 0.043325\ M$
Molarity of HCl	$0.043325\ x\ 50 = \mathbf{2.166\ M}$

APPENDIX D: Results for Reaction Kinetics Terms

Gravimetric Dissolving Power of Acid,"β"

Acid Concentration, wt. %	Dolomite Dissolving Power, β, lb_m mineral/lb_m solution
100	1.27
15	0.189
12.5	0.157
10	0.126
7.5	0.0945

Volumetric Dissolving Power, "X"

Acid concentration, wt. %	Volumetric Dissolving Power, X, ft^3 mineral/ ft^3 solution
100	0.473
15	0.071
12.5	0.0592
10	0.0473
7.5	0.0355

Reaction Order and Rate Equation

Disk Speed ω, rpm	Bulk acid concentration Cb, mole/lit	Surface acid concentration Cs, mole / ml	Reaction order, n	Rate Equation
250 rpm	4.42	0.004331	0.398	$-r_{HCl} = 2.4\ x\ 10^{-05}\ (C_{HCl})^{0.398}$
	3.64	0.003565		
	2.88	0.002797		
	2.132	0.00207		
500 rpm	4.42	0.004313	0.3151	$-r_{HCl} = 1.0\ x\ 10^{-05}\ (C_{HCl})^{0.315}$
	3.64	0.003557		
	2.88	0.002794		
	2.132	0.002051		
750 rpm	4.42	0.004305	0.3193	$-r_{HCl} = 2.0\ x\ 10^{-05}\ (C_{HCl})^{0.319}$
	3.64	0.003543		
	2.88	0.002787		
	2.132	0.002041		
1000 rpm	4.42	0.00429	0.133	$-r_{HCl} = 7.0\ x\ 10^{-06}\ (C_{HCl})^{0.133}$
	3.64	0.003531		
	2.88	0.002779		
	2.132	0.002014		
1250 rpm	4.42	0.00429	0.035	$-r_{HCl} = 4.0\ x\ 10^{-06}\ (C_{HCl})^{0.035}$
	3.64	0.003531		
	2.88	0.00276		
	2.132	0.00201		

APPENDIX E: XRD Profile and Molecular Structure of Dolomite

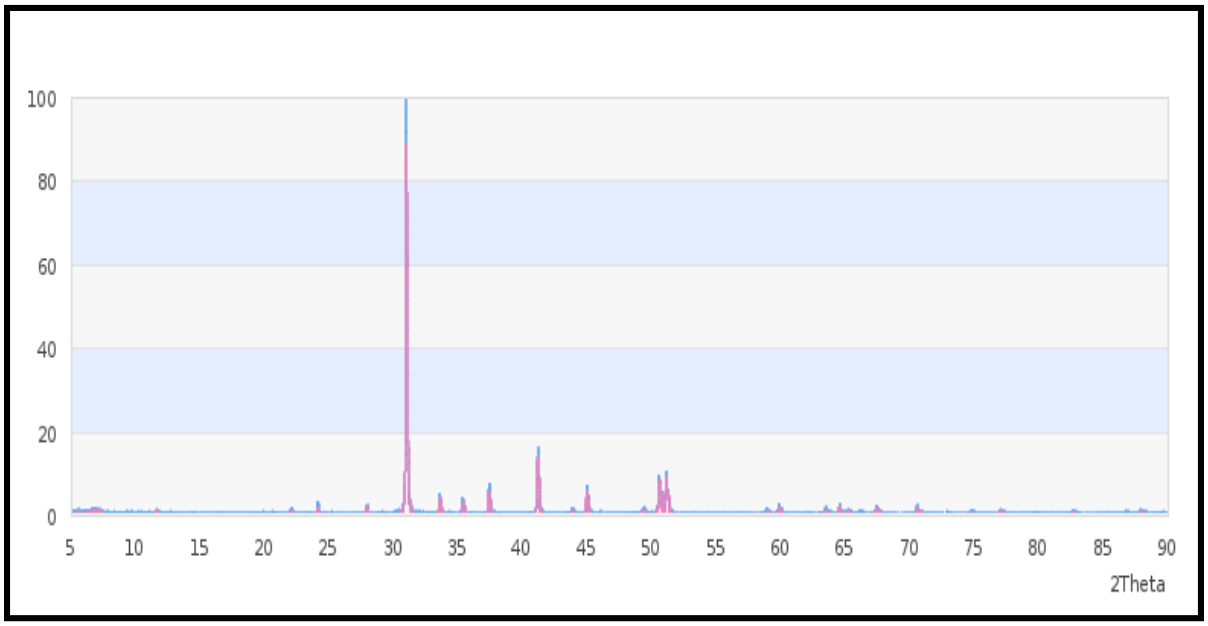

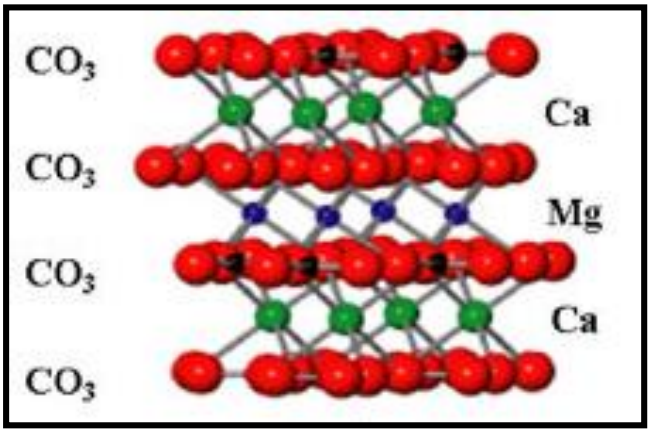

(Reference: Magalhaes, Antônio Sávio G. *et al.*, 2013)

REFERENCES

[1] Al-Douri, Sayed and Nasr-El-Din, 2013, "A New Organic Acid To Stimulate Deep Wells in Carbonate Reservoirs", SPE-164110.

[2] Rabie, Mahmoud and Nasr-El-Din, 2011, "Reaction of GLDA with Calcite: Reaction Kinetics and Transport Study", SPE-139816.

[3] Fredd and Fogler, 1999, "Optimum Conditions for Wormhole Formation in Carbonate Porous Media: Influence of Transport and Reaction", SPE-56995-PA.

[4] Fredd and Fogler, 1998, "The kinetics of calcite dissolution in acetic acid solutions", Chemical Engineering Science: Vol. 53 - pp. 3863-3874.

[5] Taylor and Nasr-El-Din, 2009, "Measurement of Acid Reaction Rates with the Rotating Disk Apparatus", PETSOC-09-06-66, Journal of Canadian Petroleum Technology: Vol. 48 - pp. 66 - 70.

[6] Taylor, Ghamdi and Nasr-El-Din, 2004, "Effect of Additives on the Acid Dissolution Rates of Calcium and Magnesium Carbonates", SPE-80256-PA.

[7] Taylor, Ghamdi and Nasr-El-Din, 2003, "Measurement of Acid Reaction Rates of a Deep Dolomitic Gas Reservoir", PETSOC-2003-068.

[8] Lund, Fogler and McCune, 1973, "Acidization—I. The dissolution of dolomite in hydrochloric acid", Chemical Engineering Science: Vol. 28 - pp. 691–700.

[9] Lund, Fogler, McCune and Ault, 1975, “Acidization—II. The dissolution of calcite in hydrochloric acid”, Chemical Engineering Science: Vol. 30 - pp. 825-835.

[10] Taylor, Nasr-El-Din and Mehta, 2006, “Anomalous Acid Reaction Rates in Carbonate Reservoir Rocks”, SPE-89417-PA.

[11] Levich, 1962, “Physicochemical hydrodynamics”, [Book] - Englewood Cliffs, N.J. : Prentice-Hall: p. 700.

[12] Sayed, Nasr-El-Din and Wolf, 2013, “Emulsified Chelating Agent: Evaluation of an Innovative Technique for High Temperature Stimulation Treatments”, SPE-165120.

[13] Anderson, 1991, “Reactivity of San Andres Dolomite”, SPE-20115-PA.

[14] Sayed and Nasr-El-Din, 2012, “Reaction Rate of Emulsified Acids and Dolomite”, SPE-151815.

[15] Pokrovsky, Golubev and Schott, 2005, “Dissolution kinetics of calcite, dolomite and magnesite at 25 °C and 0 to 50 atm pCO_2”, Ge´ochimie: Vol. 217 - pp. 239-255.

[16] Adenuga, Nasr-El-Din and Sayed, 2013, “Reactions of Simple Organic Acids and Chelating Agents with Dolomite”, SPE-164480.

[17] Plummer and Busenberg, 1982, “The kinetics of dissolution of dolomite in CO_2-H_2O systems at 1.5 to 65 C and 0 to 1 atm pCO_2”, American Journal of Science: Vol. 282 - pp. 45-78.

[18] Herman and White, 1985, “Dissolution Kinetics of Dolomite: Effects of lithology and fluid flow velocity”, Geochimica et Cosmochimica Acta: Vol. 49 - pp. 2017-2026.

[19] Qiu, Zhao, Dyer, Al-Dossary, Khan and Sultan, 2014, “Revisiting Reaction Kinetics and Wormholing Phenomena During Carbonate Acidizing”, IPTC-17285.

[20] Qiu, Zhao, Chang and Dyer, 2013, “Quantitative Modeling of Acid Wormholing in Carbonates- What Are the Gaps to Bridge”, SPE-164245.

[21] George E. King, 1986, “Acidizing Concepts – Matrix vs. Fracture Acidizing”, SPE-15279-PA, Journal of Petroleum Technology: Vol. 38 - pp. 507-508.

[22] Newman John, 1966, “Schmidt Number Corrections for the Rotating Disk”, Journal of Physical Chemistry, Vol. 70 - pp. 1327-1328.

[23] K. Lund, H.S. Fogler, C.C. McCune and J.W. Ault, 1973, “Kinetic Rate expressions for Reactions of selected minerals with HCl and HF mixtures”, SPE 4348.

[24] Fredd and Fogler, 1997, “Chelating Agents as effective Matrix Stimulation Fluids for Carbonate”, SPE 37212.

[25] J.G. Vusse, 1960, “Mass transfer with Chemical Reaction”, Chemical Engineering Science, Vol. 16 – pp. 21-30.

[26] Fogler, 2005, “Elements of Chemical Reaction Engineering, 4th edition”, [Book] Prentice-Hall: p. 1080.

[27] Lewis and Whitman, 1924, "Principles of Gas Absorption", Industrial and Engineering Chemistry, Vol. 16 – pp. 1215-1220

[28] Chang and Abbad, 2011, "Modelling Mass Transfer in a rotating disk reaction vessel".

[29] Hoefner, Fogler, Stenius and Sjoblom, 1987, "Role of Acid Diffusion in Matrix Acidizing of Carbonates", SPE 13564 PA, Journal of Petroleum Technology.

[30] N.A. Mumallah, 1991, "Factors influencing the reaction rate of Hydrochloric acid and Carbonate rock", SPE 21036.

[31] Boomer, McCune and Fogler, 1972, "Rotating Disk Apparatus for Reaction Rate studies in Corrosive Liquid Environments", The review of Scientific Instruments, Vol. 43 – pp. 225-229.

[32] Analytical Methods for Atomic Absorption Spectroscopy, 1996, The PerkinElmer Inc.

[33] Prutton and Salvage, 1945, "The Solubility of Carbon Dioxide in Calcium Chloride – Water Solutions at 75, 100, 120 º and High pressures", Vol. 67 – pp. 1550-1554.

[34] Rabie and Nasr El Din, 2011, "Measuring the Reaction Rate of Lactic Acid with Calcite using the Rotating Disk Apparatus", SPE 140167.

[35] Alkhaldi, Nasr El Din and Sarma, 2009, "Kinetics of the Reaction of Citric Acid with Calcite", SPE 118724.

[36] Conway, Asadi, Penny and Chang, 1999, "A Comparative Study of Straight/Gelled/Emulsified Hydrochloric Acid Diffusivity Coefficient Using Diaphragm Cell and Rotating Disk", SPE 56532.

[37] Higbie, R, (1935), "Trans. Am.", Inst Chem. Eng., Vol. 31, pp. 365.

[38] Magalhaes, Antônio Sávio G. *et al.*, 2013, "Superabsorbent hydrogel composite with minerals aimed at water sustainability". Journal of Brazilian Chemical Society, Vol. 24.

[39] Robert S. Schecter, 1992, "Oil Well Stimulation", [Book] Prentice-Hall.

[40] Michael Economides, Daniel Hill and Economides, 2012, "Petroleum Production Systems", [Book] Prentice-Hall.

VITAE

Name	: Muhammad Ali Khalid
Nationality	: Pakistani
Date of Birth	:1/25/1989
Email	: alikhld89@gmail.com
Address	: KFUPM Graduate Housing, Building # 811, Room # 106
Academic Background	: **MSc (Petroleum Engineering)**
	December, 2014
	King Fahd University of Petroleum and Minerals
	Dhahran, Saudi Arabia
	B.E. (Petroleum Engineering)
	December, 2010
	NED University of Engineering and Technology
	Karachi, Pakistan

Publications : X. W. Qiu, Schlumberger; M. A. Khalid and A. S. Sultan, KFUPM; 2014, “How to Determine True Acid Diffusion Coefficient to Optimize Formation Damage Treatment”, SPE-174241-MS, SPE European Formation Damage Conference, Hungary.

M. A. Khalid, S. Alnuaim and M. H. Rammay, KFUPM, 2014, “Inflow Performance Relationship For Horizontal Wells Producing From Multi-Layered Heterogeneous Solution Gas-Drive Reservoirs”, OTC-24757-MS, Offshore Technology Conference, Malaysia.